Dispersion relations in cold magnetized plasmas

Christophe Cheverry, Adrien Fontaine

▶ **To cite this version:**

Christophe Cheverry, Adrien Fontaine. Dispersion relations in cold magnetized plasmas. Kinetic and Related Models , 2017, 10 (2), pp.373-421. 10.3934/krm.2017015 . hal-01243495

HAL Id: hal-01243495
https://hal.science/hal-01243495

Submitted on 15 Dec 2015

HAL is a multi-disciplinary open access archive for the deposit and dissemination of scientific research documents, whether they are published or not. The documents may come from teaching and research institutions in France or abroad, or from public or private research centers.

L'archive ouverte pluridisciplinaire **HAL**, est destinée au dépôt et à la diffusion de documents scientifiques de niveau recherche, publiés ou non, émanant des établissements d'enseignement et de recherche français ou étrangers, des laboratoires publics ou privés.

DISPERSION RELATIONS IN COLD MAGNETIZED PLASMAS

CHRISTOPHE CHEVERRY AND ADRIEN FONTAINE

Abstract. Starting from kinetic models of cold magnetized collisionless plasmas, we provide a complete description of the characteristic variety sustaining electromagnetic wave propagation. As in [4, 12, 15], our analysis is based on some asymptotic calculus exploiting the presence at the level of dimensionless relativistic Vlasov-Maxwell equations of a large parameter: the electron gyrofrequency. Our method is inspired from geometric optics [26, 30]. It allows to unify preceding results [8, 11, 34, 28, 33, 36], while incorporating new aspects. Specifically, the non trivial effects [5, 9, 10, 21] of the spatial variations of the background density, temperature and magnetic field are exhibited. In this way, a comprehensive overview of the dispersion relations becomes available, with important possible applications in plasma physics [7, 25, 27].

Keywords. Relativistic Vlasov-Maxwell equations; Cold magnetized plasmas; Plasma phenomena out of equilibrium; Electromagnetic wave propagation; Dispersion relations; characteristic variety; Appleton-Hartree equations; eikonal equations.

Table of contents

Date: today.

1. Introduction

The Appleton-Hartree equation, sometimes referred to as the Appleton-Lassen equation, is a mathematical expression that describes the refractive index for electromagnetic wave propagation in a *cold magnetized* plasma. Historically [13], it was developed in the context of the magneto-ionic theory. The form that is still widely exploited in plasma physics [11, 27, 33] is valid in the case of a *uniform* magnetic field. It resulted from the works of E. Appleton [1] and D. Hartree [17] between 1929 and 1932. It was definitely established during the 1960s, in a series of articles [19, 32], technical notes [35] and books [18, 27].

Despite the abundance of literature on the subject, more refined models are still the focus of ongoing research. It is because numerous factors may be considered: the framework may be relativistic [8, 36]; it may look at the oblique propagation [28, 34]; it can select a special frequency range (to point out for instance whistler waves [7, 32]); it may incorporate the influence of boundaries [2, 10]; and, last but not least, it can take into account the presence of spatial inhomogeneities. The aim of the present article is to discuss this issue through a new comprehensive approach that encompasses all the foregoing elements, while adding significant additional information concerning the last one.

A complete mathematical formulation of the problem is available by coming back to the original relativistic Vlasov-Maxwell (RVM) system. The general setting is as in [14], or see directly at (2.7)-(2.8). It allows to take a principle-based approach. One challenge is to fix adequately the physical framework. This must be done with a close link to concrete situations and in accordance with the basic concepts of plasma physics. As a prototype of a cold magnetized plasma, we will consider the earth's magnetosphere. This choice allows access to exhaustive, reliable and verifiable data. Simplifications come from three basic requirements. As stated in Assumption 2.1, the temperatures and the densities of the species are supposed to undergo only slight variations. As prescribed in Assumption 2.2, partially or fully ionized space plasmas have almost the same number of positive (ions) and negative (electrons) charges, and therefore behave *quasineutral* [16]. As indicated in Assumption 2.3, most particles are in a state of local *cold* thermodynamic equilibrium [8, 28]. There remains, however, a limited but very significant fraction of the plasma which is out of equilibrium. The related nonthermal facets play a central role in many applications. They are usually tackled through some stability analysis [23].

Another key aspect of astrophysical plasmas is the decisive intervention of some exterior magnetic field $\tilde{\mathbf{B}}_e$. From this point of view, the situation is very similar to that of magnetic confinement fusion [4, 12]. The charged particles are deflected by $\tilde{\mathbf{B}}_e$ through the Lorentz force. The strong influence of $\tilde{\mathbf{B}}_e$ leads to the introduction of a small dimensionless parameter ε, with $0 < \varepsilon \ll 1$, defined at the level of (2.48), and coming from the inverse of the electron cyclotron frequency. In addition, the geomagnetic field $\tilde{\mathbf{B}}_e$ is inhomogeneous. More precisely, it can be approximated by a dipole model. With position $\mathbf{x}$ in some open set $\Omega \subset \mathbb{R}^3$, it takes the form $\tilde{\mathbf{B}}_e \equiv \varepsilon^{-1}\,\mathbf{B}_e(\mathbf{x})$, where the function $\mathbf{B}_e(\cdot)$ is subjected to Assumptions 2.4 and 2.5. As shown in (2.40), it follows that the Vlasov equation contains the penalization term $\varepsilon^{-1}\left(\mathbf{p}\times\mathbf{B}_e(\mathbf{x})\right)\cdot\nabla_{\mathbf{p}}$, where $\mathbf{p}\in\mathbb{R}^3$ is a momentum.

A work of preparation allows to extract the dimensionless version of the RVM equations. Then, the parameter ε can serve as a unit of measurement to which all the dimensionless quantities can be compared. By this way, we are led to a singular version of the RVM system. The corresponding asymptotic analysis is part of a long tradition of mathematical works in gyrokinetics [4, 12], fast rotating fluids [6] and geometric optics [26, 30]. The uniform case, that is when the function $\mathbf{B}_e(\cdot)$ is constant, has been extensively studied. However, the realistic frameworks [5, 7] imply non-constant functions $\mathbf{B}_e(\cdot)$. Now, the variations of $\mathbf{B}_e(\cdot)$ raise numerous difficulties. Their effects have not been investigated so far; they remain poorly understood; and they do not fall under the scope of classical results. The complications stem from the penalization term $\varepsilon^{-1}\,(\mathbf{p}\times\mathbf{B}_e(\mathbf{x}))\cdot\nabla_{\mathbf{p}}$ that involves a large skew-adjoint differential operator with *variable coefficients*.

The present article is starting to address this problem. It shows that the variations of $\mathbf{B}_e(\cdot)$, both in amplitude and directions, play a crucial role in electromagnetic wave propagation. In a logical order, they impact the dispersion relations, the eikonal equations, and finally the ray tracing methods [22, 37]. They have therefore important practical implications. To make our main results readable and usable, some notation is needed.

A propagating wave located at the position $(\mathbf{t},\mathbf{x})\in M:=[0,1]\times\Omega$ may be characterized by its temporal frequency $\tau\in\mathbb{R}$ and its wave vector $\xi\in\mathbb{R}^3$, with $(\tau,\xi)\in\mathbb{R}^4\setminus\{0\}$. The position $(\mathbf{t},\mathbf{x},\tau,\xi)\in T^*M$ must satisfy restrictions. It must belong to a subset $\mathscr{V}$ of T^*M called the *characteristic variety*, and specified in Paragraph 3.2.1 (see Definition 3.1). In practice, $(\mathbf{t},\mathbf{x},\tau,\xi)\in\mathscr{V}$ if and only if τ and ξ are linked by dispersion relations. These relations appear to depend on $\mathbf{x}\in\Omega$, on $|\tau|\in\mathbb{R}_+$, on $r:=|\xi|\in\mathbb{R}_+$ and on the angle $\varpi\in[0,\pi]$ between ξ and $\mathbf{B}_e(\mathbf{x})$. On the other hand, they do not involve the time $\mathbf{t}\in[0,1]$ and the polar angle $\omega\in[0,2\,\pi]$. In other words, the relation $(\mathbf{t},\mathbf{x},\tau,\xi)\in\mathscr{V}$ is equivalent to impose $(|\tau|,r)\in\mathrm{V}(\mathbf{x},\varpi)$ for some subset $\mathrm{V}(\mathbf{x},\varpi)$ of the quadrant $\mathbb{R}_+\times\mathbb{R}_+$.

In the magnetosphere, signals split up into two characteristic components. In the case of *oblique* propagation ($\varpi\neq 0$), this translates into a partition $\mathrm{V}(\mathbf{x},\varpi)=\mathrm{V}_o(\mathbf{x},\varpi)\sqcup\mathrm{V}_x(\mathbf{x},\varpi)$. The part $\mathrm{V}_o(\mathbf{x},\varpi)$ is associated to *ordinary* waves (o-waves), whereas the subset $\mathrm{V}_x(\mathbf{x},\varpi)$ is related to *extraordinary* waves (x-waves). A precise definition of $\mathrm{V}_o(\mathbf{x},\varpi)$ and $\mathrm{V}_x(\mathbf{x},\varpi)$ is given in the statement below.

Theorem 1. *[oblique dispersion relations, when $\varpi\neq 0(\pi)$] Introduce as in Definition 3.3 the resonance frequencies $\tau^{\pm}_{\infty}(\cdot)$ with $\tau^{-}_{\infty}(\mathbf{x},\varpi)<\tau^{+}_{\infty}(\mathbf{x},\varpi)$, and as in Definition 3.2 the cutoff frequencies $\tau^{\pm}_{0}(\cdot)$ with $\tau^{-}_{0}(\mathbf{x})<\tau^{+}_{0}(\mathbf{x})$. With the functions $g_{\pm}(\cdot)$ of Definition 3.4, both sets $\mathrm{V}_o(\mathbf{x},\varpi)$ and $\mathrm{V}_x(\mathbf{x},\varpi)$ consist of two connected components, namely:*

$$\mathrm{V}_o(\mathbf{x},\varpi)=\mathrm{V}_o^+(\mathbf{x},\varpi)\sqcup\mathrm{V}_o^-(\mathbf{x},\varpi)\,,\qquad \mathrm{V}_x(\mathbf{x},\varpi)=\mathrm{V}_x^+(\mathbf{x},\varpi)\sqcup\mathrm{V}_x^-(\mathbf{x},\varpi)\,,$$

with the explicit formulas:

$$\mathrm{V}_o^-(\mathbf{x},\varpi):=\big\{(\tau,r)\in\mathbb{R}_+\times\mathbb{R}_+\,;\,\tau\leq\tau^-_\infty(\mathbf{x},\varpi)\,,\,r^2=g_+(\mathbf{x},\varpi,\tau)\,\big\}\,, \tag{1.1a}$$

$$\mathrm{V}_o^+(\mathbf{x},\varpi):=\big\{(\tau,r)\in\mathbb{R}_+\times\mathbb{R}_+\,;\,\kappa\leq\tau\,,\,r^2=g_+(\mathbf{x},\varpi,\tau)\,\big\}\,, \tag{1.1b}$$

$$\mathrm{V}_x^-(\mathbf{x},\varpi):=\big\{(\tau,r)\in\mathbb{R}_+\times\mathbb{R}_+\,;\,\tau^-_0(\mathbf{x})<\tau<\tau^+_\infty(\mathbf{x},\varpi)\,,\,r^2=g_-(\mathbf{x},\varpi,\tau)\,\big\}\,, \tag{1.1c}$$

$$\mathrm{V}_x^+(\mathbf{x},\varpi):=\big\{(\tau,r)\in\mathbb{R}_+\times\mathbb{R}_+\,;\,\tau^+_0(\mathbf{x})\leq\tau\,,\,r^2=g_-(\mathbf{x},\varpi,\tau)\,\big\}\,. \tag{1.1d}$$

The description of the characteristic variety $\mathscr{V}$ through (1.1) is directly applicable in a large number of situations. That is why it is highlighted in this introduction. However, this representation implies a special choice of parameterization, which is not appropriate in the case $\varpi = 0$. Precisely, one important contribution of the present article is also to provide a global and intrinsic view of $\mathscr{V}$ (Definition 3.1) that allows to study $\mathscr{V}$ in its different facets (Section 3.4). In particular, in Paragraph 3.4.2, we investigate what happens if we fix $\tau \in \mathbb{R}_+^*$, that is if we consider sets given by $\{\xi \in \mathbb{R}^3\,;\, (\mathbf{t}, \mathbf{x}, \tau, \xi) \in \mathscr{V}\}$. By this way, according to the values of τ, we can recover various pictures. This could include one or two (more or less) nested spheres (Figures 12 and 13). This can also result in one or two connected unbounded sets with conic shape (Figures 10 and 11).

Another significant aspect of our study is the topological decomposition (valid only in the oblique case $\varpi \neq 0$) of $\mathscr{V}$ into connected components. From this perspective, the case of *parallel* propagation ($\varpi = 0$), which is often presented as being indicative of the general situation, appears rather to be a very singular situation. As revealed in Paragraph 3.3.3, as can be seen by comparing Figure 7 ($\varpi = 0$) and Figure 8 ($\varpi \to 0$), and as you can guess by looking at Figure 9, it is a composite of ordinary and extraordinary waves. The classical physical nomenclature (in terms of *Alfvèn*, *whistler*, ... and *electrostatic* waves) which is recalled in Paragraph 3.3.1 does not take into account this mixture. As a matter of fact, it is based on other considerations.

Theorem 1 gives access to rigorously justified eikonal equations (Lemmas 3.18 and 3.20) governing the propagation of the phases ϕ. To this end, it suffices to replace in (3.40) the variables τ and ξ respectively by $\partial_{\mathbf{t}}\phi(\mathbf{t}, \mathbf{x})$ and $\nabla_{\mathbf{x}}\phi(\mathbf{t}, \mathbf{x})$. The variations of $\mathbf{B}_e(\cdot)$ come into play through the dependence of ϖ and $g_\pm(\cdot)$ on $\mathbf{B}_e(\cdot)$, see (3.38) and Definition 3.4. As a by product, as shown in Section 3.4, purely parallel propagation cannot occur.

In the following text, special emphasis will be placed on frequencies which are in a range around or below, but comparable to the electron cyclotron frequency ε^{-1}. The reasons for this are the following. First, this range is where the exterior magnetic field $\mathbf{B}_e(\cdot)$ has the most influence by a clear separation between ordinary waves and extraordinary waves, and by the appearance of exactly two *cutoff* frequencies and two *resonance* frequencies. Secondly, as is well-known [19, 25, 36], this is where the propagation can be responsible for the energisation of confined plasmas and particle loss [34] through a mechanism of wave-particle interaction [7].

Now, when dealing with the plasmasphere, looking at such frequencies means to focus on Very Low Frequency waves (VLF radio frequencies in the range of 100 Hz to 10 kHz). Experimentally (Figure 17), there are a lower band and a upper band (corresponding to the two resonance frequencies) where VLF emissions arise. The monochromatic elements forming the fine structure of chorus have been mathematically interpreted in [7] as coming from a mesoscopic caustic effect. It was done on the basis of the classical toy model of [11, 27, 33], which is derived from *parallel* propagation ($\varpi = 0$) in the presence of a *uniform* magnetic field. Beyond this preliminary approach, to fully understand the morphological properties of chorus emissions, Theorem 1 is required. As outlined in Paragraph 3.4.5, a lot of information about chorus emissions [24, 25, 31, 37] can be extracted from it.

2. Kinetic descriptions issued from plasma physics

To model the behavior of a real plasma, we may simplify its characteristics. This is what is done in this Section 2. The basic equations are the Relativistic Vlasov-Maxwell equations (RVM equations) recalled in Paragraph 2.1. Exact solutions can be produced by looking at local thermodynamic equilibria (Paragraph 2.2). However, there are many situations where complex plasma phenomena (Paragraph 2.3) play a decisive part.

In Paragraph 2.4, we present such a framework issued from near-Earth space plasmas. This application involves a strong external magnetic field, satisfying special assumptions (Paragraph 2.5). In Paragraph 2.6, we derive the dimensionless form of RVM equations. By this way, we get a basic model (Paragraph 2.7) which can serve for the description of electromagnetic waves (Paragraph 2.8).

2.1. **Relativistic Vlasov-Maxwell equations.** The topic of RVM equations has been widely discussed [4, 7, 12, 14, 23]. The corresponding framework is recalled hereafter. The speed of light is $c_0 \simeq 2,99 \times 10^8\, m\, s^{-1}$. Let $L \in \mathbb{R}_+^*$ be a characteristic spatial length. The original spatial variable is $\tilde{\mathbf{x}} \in \tilde{\Omega}$, where $\tilde{\Omega}$ is some non-empty open set of $\mathbb{R}^3$. We fix the observation time $T \in \mathbb{R}_+^*$ as $T := L/c_0$. The original time variable is $\tilde{\mathbf{t}} \in [0,T]$. There are corresponding rescaled versions:

$$\mathbf{t} := \frac{\tilde{\mathbf{t}}}{T} \in [0,1]\,, \qquad \mathbf{x} = (\mathbf{x}^1,\mathbf{x}^2,\mathbf{x}^3) := \frac{\tilde{\mathbf{x}}}{L} \in \Omega := \left\{\frac{\tilde{\mathbf{x}}}{L}\,;\, \tilde{\mathbf{x}} \in \tilde{\Omega}\right\}. \tag{2.1}$$

The original space and momentum variables are $(\tilde{\mathbf{x}}, \tilde{\mathbf{p}})$ with:

$$\tilde{\mathbf{x}} = (\tilde{\mathbf{x}}^1,\tilde{\mathbf{x}}^2,\tilde{\mathbf{x}}^3) \in \tilde{\Omega} \subset \mathbb{R}^3\,, \qquad \tilde{\mathbf{p}} = (\tilde{\mathbf{p}}^1,\tilde{\mathbf{p}}^2,\tilde{\mathbf{p}}^3) \in \mathbb{R}^3\,.$$

We consider a plasma which is confined inside $\tilde{\Omega}$, and which consists of N distinct species labelled by $\alpha \in \{1,\cdots,N\}$. The particles of the α^{th} species have charge e_α and rest mass m_α. The number $\alpha = 1$ will be associated with electrons. Thus, the elementary charge is $e \equiv -e_1 \simeq 1,6 \times 10^{-19}\, C$ and the electron rest mass is $m_e \equiv m_1 \simeq 9,1 \times 10^{-31}\, kg$. Recall that the proton-to-electron mass ratio $\beta \simeq 1836$ is a dimensionless quantity, so that:

$$\iota_1 := \frac{m_1}{m_e} = 1\,, \qquad \iota_\alpha := \frac{m_1}{m_\alpha} \lesssim \beta^{-1} \simeq 10^{-3}\,, \qquad \forall\, \alpha \in \{2,\cdots,N\}\,. \tag{2.2}$$

On the other hand, the charge e_α is an integer multiple of e. More precisely:

$$\forall\, \alpha \in \{2,\cdots,N\}\,, \qquad \exists\, k_\alpha \in \mathbb{N}^*\,; \qquad k_\alpha \simeq 1\,, \qquad e_\alpha = k_\alpha\, e\,. \tag{2.3}$$

The velocity $\tilde{\mathbf{v}}_\alpha$ of a particle of type α is limited by $|\tilde{\mathbf{v}}_\alpha| \leq c_0$, and it is linked to the momentum $\tilde{\mathbf{p}} \in \mathbb{R}^3$ through:

$$\frac{\tilde{\mathbf{v}}_\alpha(\tilde{\mathbf{p}})}{c_0} = \frac{\tilde{\mathbf{p}}}{m_\alpha\, c_0}\left(1 + \frac{|\tilde{\mathbf{p}}|^2}{m_\alpha^2\, c_0^2}\right)^{-1/2}, \qquad \frac{\tilde{\mathbf{p}}(\tilde{\mathbf{v}}_\alpha)}{m_\alpha\, c_0} = \frac{\tilde{\mathbf{v}}_\alpha}{c_0}\left(1 - \frac{|\tilde{\mathbf{v}}_\alpha|^2}{c_0^2}\right)^{-1/2}. \tag{2.4}$$

The kinetic distribution function (KDF) of the α^{th} species is denoted by $\tilde{\mathrm{f}}_\alpha^{\mathrm{k}}(\tilde{\mathbf{t}},\tilde{\mathbf{x}},\tilde{\mathbf{p}})$. It is composed of:

- A *dominant stationary* part $\tilde{\mathrm{f}}_\alpha^{\mathrm{d}}(\tilde{\mathbf{x}},\tilde{\mathbf{p}})$;
- A *smaller moving* part $\tilde{\mathrm{f}}_\alpha^{\mathrm{s}}(\tilde{\mathbf{t}},\tilde{\mathbf{x}},\tilde{\mathbf{p}})$.

The density ratio $\nu \in \mathbb{R}_+^*$ between these two populations is assumed to be small and independant of α:

$$\tilde{f}_\alpha^{\rm k}(\tilde{t},\tilde{x},\tilde{p}) = \tilde{f}_\alpha^{\rm d}(\tilde{x},\tilde{p}) + \nu\, \tilde{f}_\alpha^{\rm s}(\tilde{t},\tilde{x},\tilde{p})\,, \quad (\tilde{t},\tilde{x},\tilde{p}) \in \mathbb{R}_+ \times \tilde{\Omega} \times \mathbb{R}^3\,, \quad \nu \ll 1\,. \tag{2.5}$$

The charge density $\tilde{\rho}$ and the current density $\tilde{\jmath}$ are given by:

$$\tilde{\rho} \equiv \tilde{\rho}(\tilde{f}_1^{\rm k},\cdots,\tilde{f}_N^{\rm k})(\tilde{t},\tilde{x}) \equiv \tilde{\rho}(\tilde{f}_\alpha^{\rm k})(\tilde{t},\tilde{x}) := \sum_{\alpha=1}^{N} \int_{\mathbb{R}^3} e_\alpha\, \tilde{f}_\alpha^{\rm k}(\tilde{t},\tilde{x},\tilde{p})\, d\tilde{p}\,, \tag{2.6a}$$

$$\tilde{\jmath} \equiv \tilde{\jmath}(\tilde{f}_1^{\rm k},\cdots,\tilde{f}_N^{\rm k})(\tilde{t},\tilde{x}) \equiv \tilde{\jmath}(\tilde{f}_\alpha^{\rm k})(\tilde{t},\tilde{x}) := \sum_{\alpha=1}^{N} \int_{\mathbb{R}^3} e_\alpha\, \tilde{v}_\alpha(\tilde{p})\, \tilde{f}_\alpha^{\rm k}(\tilde{t},\tilde{x},\tilde{p})\, d\tilde{p}\,. \tag{2.6b}$$

We impose a (stationary, divergence and curl-free) external magnetic field $\tilde{B}_e : \tilde{\Omega} \longrightarrow \mathbb{R}^3$. We also take into account some collective self-consistent electromagnetic field $(\tilde{E},\tilde{B})(\tilde{t},\tilde{x})$, which is created by all plasma particles. Then, neglecting the collisional effects, the time evolution of the KDF can be modelled through the Vlasov equation:

$$\partial_{\tilde{t}} \tilde{f}_\alpha^{\rm k} + \tilde{v}_\alpha(\tilde{p}) \cdot \nabla_{\tilde{x}} \tilde{f}_\alpha^{\rm k} + e_\alpha \left[\tilde{E}(\tilde{t},\tilde{x}) + \tilde{v}_\alpha(\tilde{p}) \times \big(\tilde{B}(\tilde{t},\tilde{x}) + \tilde{B}_e(\tilde{x})\big)\right] \cdot \nabla_{\tilde{p}} \tilde{f}_\alpha^{\rm k} = 0\,. \tag{2.7}$$

On the other hand, the self-consistent electromagnetic field $(\tilde{E},\tilde{B})(\tilde{t},\tilde{x})$ is subjected to the Maxwell equations:

$$\partial_{\tilde{t}} \tilde{E} - c_0^2\, \nabla_{\tilde{x}} \times \tilde{B} = -\,\epsilon_0^{-1}\, \tilde{\jmath}(\tilde{f}_\alpha^{\rm k})\,, \qquad \nabla_{\tilde{x}} \cdot \tilde{E} = \epsilon_0^{-1}\, \tilde{\rho}(\tilde{f}_\alpha^{\rm k})\,, \tag{2.8a}$$

$$\partial_{\tilde{t}} \tilde{B} + \nabla_{\tilde{x}} \times \tilde{E} = 0\,, \qquad \nabla_{\tilde{x}} \cdot \tilde{B} = 0\,. \tag{2.8b}$$

In (2.8), the physical constant $\epsilon_0 \simeq 8,8 \times 10^{-12}\, F\, m^{-1}$ stands for the vacuum permitivity.

2.2. **A dominant stationary part in a state of local thermodynamic equilibrium.** The unknowns in (2.7)-(2.8) are the $\tilde{f}_\alpha^{\rm k}(\cdot)$ and $(\tilde{E},\tilde{B})(\cdot)$. For $\nu = 0$ and $(\tilde{E},\tilde{B}) = (0,0)$, we simply find:

$$(\tilde{f}_1^{\rm k}(\tilde{t},\tilde{x},\tilde{p}),\cdots,\tilde{f}_N^{\rm k}(\tilde{t},\tilde{x},\tilde{p}),\tilde{E}(\tilde{t},\tilde{x}),\tilde{B}(\tilde{t},\tilde{x})) = (\tilde{f}_1^{\rm d}(\tilde{x},\tilde{p}),\cdots,\tilde{f}_N^{\rm d}(\tilde{x},\tilde{p}),0,0)\,. \tag{2.9}$$

This expression is assumed to satisfy (2.7) modulo some small term (to be specified later):

$$\tilde{v}_\alpha(\tilde{p}) \cdot \nabla_{\tilde{x}} \tilde{f}_\alpha^{\rm d} + e_\alpha \left[\tilde{v}_\alpha(\tilde{p}) \times \tilde{B}_e(\tilde{x})\right] \cdot \nabla_{\tilde{p}} \tilde{f}_\alpha^{\rm d} \simeq 0\,, \qquad \forall\, \alpha \in \{1,\cdots,N\}\,. \tag{2.10}$$

It is also an equilibrium from the viewpoint of waves, meaning that:

$$\epsilon_0^{-1}\, \tilde{\jmath}(\tilde{f}_\alpha^{\rm d})(\tilde{x}) = 0\,, \tag{2.11a}$$

$$\tilde{\rho}(\tilde{f}_\alpha^{\rm d})(\tilde{x}) = 0\,. \tag{2.11b}$$

The aim of this subsection 2.2 is to give a detailed description of special functions $\tilde{f}_\alpha^{\rm d}(\cdot)$ satisfying (2.10) and (2.11), together with a number of other relevant physical constraints. As a matter of fact, the two paragraphs 2.2.1 and 2.2.2 will consider (2.11b). On the other hand, the paragraph 2.2.3 will give a precise description of $\tilde{f}_\alpha^{\rm d}(\cdot)$, complemented by the examination of (2.10) and the verification of (2.11a).

2.2.1. *Cold, warm and hot plasma temperatures.* A plasma which turns to be spatially in Local Thermodynamic Equilibrium (LTE) can be characterized at the position $\tilde{\mathbf{x}}$ with a few parameters, like the temperatures $\tilde{\theta}^{\mathrm{d}}_{\alpha}(\tilde{\mathbf{x}})$ and the densities $\tilde{\mathbf{n}}^{\mathrm{d}}_{\alpha}(\tilde{\mathbf{x}})$ of the α^{th} species. Both $\tilde{\theta}^{\mathrm{d}}_{\alpha}(\cdot)$ and $\tilde{\mathbf{n}}^{\mathrm{d}}_{\alpha}(\cdot)$ are building blocks in the construction of $\tilde{\mathrm{f}}^{\mathrm{d}}_{\alpha}(\cdot)$. Retain for instance that $\tilde{\mathbf{n}}^{\mathrm{d}}_{\alpha}(\cdot)$ can be recovered from $\tilde{\mathrm{f}}^{\mathrm{d}}_{\alpha}(\cdot)$ through the integral formula:

$$\tilde{\mathbf{n}}^{\mathrm{d}}_{\alpha}(\tilde{\mathbf{x}}) := \int_{\mathbb{R}^3} \tilde{\mathrm{f}}^{\mathrm{d}}_{\alpha}(\tilde{\mathbf{x}}, \tilde{\mathbf{p}})\, d\tilde{\mathbf{p}}\,, \qquad \tilde{\mathbf{x}} \in \tilde{\Omega}\,, \qquad \alpha \in \{1, \cdots, N\}\,. \tag{2.12}$$

Denote simply by $\theta^{\mathrm{d}}_{\alpha} \in \mathbb{R}^*_+$ and $n^{\mathrm{d}}_{\alpha} \in \mathbb{R}^*_+$ typical sizes of $\tilde{\theta}^{\mathrm{d}}_{\alpha}(\cdot)$ and $\tilde{\mathbf{n}}^{\mathrm{d}}_{\alpha}(\cdot)$. We require that the two quantities $\tilde{\theta}^{\mathrm{d}}_{\alpha}(\tilde{\mathbf{x}})$ and $\tilde{\mathbf{n}}^{\mathrm{d}}_{\alpha}(\tilde{\mathbf{x}})$ do not deviate too far from $\theta^{\mathrm{d}}_{\alpha}$ and n^{d}_{α}. In other words:

Assumption 2.1. *[possible but slight variations in temperatures and densities] There is a constant $c \in]0,1[$ such that:*

$$0 < c\, \theta^{\mathrm{d}}_{\alpha} \le \tilde{\theta}^{\mathrm{d}}_{\alpha}(\tilde{\mathbf{x}}) \le c^{-1}\, \theta^{\mathrm{d}}_{\alpha}\,, \qquad 0 < c\, n^{\mathrm{d}}_{\alpha} \le \tilde{\mathbf{n}}^{\mathrm{d}}_{\alpha}(\tilde{\mathbf{x}}) \le c^{-1}\, n^{\mathrm{d}}_{\alpha}\,, \qquad \forall\, \tilde{\mathbf{x}} \in \tilde{\Omega}\,. \tag{2.13}$$

Recall that $k_B \simeq 1,38 \times 10^{-23}\, m^2\, kg\, s^{-2}\, K^{-1}$ stands for the Boltzmann constant, and also retain the relationship $1\, eV \simeq 1,16 \times 10^4\, k_B\, K$. The electron temperature ($T_e \equiv T_1$) and the ion temperatures (denoted by T_α for $\alpha > 1$) can be expressed either in kelvin (K) or in electronvolt (eV). Because of the large difference in mass, the electrons will come to thermodynamic equilibrium amongst themselves much faster than they will come into equilibrium with the ions or neutral atoms. For this reason, the ion temperatures may be very different from (usually much lower than) the electron temperature:

$$T_\alpha \le T_e \equiv T_1\,, \qquad \forall\, \alpha \in \{1, \cdots, N\}\,. \tag{2.14}$$

Based on the relative temperatures of the electrons, ions and neutrals, plasmas are classified as thermal or non-thermal. Introduce the thermal speed:

$$v^{th}_{\alpha} := \Big(\frac{k_B\, T_\alpha}{m_\alpha}\Big)^{1/2} \in \mathbb{R}^*_+\,. \tag{2.15}$$

It is linked to the dimensionless parameter $\theta^{\mathrm{d}}_{\alpha}$ through:

$$\theta^{\mathrm{d}}_{\alpha} := \frac{v^{th}_{\alpha}}{c_0} \in \mathbb{R}^*_+\,. \tag{2.16}$$

These two quantities v^{th}_{α} and $\theta^{\mathrm{d}}_{\alpha}$ can also be viewed as measures of temperature. Combining (2.2) and (2.14), we get:

$$\frac{v^{th}_{\alpha}}{v^{th}_{1}} = \frac{\theta^{\mathrm{d}}_{\alpha}}{\theta^{\mathrm{d}}_{1}} = \Big(\frac{T_\alpha}{T_1}\Big)^{1/2} \times \Big(\frac{m_1}{m_\alpha}\Big)^{1/2} \lesssim \Big(\frac{T_\alpha}{T_1}\Big)^{1/2} \times \Big(\frac{1}{\beta}\Big)^{1/2} \ll 1\,. \tag{2.17}$$

As a rule of thumb, temperatures T_α well below $100\, eV$ are said *cold*; those which are about $100\, eV$ ($\theta^{\mathrm{d}}_{\alpha} \simeq 10^{-2}$) are considered *warm*; those with T_α ranging from $100\, eV$ to $10\, keV$ ($10^{-2} \lesssim \theta^{\mathrm{d}}_{\alpha} \lesssim 1$) become progressively *hot*; particles with higher energies ($1 \lesssim \theta^{\mathrm{d}}_{\alpha}$) are termed *energetic* or *relativistic*.

2.2.2. *Quasi-neutrality.* A plasma consists of approximately equal numbers of positively charged ions and negatively charged electrons. This property is expressed by (2.11b). In view of (2.6a) and (2.12), this can also take the following equivalent form.

Assumption 2.2. *The plasma is quasi-neutral in the sense that:*

$$e\,\tilde{\mathbf{n}}_1^{\mathrm{d}}(\tilde{\mathbf{x}}) \,=\, \sum_{\alpha=2}^{N} e_\alpha\,\tilde{\mathbf{n}}_\alpha^{\mathrm{d}}(\tilde{\mathbf{x}})\,, \qquad \forall\,\tilde{\mathbf{x}}\in\tilde{\Omega}\,. \tag{2.18}$$

The interpretation of (2.18) is the existence of a background neutralizing ion population. In view of (2.3), (2.13) and (2.18), we can infer that:

$$e\,n_1^{\mathrm{d}} \,\simeq\, \sum_{\alpha=2}^{N} e_\alpha\,n_\alpha^{\mathrm{d}}\,, \qquad n_\alpha^{\mathrm{d}}\simeq n_1^{\mathrm{d}}\,, \qquad \forall\,\alpha\in\{2,\cdots,N\}\,. \tag{2.19}$$

2.2.3. *Velocity distribution function.* Several existing models can be used to describe $\tilde{\mathrm{f}}_\alpha^{\mathrm{d}}(\cdot)$. The basic descriptions rely on the following choice.

Definition 2.1. *The Maxwell-Boltzmann distribution is given by:*

$$\tilde{\mathrm{f}}_\alpha^{\mathrm{d}}(\tilde{\mathbf{x}},\tilde{\mathbf{p}}) = \frac{\tilde{\mathbf{n}}_\alpha^{\mathrm{d}}(\tilde{\mathbf{x}})}{m_\alpha^3\,c_0^3}\;\mathcal{M}^b_{\tilde{\theta}_\alpha^{\mathrm{d}}(\tilde{\mathbf{x}})}\Big(\frac{|\tilde{\mathbf{p}}|}{m_\alpha\,c_0}\Big)\,, \qquad \mathcal{M}^b_\theta(r) := \frac{1}{\pi^{3/2}}\;\frac{1}{\theta^3}\;\exp\Big(-\frac{r^2}{\theta^2}\Big)\,. \tag{2.20}$$

Retain that:

$$\partial_\theta\mathcal{M}^b_\theta(r) = \frac{1}{\theta}\;\mathfrak{m}^b_\theta(r)\;\mathcal{M}^b_\theta(r)\,, \qquad \mathfrak{m}^b_\theta(r) := -\,3+2\,\Big(\frac{r}{\theta}\Big)^2\,. \tag{2.21}$$

Moreover, $\mathcal{M}^b_\theta(\cdot)$ is a smooth probability density function (for the measure $4\,\pi\,r^2\,dr$):

$$\int_{\mathbb{R}^3}\mathcal{M}^b_\theta(|\mathbf{p}|)\;d\mathbf{p} \;=\; 4\;\pi\int_0^{+\infty}\mathcal{M}^b_\theta(r)\;r^2\;dr \;=\; 1\,, \qquad \forall\,\theta\in\mathbb{R}_+^*\,. \tag{2.22}$$

Assumption 2.3. *[the dominant stationnary parts of all species are in a state of local cold thermodynamic equilibrium] For all $\alpha\in\{1,\cdots,N\}$, we have (2.20) and the relation (2.13) is satisfied for some $\theta_\alpha^{\mathrm{d}}\lesssim 10^{-2}$.*

In the scientific literature [20, 36], the term *cold plasma* is sometimes associated with a Dirac mass in the momentum $\tilde{\mathbf{p}}$, in which case $\theta=0$ or equivalently $\mathcal{M}(r)\equiv(4\,\pi)^{-1}\,r^{-2}\,\delta_{|r=0}$. However, the temperatures are not zero. The use of (2.20) is therefore more refined, while keeping track of concentration effects through the (possible) smallness of θ.

Electrons are lighter than ions and neutral atoms. This is why they can easier reach higher energies. This is especially true in the case of the outer Van Allen belt as it will be explained in Paragraph 2.4. It follows that the dominant populations can inherit more complex structures than (2.20). As long as $\theta_\alpha^{\mathrm{d}}\lesssim 10^{-2}$, we can keep (2.20) to describe $\tilde{\mathrm{f}}_\alpha^{\mathrm{d}}(\cdot)$. But beyond, that is for hot plasmas ($10^{-2}\lesssim\theta_\alpha^{\mathrm{d}}\lesssim 1$) and all the more so for relativistic beams ($1\lesssim\theta_\alpha^{\mathrm{d}}$), it might be preferable to select a Maxwell-Jüttner distribution function. Such relativistic aspects will be examined in a forthcoming publication. Here, we will stay in the context of (2.20). Assuming (2.20), we find that:

$$\begin{aligned}\big[\tilde{\mathbf{v}}_\alpha\cdot\nabla_{\tilde{\mathbf{x}}} + e_\alpha\,(\tilde{\mathbf{v}}_\alpha\times\tilde{\mathbf{B}}_e)\cdot\nabla_{\tilde{\mathbf{p}}}\big](\ln\tilde{\mathrm{f}}_\alpha^{\mathrm{d}}) &= \tilde{\mathbf{v}}_\alpha\cdot\nabla_{\tilde{\mathbf{x}}}(\ln\tilde{\mathrm{f}}_\alpha^{\mathrm{d}})\\ &= \tilde{\mathbf{v}}_\alpha\cdot\nabla_{\tilde{\mathbf{x}}}(\ln\tilde{\mathbf{n}}_\alpha^{\mathrm{d}}) + \tilde{\mathbf{v}}_\alpha\cdot\nabla_{\tilde{\mathbf{x}}}(\ln\tilde{\theta}_\alpha^{\mathrm{d}})\;\mathfrak{m}^b_{\tilde{\theta}_\alpha^{\mathrm{d}}}\Big(\frac{|\tilde{\mathbf{p}}|}{m_\alpha\,c_0}\Big)\,.\end{aligned} \tag{2.23}$$

If the temperature and the density are constant, that is if $\tilde{\theta}^{\rm d}_\alpha(\cdot) \equiv \theta^{\rm d}_\alpha$ and $\tilde{\mathbf{n}}^{\rm d}_\alpha(\cdot) \equiv n^{\rm d}_\alpha$, the right-hand term of (2.23) disappears. Then, the expression (2.20) yields exact solutions to the equation (2.10). On the contrary, when $\nabla_{\tilde{\mathbf{x}}}(\ln \tilde{\theta}^{\rm d}_\alpha) \not\equiv 0$ or when $\nabla_{\tilde{\mathbf{x}}}(\ln \tilde{\mathbf{n}}^{\rm d}_\alpha) \not\equiv 0$, this term is sure to contribute (more or less strongly). As revealed by the dimensionless version of the equations (see Paragraph 2.6), the induced effect depends on the variations of $\tilde{\theta}^{\rm d}_\alpha(\cdot)$ and $\tilde{\mathbf{n}}^{\rm d}_\alpha(\cdot)$ in $\tilde{\mathbf{x}}$, but also on the size of the temperature $\theta^{\rm d}_\alpha$.
The expression $\tilde{\rm f}^{\rm d}_\alpha(\cdot)$ issued from (2.20) involves even functions. It makes no contribution to the current density in (2.6b). When dealing with (2.20), the constraint (2.11a) is sure to be satisfied.

2.3. **Plasma phenomena out of equilibrium.** *Collisionless* plasmas are characterized by a Knudsen number K_n larger than one. It follows that the possible discrepencies from the Maxwell-Boltzmann distributions are not immediately relaxed. Expressions like (2.9), where the $\tilde{\rm f}^{\rm d}_\alpha(\cdot)$ are adjusted as in (2.20), are therefore not sufficiently exhaustive to fully describe the realistic plasmas. In particular, in connection with some observed phenomena, the following aspects may need to be incorporated:

- *Spatial variations in the position* $\tilde{\mathbf{x}}$**:** As already taken into account, most concrete situations involve non constant functions $\tilde{\mathbf{n}}^{\rm d}_\alpha(\cdot) - n^{\rm d}_\alpha$ and $\tilde{\theta}^{\rm d}_\alpha(\cdot) - \theta^{\rm d}_\alpha$. A perturbative approach is required to absorb the remainders obtained when computing (2.7), see the right-hand term of (2.23).
- *Anisotropic effects in the momentum* $\tilde{\mathbf{p}}$**:** There is a plethora of factors that produce inhomogeneities according to the different directions $|\tilde{\mathbf{p}}|^{-1}\,\tilde{\mathbf{p}} \in \mathbb{S}^2$ of $\tilde{\mathbf{p}}$. Examples include lighting strikes, solar flares, ohming heating, neutral beam injections, high-frequency and radio-frequency waves. Obviously, such features cannot be included inside (2.20), because this expression depends only on $|\tilde{\mathbf{p}}|$.
- *Dynamical aspects*: The anisotropy in $\tilde{\mathbf{p}}$ can be enhanced by the external magnetic field $\tilde{\mathbf{B}}_e(\cdot)$ through the Lorentz force. This results in microscopic time-dependent instabilities, known as anomalous transport.
- *Electromagnetic perturbations*: In practice, fluctuations of the electric field and of the magnetic field (near $\tilde{\mathbf{B}}_e$) are recorded. In contrast with (2.9), the self-consistent field $(\tilde{\mathbf{E}}, \tilde{\mathbf{B}})(\cdot)$ is in general non-trivial.

To grasp plasma instabilities or plasma processes which are not in thermal equilibrium, we can perform a stability analysis in the vicinity of (2.9). This amounts to take $\nu \in \mathbb{R}^*_+$ with $\nu \ll 1$ in (2.5). From now on, the focus will be on (2.7)-(2.8) in the context of the perturbative regime (2.5). With a dominant stationary part adjusted as in (2.20), we look at the extra part $\tilde{\rm f}^{\rm s}_\alpha(\cdot)$, which is governed by:

$$\left\{\begin{array}{l} \partial_{\tilde{\mathbf{t}}}\tilde{\rm f}^{\rm s}_\alpha + \tilde{\mathbf{v}}_\alpha(\tilde{\mathbf{p}})\cdot\nabla_{\tilde{\mathbf{x}}}\tilde{\rm f}^{\rm s}_\alpha + e_\alpha\,\big[\,\tilde{\mathbf{E}} + \tilde{\mathbf{v}}_\alpha(\tilde{\mathbf{p}})\times(\tilde{\mathbf{B}}+\tilde{\mathbf{B}}_e)\,\big]\cdot\nabla_{\tilde{\mathbf{p}}}\tilde{\rm f}^{\rm s}_\alpha \\ \qquad\qquad = -\,\nu^{-1}\,\tilde{\mathbf{v}}_\alpha(\tilde{\mathbf{p}})\cdot\nabla_{\tilde{\mathbf{x}}}\tilde{\rm f}^{\rm d}_\alpha - \nu^{-1}e_\alpha\,\tilde{\mathbf{E}}\cdot\nabla_{\tilde{\mathbf{p}}}\tilde{\rm f}^{\rm d}_\alpha\,, \\ \partial_{\tilde{\mathbf{t}}}\tilde{\mathbf{B}} + \nabla_{\tilde{\mathbf{x}}}\times\tilde{\mathbf{E}} = 0\,, \\ \partial_{\tilde{\mathbf{t}}}\tilde{\mathbf{E}} - c_0^2\,\nabla_{\tilde{\mathbf{x}}}\times\tilde{\mathbf{B}} = -\,\epsilon_0^{-1}\nu\;\tilde{\jmath}(\tilde{\rm f}^{\rm s}_1,\cdots,\tilde{\rm f}^{\rm s}_N)\,, \end{array}\right. \tag{2.24}$$

together with:

$$\nabla_{\tilde{\mathbf{x}}}\cdot\tilde{\mathbf{E}} = \epsilon_0^{-1}\nu\;\tilde{\rho}(\tilde{\rm f}^{\rm s}_1,\cdots,\tilde{\rm f}^{\rm s}_N)\,, \qquad \nabla_{\tilde{\mathbf{x}}}\cdot\tilde{\mathbf{B}} = 0\,. \tag{2.25}$$

2.4. **Some concrete situation.** The description through (2.20) of the underlying medium can be further specified with regard to the applications in physics. We will consider the case of Near-Earth space plasmas [21], inside the exosphere (where $K_n > 1$). In the inner magnetosphere, we can distinguish two types of particle structures, which can involve special values of temperatures and densities, falling into the context of the description of cold plasmas from Paragraph 2.2.

• **C1**. The plasmasphere is a doughnut-shaped region which rotates with the Earth. It is a cold plasma ($\simeq 1\,\mathrm{eV}$) made of H^+ (nominally about 80%), He^+ (10 − 20%) and O^+ (a few percent). As noted in [9], the average electronic temperature is $T_e \simeq 6 \times 10^3\, K$, so that $\theta_1^{\mathrm{d}} \simeq 10^{-3}$. As a result, the selection of (2.20) for all $\alpha \in \{1, \cdots, N\}$ is adequate. The plasmaspheric concentration is around a mean value which is close to $n_1^{\mathrm{d}} = 10^8\, electons/m^3$. The functions $\tilde{\mathbf{n}}_\alpha^{\mathrm{d}}(\cdot)$ may vary slightly from place to place, especially when crossing the slot region. Global realistic profiles for $\tilde{\mathbf{n}}_\alpha^{\mathrm{d}}(\cdot)$ are suggested in [9, 21]. ◦

• **C2**. The outer Van Allen belt partly overlaps with the plasmasphere. It is a concentric, tyre-shaped belt containing ionic and neutral species which may be globally cold, warm, or possibly hot (but certainly not beyond). This belt can also implicate *highly energetic* ($\simeq 1\,\mathrm{MeV}$) electron fluxes which may be trapped [5, 7] by the geomagnetic field. These fast charged parcticles travel along the field lines. They stay approximately at a fixed L-shell, where the density is almost constant. We can therefore take $\tilde{\mathbf{n}}_\alpha^{\mathrm{d}}(\cdot) \equiv n_\alpha^{\mathrm{d}}$ for all $\alpha \in \{1, \cdots, N\}$. In particular, as in **C1.**, we can fix $n_1^{\mathrm{d}} = 10^8\, electrons/m^3$. Moreover, as long as the fraction of hot and energetic particles remains small, even for $\alpha = 1$, we can still select (2.20) and incorporate the relativistic aspects inside $\tilde{\mathrm{f}}_1^{\mathrm{s}}$. ◦

In what follows, the two above contexts will be systematically tested. This will appear throughout the text inside paragraphs that will be preceded by the title **Discussion**.

2.5. **Inhomogeneous magnetized plasmas.** Most cold plasmas [4, 7, 12, 16] are under the influence of a strong external magnetic field which can be prescribed through some adequate function $\tilde{\mathbf{B}}_e : \tilde{\Omega} \longrightarrow \mathbb{R}^3$, with amplitude $\tilde{\mathbf{b}}_e(\tilde{\mathbf{x}}) := |\tilde{\mathbf{B}}_e(\tilde{\mathbf{x}})|$. The function $\tilde{\mathbf{b}}_e(\cdot)$ is assumed to be of the order $b_e \in \mathbb{R}_+^*$. More precisely, we can find $c \in]0, 1[$ such that:

$$0 < c\, b_e \leq \tilde{\mathbf{b}}_e(\tilde{\mathbf{x}}) \leq c^{-1}\, b_e\,, \qquad \forall\, \tilde{\mathbf{x}} \in \tilde{\Omega}\,. \tag{2.26}$$

In view of (2.1), we can consider the following rescaled version of $\tilde{\mathbf{B}}_e(\cdot)$:

$$\mathbf{B}_e(\mathbf{x}) := \frac{\tilde{\mathbf{B}}_e(L\,\mathbf{x})}{b_e}\,, \qquad \mathbf{b}_e(\mathbf{x}) := |\mathbf{B}_e(\mathbf{x})|\,. \tag{2.27}$$

Then, the condition (2.26) becomes:

Assumption 2.4. *[nowhere-vanishing external magnetic field] There is $c \in]0, 1[$ such that:*

$$0 < c \leq \mathbf{b}_e(\mathbf{x}) \leq c^{-1}\,, \qquad \forall\, \mathbf{x} \in \Omega\,. \tag{2.28}$$

The function $\mathbf{B}_e(\cdot)$ generates a unit vector field:

$$e_3(\mathbf{x}) := \mathbf{b}_e(\mathbf{x})^{-1}\, \mathbf{B}_e(\mathbf{x}) \in \mathbb{S}^2 := \{\mathbf{x} \in \mathbb{R}^3\,;\, |\mathbf{x}| = 1\}\,. \tag{2.29}$$

Complete $e_3(\mathbf{x})$ into some right-handed orthonormal basis $(e_1, e_2, e_3)(\mathbf{x})$, with:

$$e_j(\cdot) = {}^t(e_j^1, e_j^2, e_j^3)(\cdot) \in \mathcal{C}^\infty(\Omega; \mathbb{S}^2)\,, \qquad \forall\, j \in \{1,2,3\}\,. \tag{2.30}$$

With the preceding ingredients, we can define some orthogonal matrix $O(\mathbf{x})$ and some constant skew-symmetric matrix Λ according to:

$$O := \begin{pmatrix} e_1^1 & e_2^1 & e_3^1 \\ e_1^2 & e_2^2 & e_3^2 \\ e_1^3 & e_2^3 & e_3^3 \end{pmatrix} = {}^tO^{-1}\,, \qquad \Lambda := \begin{pmatrix} 0 & 1 & 0 \\ -1 & 0 & 0 \\ 0 & 0 & 0 \end{pmatrix} = -\,{}^t\Lambda\,. \tag{2.31}$$

Assumption 2.5. *[divergence and curl-free external magnetic field] The function $\mathbf{B}_e(\cdot)$ is smooth, with $\mathbf{B}_e \in \mathcal{C}^\infty(\Omega; \mathbb{R}^3)$. It is such that:*

$$\nabla_{\mathbf{x}} \cdot \mathbf{B}_e(\mathbf{x}) = 0\,, \qquad \forall\, \mathbf{x} \in \Omega\,, \tag{2.32a}$$

$$\nabla_{\mathbf{x}} \times \mathbf{B}_e(\mathbf{x}) = 0\,, \qquad \forall\, \mathbf{x} \in \Omega\,. \tag{2.32b}$$

Generally, magnetic field lines are curved. In most concrete situations, the function $\mathbf{B}_e(\cdot)$ is a well-known non constant function of $\mathbf{x} \in \mathbb{R}^3$. As depicted below, cylindrical coordinates $(\rho, \varphi, z) \in \mathbb{R}_+^* \times \mathbb{R}^2$ can be used to mark the position of $\mathbf{x}$. Recall that, for any vector field $\mathbf{A} = A_\rho\, e_\rho + A_\varphi\, e_\varphi + A_z\, e_z$, the divergence and the curl are given by the dipole model:

$$\nabla \cdot \mathbf{A} = \frac{1}{\rho}\frac{\partial}{\partial \rho}(\rho A_\rho) + \frac{1}{\rho}\frac{\partial A_\varphi}{\partial \varphi} + \frac{\partial A_z}{\partial z}\,, \tag{2.33a}$$

$$\nabla \times \mathbf{A} = \left(\frac{1}{\rho}\frac{\partial A_z}{\partial \varphi} - \frac{\partial A_\varphi}{\partial z}\right) e_\rho + \left(\frac{\partial A_\rho}{\partial z} - \frac{\partial A_z}{\partial \rho}\right) e_\varphi + \frac{1}{\rho}\left(\frac{\partial}{\partial \rho}(\rho A_\rho) - \frac{\partial A_\rho}{\partial \varphi}\right) e_z\,. \tag{2.33b}$$

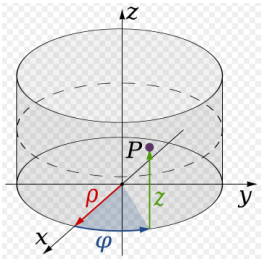

Discussion 2.1. *[external magnetic field] In the case of Near-Earth plasmas, just take $L = R^e$, where $R^e \simeq 6,3 \times 10^6\, m$ is the Earth radius. The plasmasphere and the two Van Allen belts occupy some area between altitudes of $2\,R^e$ and $8\,R^e$. We can work with:*

$$\Omega^e := \{\, (\rho, \varphi, z) \in \mathbb{R}_+^* \times \mathbb{R}^2\,;\, 2 < \rho^2 + z^2 < 8\,\}\,.$$

The magnitude of the geomagnetic field, as it can be measured at the surface of the earth, is about $b_e \simeq 10^{-5}\, T$. The Earth's magnetic field $\mathbf{B}_e \equiv \mathbf{B}_e^e$ does not depend on the angle φ. As mentioned for instance in [5, 7], it can be approximated by:

$$\mathbf{B}_e^e(\rho, z) := \frac{1}{(\rho^2 + z^2)^{5/2}} \begin{pmatrix} -\,3\,\rho\, z \\ 0 \\ \rho^2 - 2\, z^2 \end{pmatrix}, \qquad \mathbf{b}_e^e \equiv |\mathbf{B}_e^e| = \frac{(\rho^2 + 4\, z^2)^{1/2}}{(\rho^2 + z^2)^2}\,. \tag{2.34}$$

Observe that the two functions $\mathbf{B}_e^e(\cdot)$ and $\mathbf{b}_e^e(\cdot)$ are homogeneous in (ρ, z) of degree -3. We can recover (2.28) with $c = 8^{-3}$. Applying (2.33a) and (2.33b), we see easily that both conditions (2.32a) and (2.32b) are met. ∘

2.6. **Dimensionless equations.** The aim here is to write the system (2.24)-(2.25) in dimensionless form (Paragraph 2.6.1). By doing so, we have to take into account the effects induced by the spatial variations of $\tilde{\mathbf{n}}^{\mathrm{d}}_\alpha(\tilde{\mathbf{x}})$, $\tilde{\theta}^{\mathrm{d}}_\alpha(\tilde{\mathbf{x}})$ and $\tilde{\mathbf{B}}_e(\tilde{\mathbf{x}})$. Then, it is useful to straighten the field lines (Paragraph 2.6.2). Moreover, in connection with the application to the earth's context, it is important to give (Paragraph 2.6.3) a precise description of (the relative sizes of) the various physical parameters.

2.6.1. *Rescalings.* Let us recall (2.27), and define rescaled versions of $\tilde{\mathbf{n}}^{\mathrm{d}}_\alpha(\cdot)$ and $\tilde{\theta}^{\mathrm{d}}_\alpha(\cdot)$:

$$\mathbf{n}^{\mathrm{d}}_\alpha(\mathbf{x}) := (n^{\mathrm{d}}_\alpha)^{-1}\tilde{\mathbf{n}}^{\mathrm{d}}_\alpha(L\,\mathbf{x}) \simeq 1\,, \qquad \theta^{\mathrm{d}}_\alpha(\mathbf{x}) := (\theta^{\mathrm{d}}_\alpha)^{-1}\tilde{\theta}^{\mathrm{d}}_\alpha(L\,\mathbf{x}) \simeq 1\,. \tag{2.35}$$

This says nothing about the comparison of the selfconsistent magnetic field $\tilde{\mathbf{B}}$ to the typical size b_e of $\tilde{\mathbf{b}}_e(\cdot)$. From the Ampère's law in (2.24), we can infer that $\tilde{\mathbf{B}} \simeq \nu\,\theta^{\mathrm{d}}_\alpha\,b_e$. With this in mind, we can further define new unknowns by the relations:

$$\mathbf{v}_\alpha(\mathbf{p}) := (c_0)^{-1}\tilde{\mathbf{v}}_\alpha(\tilde{\mathbf{p}})\,, \qquad \mathbf{p}_\alpha := (m_\alpha\; c_0\,\theta^{\mathrm{d}}_\alpha)^{-1}\tilde{\mathbf{p}}_\alpha\,, \qquad \forall\,\alpha\in\{1,\cdots,N\}\,, \tag{2.36a}$$

$$\mathrm{f}_\alpha(\mathbf{t},\mathbf{x},\mathbf{p}_\alpha) := (n^{\mathrm{d}}_\alpha)^{-1}m^3_\alpha\;c_0^3\;(\theta^{\mathrm{d}}_\alpha)^3\;\tilde{\mathrm{f}}^{\mathrm{s}}_\alpha(\tilde{\mathrm{t}},\tilde{\mathbf{x}},\tilde{\mathbf{p}})\,, \qquad \forall\,\alpha\in\{1,\cdots,N\}\,, \tag{2.36b}$$

$$\mathbf{E}(\mathbf{t},\mathbf{x}) := (\nu\;\theta^{\mathrm{d}}_1\;c_0\;b_e)^{-1}\;\tilde{\mathbf{E}}(\tilde{\mathrm{t}},\tilde{\mathbf{x}})\,, \qquad \mathbf{B}(\mathbf{t},\mathbf{x}) := (\nu\;\theta^{\mathrm{d}}_1\;b_e)^{-1}\;\tilde{\mathbf{B}}(\tilde{\mathrm{t}},\tilde{\mathbf{x}})\,. \tag{2.36c}$$

From now on, the time-spatial position is $(\mathbf{t},\mathbf{x})$, with $(\mathbf{t},\mathbf{x})\in M := [0,1]\times\Omega$. Let T^*M be the cotangent bundle associated with M. With (2.36a), the vectors $\mathbf{v}_\alpha$ and $\mathbf{p}_\alpha$ are linked by the relations issued from (2.4), that is:

$$\mathbf{p}_\alpha(\mathbf{v}_\alpha) := \frac{\mathbf{v}_\alpha}{\theta^{\mathrm{d}}_\alpha\;(1-|\mathbf{v}_\alpha|^2)^{1/2}}\,, \qquad \mathbf{v}_\alpha(\mathbf{p}_\alpha) := \frac{\theta^{\mathrm{d}}_\alpha\;\mathbf{p}_\alpha}{\langle\theta^{\mathrm{d}}_\alpha\;|\mathbf{p}_\alpha|\rangle}\,, \qquad \langle r\rangle := \sqrt{1+r^2}\,. \tag{2.37}$$

Among the fundamental plasma parameters, we can mention (for $\alpha=1$) the electron gyrofrequency (or cyclotron frequency) $\omega_{ce}\equiv\omega_{c1}$ and the electron plasma frequency (or plasma oscillation) $\omega_{pe}\equiv\omega_{p1}$. For $\alpha\in\{2,\cdots,N\}$, we could cite the ion gyrofrequencies $\omega_{c\alpha}$ and the ion plasma frequencies $\omega_{p\alpha}$. For simplicity of presentation, we define below these quantities with an algebraic sign:

$$\omega_{c\alpha} := \frac{e_\alpha\;b_e}{m_\alpha}\,, \qquad \omega_{p\alpha} := \sqrt{\frac{n^{\mathrm{d}}_\alpha\;e^2_\alpha}{m_\alpha\;\epsilon_0}}\,, \qquad \forall\,\alpha\in\{1,\cdots,N\}\,. \tag{2.38}$$

There are corresponding dimensionless coefficients ε_α and μ_α, given by:

$$\varepsilon_\alpha := (L\,\omega_{c\alpha})^{-1}c_0\,, \qquad \mu_\alpha := (\omega_{c\alpha})^{-1}\omega_{p\alpha}\,, \qquad \forall\,\alpha\in\{1,\cdots,N\}\,. \tag{2.39}$$

Then, the new Vlasov equation is:

$$\begin{aligned}
&\partial_{\mathbf{t}}\mathrm{f}_\alpha + \frac{\theta^{\mathrm{d}}_\alpha}{\langle\theta^{\mathrm{d}}_\alpha\,|\mathbf{p}_\alpha|\rangle}\;\mathbf{p}_\alpha\cdot\nabla_{\mathbf{x}}\mathrm{f}_\alpha + \frac{\theta^{\mathrm{d}}_1}{\theta^{\mathrm{d}}_\alpha}\;\frac{\nu}{\varepsilon_\alpha}\;\Big[\mathbf{E}+\frac{\theta^{\mathrm{d}}_\alpha}{\langle\theta^{\mathrm{d}}_\alpha\,|\mathbf{p}_\alpha|\rangle}\;\mathbf{p}_\alpha\times\mathbf{B}\Big]\cdot\nabla_{\mathbf{p}_\alpha}\mathrm{f}_\alpha \\
&+\frac{1}{\varepsilon_\alpha}\;\frac{1}{\langle\theta^{\mathrm{d}}_\alpha\,|\mathbf{p}_\alpha|\rangle}\;(\mathbf{p}_\alpha\times\mathbf{B}_e(\mathbf{x}))\cdot\nabla_{\mathbf{p}_\alpha}\mathrm{f}_\alpha + \frac{\theta^{\mathrm{d}}_1}{\theta^{\mathrm{d}}_\alpha}\;\frac{\mathbf{n}^{\mathrm{d}}_\alpha}{\varepsilon_\alpha}\;\partial_r\mathcal{M}^b_{\theta^{\mathrm{d}}_\alpha(\mathbf{x})}\Big(|\mathbf{p}_\alpha|\Big)\;\frac{\mathbf{p}_\alpha\cdot\mathbf{E}}{|\mathbf{p}_\alpha|} \\
&+\frac{1}{\nu}\;\frac{\theta^{\mathrm{d}}_\alpha}{\langle\theta^{\mathrm{d}}_\alpha\,|\mathbf{p}_\alpha|\rangle}\;\mathbf{p}_\alpha\cdot\nabla_{\mathbf{x}}\mathbf{n}^{\mathrm{d}}_\alpha\;\mathcal{M}^b_{\theta^{\mathrm{d}}_\alpha(\mathbf{x})}(|\mathbf{p}_\alpha|) \\
&+\frac{1}{\nu}\;\mathbf{n}^{\mathrm{d}}_\alpha\;\frac{\theta^{\mathrm{d}}_\alpha}{\langle\theta^{\mathrm{d}}_\alpha\,|\mathbf{p}_\alpha|\rangle}\;\mathbf{p}_\alpha\cdot\nabla_{\mathbf{x}}(\ln\,\theta^{\mathrm{d}}_\alpha)\;(\mathfrak{m}^b_{\theta^{\mathrm{d}}_\alpha(\mathbf{x})}\,\mathcal{M}^b_{\theta^{\mathrm{d}}_\alpha(\mathbf{x})})(|\mathbf{p}_\alpha|) \;=\; 0\,.
\end{aligned} \tag{2.40}$$

On the other hand, the Maxwell's equations become:

$$\partial_{\mathbf{t}}\mathbf{B} + \nabla_{\mathbf{x}} \times \mathbf{E} = 0\,, \qquad \partial_{\mathbf{t}}\mathbf{E} - \nabla_{\mathbf{x}} \times \mathbf{B} = -\jmath(\mathrm{f}_\alpha)\,, \tag{2.41a}$$

$$\nabla_{\mathbf{x}} \cdot \mathbf{B} = 0\,, \qquad \nabla_{\mathbf{x}} \cdot \mathbf{E} = \rho(\mathrm{f}_\alpha)\,, \tag{2.41b}$$

where we have introduced:

$$\rho(\mathrm{f}_1, \cdots, \mathrm{f}_N)(\mathbf{t}, \mathbf{x}) \equiv \rho(\mathrm{f}_\alpha)(\mathbf{t}, \mathbf{x}) := \sum_{\alpha=1}^{N} \frac{1}{\theta_1^{\mathrm{d}}} \frac{\mu_\alpha^2}{\varepsilon_\alpha} \int_{\mathbb{R}^3} \mathrm{f}_\alpha(\mathbf{t}, \mathbf{x}, \mathbf{p}_\alpha)\, d\mathbf{p}_\alpha\,, \tag{2.42a}$$

$$\jmath(\mathrm{f}_1, \cdots, \mathrm{f}_N)(\mathbf{t}, \mathbf{x}) \equiv \jmath(\mathrm{f}_\alpha)(\mathbf{t}, \mathbf{x}) := \sum_{\alpha=1}^{N} \frac{\theta_\alpha^{\mathrm{d}}}{\theta_1^{\mathrm{d}}} \frac{\mu_\alpha^2}{\varepsilon_\alpha} \int_{\mathbb{R}^3} \frac{\mathbf{p}_\alpha}{\langle \theta_\alpha^{\mathrm{d}} |\mathbf{p}_\alpha| \rangle}\, \mathrm{f}_\alpha(\mathbf{t}, \mathbf{x}, \mathbf{p}_\alpha)\, d\mathbf{p}_\alpha\,. \tag{2.42b}$$

A quick calculation indicates that the two relations of (2.41b) are propagated by the evolution equation (2.40)-(2.41a). Therefore, it suffices to check (2.41b) at the time $t = 0$, and then to focuss on (2.41a).

2.6.2. *Straightening the field lines.* Equation (2.40) is not yet in a suitable form. Still, we need to straighten out the field lines. Recall (2.29)-(2.31) so that:

$$\mathbf{B}_e(\mathbf{x}) = \mathbf{b}_e(\mathbf{x})\; e_3(\mathbf{x}) = \mathbf{b}_e(\mathbf{x})\; O(\mathbf{x})\; {}^t(0,0,1)\,, \qquad \forall\, \mathbf{x} \in \Omega\,. \tag{2.43}$$

In view of Discussion 2.1, the directions of the unit vector field $e_3(\cdot)$, and therefore of $\mathbf{B}_e(\cdot)$, can vary with changes in $\mathbf{x} \in \Omega$. To remedy this situation, we replace simultaneously $\mathbf{B}_e$, $\mathbf{B}$, $\mathbf{E}$ and $\mathbf{p}_\alpha$ according to:

$$\mathbf{b}_e\, {}^t(0,0,1) = {}^tO\, \mathbf{B}_e\,, \qquad B := {}^tO\, \mathbf{B}\,, \qquad E := {}^tO\, \mathbf{E}\,, \qquad p_\alpha := {}^tO\, \mathbf{p}_\alpha\,. \tag{2.44}$$

For the sake of simplicity, the subscript α that identifies the different momentum variables p_α will be omitted. Concerning $p \equiv p_\alpha \in \mathbb{R}^3$, we can pass from cartesian to spherical coordinates, with orthonormal basis $(e_r, e_\varpi, e_\omega)$. This gives rise to:

$$p = r\; {}^t(\cos\omega\, \sin\varpi, \sin\omega\, \sin\varpi, \cos\varpi)\,, \qquad (\varpi, \omega, r) \in \mathbb{T}^2 \times \mathbb{R}_+\,, \qquad r = |p| = |\mathbf{p}|\,. \tag{2.45}$$

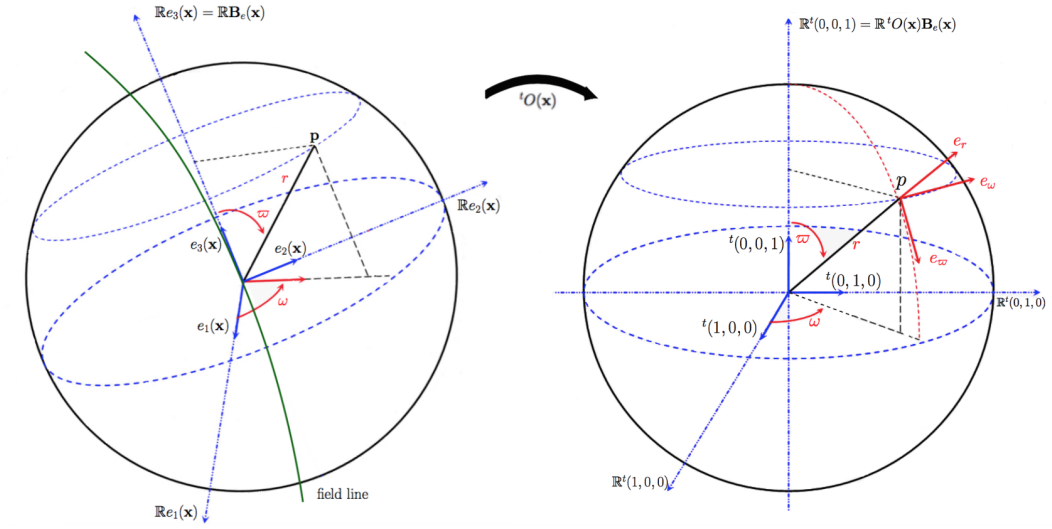

FIGURE 1. Spherical coordinates of $p \in \mathbb{R}^3$ after straigntening.

From now on, the spatial-velocity position is marked by $\mathbf{y} := (\mathbf{x}, \varpi, \omega, r) \in \Omega \times \mathbb{T}^2 \times \mathbb{R}_+$. We modify $\mathrm{f}_\alpha(\cdot)$ to fit with the preceding adjustements:

$$f_\alpha(\mathbf{t}, \mathbf{y}) \equiv f(\mathbf{t}, \mathbf{x}, \varpi, \omega, r) := \mathrm{f}_\alpha\big(\mathbf{t}, \mathbf{x}, r\, O(\mathbf{x})\, (\cos\omega\, \sin\varpi, \sin\omega\, \sin\varpi, \cos\varpi)\big)\,.$$

As usual, the symbol $\mathcal{S}$ refers to the Schwartz space. We consider functions $f(\cdot)$ satisfying uniformly in $(\mathbf{t}, \mathbf{x}, \varpi, \omega) \in M \times \mathbb{T}^2$ the conditions:

$$f \in \mathcal{C}^\infty(M \times \mathbb{T}^2 \times \mathbb{R}_+; \mathbb{R})\,, \qquad f(\mathbf{t}, \mathbf{x}, \varpi, \omega, \cdot) \in \mathcal{S}(\mathbb{R}_+; \mathbb{R})\,. \tag{2.46}$$

The gradient $\nabla_{\mathbf{p}}$ is converted into the spherical gradient ∇_p, with:

$$\nabla_p f := \frac{\partial f}{\partial r}\, e_r + \frac{1}{r}\, \frac{\partial f}{\partial \varpi}\, e_\varpi + \frac{1}{r\, \sin\varpi}\, \frac{\partial f}{\partial \omega}\, e_\omega\,.$$

The change of variables $(\mathbf{x}, \mathbf{p}) \to (\mathbf{x}, p)$ on the right of (2.44) induces some extra term when transforming $(\mathbf{v} \cdot \nabla_{\mathbf{x}})\mathrm{f}$ accordingly. Some application $Q(\cdot)$ does appear. This is a vector valued quadratic form in p, namely:

$$Q(\mathbf{x}, p) := \begin{pmatrix} O(\mathbf{x})\, p \cdot \partial_{\mathbf{x}^1} e_1 & O(\mathbf{x})\, p \cdot \partial_{\mathbf{x}^2} e_1 & O(\mathbf{x})\, p \cdot \partial_{\mathbf{x}^3} e_1 \\ O(\mathbf{x})\, p \cdot \partial_{\mathbf{x}^1} e_2 & O(\mathbf{x})\, p \cdot \partial_{\mathbf{x}^2} e_2 & O(\mathbf{x})\, p \cdot \partial_{\mathbf{x}^3} e_2 \\ O(\mathbf{x})\, p \cdot \partial_{\mathbf{x}^1} e_3 & O(\mathbf{x})\, p \cdot \partial_{\mathbf{x}^2} e_3 & O(\mathbf{x})\, p \cdot \partial_{\mathbf{x}^3} e_3 \end{pmatrix} O(\mathbf{x})\, p \in \mathbb{R}^3\,.$$

Put aside the integral operators:

$$\rho(f) := \int_0^{+\infty} \int_0^\pi \int_{-\pi}^\pi f(\varpi, \omega, r)\; r^2\, \sin\varpi\; dr\, d\varpi\, d\omega\,, \tag{2.47a}$$

$$\mathcal{J}(\theta; f) := \int_0^{+\infty} \int_0^\pi \int_{-\pi}^\pi \frac{r^3}{\langle \theta\, r\rangle} \begin{pmatrix} \cos\omega\, \sin\varpi \\ \sin\omega\, \sin\varpi \\ \cos\varpi \end{pmatrix} f(\varpi, \omega, r)\; \sin\varpi\; dr\, d\varpi\, d\omega\,. \tag{2.47b}$$

2.6.3. *The hierarchy between dimensionless parameters.* For further analysis, it is crucial to produce values for the parameters ε_α, $\theta_\alpha^{\mathrm{d}}$ and μ_α which could be meaningful from a physical point of view. It is also important to compare these quantities to one another. To this end, the following dimensionless number (which comes from the inverse of the electron cyclotron frequency):

$$\varepsilon \equiv |\varepsilon_1| := \frac{c_0}{L\, |\omega_{c1}|} = \frac{c_0\, m_e}{L\, e\, b_e} \simeq \frac{10^{-3}}{L\, b_e}\,, \tag{2.48}$$

will serve as a unit of measure.

Discussion 2.2. *[about the size of ε] As indicated in (2.39), the number ε appears to be the ratio beween the reference frequency $1/T = c_0/L$ and the gyrofrequency ω_{ce}. This appears to be a small parameter. The plasmasphere begins above the upper ionosphere and extends outwards. It contains the inner Van Allen belt, which is located between $1\, R^e$ and $2\, R^e$. Its outer boundary, known as the plasmapause, can vary with geomagnetic activity. During quiet period, it can expand outward to $7\, R^e$ or beyond. On the contrary, during magnetic storms, it moves at around $5\, R^e$. The outer Van Allen belt covers altitudes of approximately 4 to $8\, R^e$. In short, we can take the mean value $L \simeq 5\, R^e$, so that $\varepsilon \simeq 10^{-4}$.* ∘

From now on, we take $\varepsilon := 10^{-4} \ll 1$ as the small reference parameter to which all other quantities will be compared. For instance, with (2.2), keep in mind that:

$$|\varepsilon_\alpha| = \frac{e}{|e_\alpha|}\,\frac{m_\alpha}{m_e}\,\varepsilon \simeq \frac{\varepsilon}{\iota_\alpha} \gtrsim \beta\,\varepsilon \simeq 1\,, \qquad \forall\,\alpha \in \{2,\cdots,N\}\,. \tag{2.49}$$

Discussion 2.3. *[about the size of the coefficients $\theta_\alpha^{\rm d}$] The measurements recorded in the plasmasphere indicate that $\theta_1^{\rm d} \simeq \varepsilon$. The ratio $\theta_\alpha^{\rm d}/\theta_1^{\rm d}$ is given by (2.17). In view of (2.2) and (2.14), it is very small. The model (2.20) is therefore suitable for all α. In the limit ε goes to zero, we can even say that the kinetic distribution functions are given by Dirac masses. This explains the cold plasma approximation, which is sometimes applied in geophysical research [20, 36]. As regards the outer Van Allen belt, the situation is more problematic. It may still be considered that $\theta_\alpha^{\rm d} \lesssim \varepsilon$ and that $\mathrm{f}_\alpha^{\rm d}(\cdot)$ is as in (2.20) for all $\alpha \in \{2,\cdots,N\}$. However, the presence sometimes of a large amount of hot electrons might also point in favour of a Maxwell-Jüttner distribution.* ∘

Discussion 2.4. *[about the size of the coefficients μ_α] In view of (2.39), the access to μ_1 requires to evaluate b_e, m_e and $n_1^{\rm d}$. How to fix these quantities has already been explained. We find that $\mu := |\mu_1| \simeq 1$. We remark that:*

$$|\mu_\alpha| = \Big(\frac{n_\alpha^{\rm d}\,m_\alpha}{\epsilon_0}\Big)^{1/2}\,\frac{1}{b_e} = \Big(\frac{n_\alpha^{\rm d}\,m_\alpha}{n_1^{\rm d}\,m_1}\Big)^{1/2}\,|\mu_1| \geq \mu\,, \qquad \forall\,\alpha \in \{1,\cdots,N\}\,. \tag{2.50}$$

We can also find that:

$$\frac{\mu_\alpha^2}{\varepsilon_\alpha} = \frac{e_\alpha\,n_\alpha^{\rm d}}{e_1\,n_1^{\rm d}}\,\frac{\mu^2}{\varepsilon} \simeq \frac{\mu^2}{\varepsilon}\,, \qquad \forall\,\alpha \in \{1,\cdots,N\}\,. \tag{2.51}$$

∘

In practice, the value of $\mu := |\mu_1|$ is of size 1. As indicated in Definition 3.8, it can be locally compared to $\mathbf{b}_e(\mathbf{x}) \simeq 1$. The plasma is termed underdense when $\mu < \mathbf{b}_e(\mathbf{x})$ and overdense when $\mathbf{b}_e(\mathbf{x}) < \mu$. To track the influence of μ, this parameter will not be normalized in what follows. At all events, retain that the size of ε is always small, and far below μ.

Discussion 2.5. *[about the size of ν] We will adjust ν in such a way that $\nu \lesssim \varepsilon$. By this way, we can stay in a perturbative regime, even if $\theta_1^{\rm d} \simeq 1$. Indeed:*

- *Smallness of $\tilde{\mathbf{B}}$ in comparison with $\tilde{\mathbf{B}}_e$:* In view of (2.36c), the condition $\mathbf{B} \simeq 1$ implies $\tilde{\mathbf{B}} \simeq \nu\,\theta_1^{\rm d}\,b_e \lesssim \varepsilon\,b_e$. With (2.26), we can be sure that $|\tilde{\mathbf{B}}| \lesssim \varepsilon\,|\tilde{\mathbf{B}}_e|$.
- *Smallness of $\nu\,\tilde{\mathrm{f}}_\alpha^{\rm s}$ in comparison with $\tilde{\mathrm{f}}_\alpha^{\rm d}$:* When computing $\tilde{\mathrm{f}}_\alpha^{\rm k}(\cdot)$ through (2.5), the part $\nu\,\tilde{\mathrm{f}}_\alpha^{\rm s}(\cdot)$ appears as a small modification of $\tilde{\mathrm{f}}_\alpha^{\rm d}(\cdot)$. This makes sense whatever the parameter $\theta_\alpha^{\rm d}$ is, small or large. Indeed, the amplitude of $\tilde{\mathrm{f}}_\alpha^{\rm s}(\cdot)$ as prescribed by (2.36b) with $\mathrm{f}_\alpha \simeq 1$ is equivalent to the amplitude of $\tilde{\mathrm{f}}_\alpha^{\rm d}(\cdot)$ given by (2.20).

In concrete terms, we will impose $\nu \sim \varepsilon$.

2.7. **The cold asymptotic regime.** The discussion can be put in the context of some asymptotic analysis (when ε goes to 0). To this end, the coefficients ε_α, $\theta^{\rm d}_\alpha$ and μ_α must be viewed as functions of $\varepsilon \in]0,1]$. In view of the preceding study, when dealing with the plasmasphere, the three following assumptions can be retained:

- *(Cp1)*: For all $\alpha \in \{1,\cdots,N\}$, we have $\theta^{\rm d}_\alpha(\varepsilon) \sim \varepsilon$ with $\varepsilon \ll 1$.
- *(Cp2)*: For all $\alpha \in \{1,\cdots,N\}$, the dominant stationary part $\tilde{\rm f}^{\rm d}_\alpha(\cdot)$ is given by the Maxwell-Boltzmann KDF (2.20).
- *(Cp3)*: The perturbation is such that $\nu \sim \varepsilon$.

As already explained, the hypotheses *(Cp1)* and *(Cp2)* correspond to a cold thermal plasma. On the other hand, the hypothesis *(Cp3)* means that only a small fraction of the plasma is out of equilibrium. By combining information from Section 2.6 with *(Cp1)*, *(Cp2)* and *(Cp3)*, we can simplify (2.40)-(2.41a)-(2.41b) as indicated below. First, due to *(Cp2)*, there is almost no distinction between the cases $\alpha = 1$ and $\alpha \in \{2,\cdots,N\}$. The only difference is that $|\varepsilon_\alpha| \simeq 1$ for all $\alpha \in \{2,\cdots,N\}$, whereas $|\varepsilon_1| = \varepsilon \ll 1$. Thus, for all $\alpha \in \{1,\cdots,N\}$, we can impose:

$$
\begin{aligned}
&\partial_{\mathbf{t}} f_\alpha + \frac{\varepsilon}{\langle \varepsilon\, r\rangle}\, O(\mathbf{x})\, p\cdot\nabla_{\mathbf{x}} f_\alpha + \frac{\varepsilon}{\langle \varepsilon\, r\rangle}\, Q(\mathbf{x},p)\cdot\nabla_p f_\alpha \\
&\quad + \frac{\varepsilon}{\varepsilon_\alpha}\Big[E + \frac{\varepsilon}{\langle \varepsilon\, r\rangle}\, p\times B\Big]\cdot\nabla_p f_\alpha - \frac{1}{\varepsilon_\alpha}\,\frac{\mathbf{b}_e(\mathbf{x})}{\langle \varepsilon\, r\rangle}\,\partial_\omega f_\alpha \\
&\quad + \frac{\mathbf{n}^{\rm d}_\alpha(\mathbf{x})}{\varepsilon_\alpha}\,\partial_r \mathcal{M}^b_{\theta^{\rm d}_\alpha(\mathbf{x})}(r)\,\frac{p\cdot E}{r} + \frac{1}{\langle \varepsilon\, r\rangle}\, O(\mathbf{x})\, p\cdot\nabla_{\mathbf{x}}\mathbf{n}^{\rm d}_\alpha(\mathbf{x})\,\mathcal{M}^b_{\theta^{\rm d}_\alpha(\mathbf{x})}(r) \\
&\quad + \frac{1}{\langle \varepsilon\, r\rangle}\,\mathbf{n}^{\rm d}_\alpha(\mathbf{x})\, O(\mathbf{x})\, p\cdot\nabla_{\mathbf{x}}(\ln\,\theta^{\rm d}_\alpha)(\mathbf{x})\,(\mathfrak{m}^b_{\theta^{\rm d}_\alpha(\mathbf{x})}\,\mathcal{M}^b_{\theta^{\rm d}_\alpha(\mathbf{x})})(r) \,=\, 0\,.
\end{aligned}
\tag{2.52}
$$

For $\alpha \in \{2,\cdots,N\}$, this equation (2.52) contains no singular term (of the order ε^{-1}), and it is weakly nonlinear. On the contrary, for $\alpha = 1$, we can note the presence of a fast rotating term (of the order ε^{-1}), of a large source term (of size ε^{-1}), and of some $O(1)$ nonlinear contribution (of the form $E\cdot\nabla_p f_\alpha$).

The equation (2.41) does not need to be changed, except that the compatibility conditions contained in (2.41b) must be conveniently weighted:

$$
\partial_{\mathbf{t}}\mathbf{B} + \nabla_{\mathbf{x}}\times\mathbf{E} = 0\,, \qquad \nabla_{\mathbf{x}}\cdot\mathbf{B} = 0\,, \tag{2.53a}
$$

$$
\partial_{\mathbf{t}}\mathbf{E} - \nabla_{\mathbf{x}}\times\mathbf{B} = -\,\jmath(\mathrm{f}_\alpha)\,, \qquad \varepsilon\,\nabla_{\mathbf{x}}\cdot\mathbf{E} = \varepsilon\,\rho(\mathrm{f}_\alpha)\,, \tag{2.53b}
$$

and except that the two expressions $\rho(\mathrm{f}_\alpha)$ and $\jmath(\mathrm{f}_\alpha)$ can be further specified by using *(Cp1)* and (2.51) in order to find:

$$
\rho(\mathrm{f}_\alpha)(\mathbf{t},\mathbf{x}) \equiv \rho^{\rm c}(f_\alpha)(\mathbf{t},\mathbf{x}) := -\,\frac{\mu^2}{\varepsilon^2}\int_{\mathbb{R}^3} f_1\,dp + \sum_{\alpha=2}^{N}\frac{\mu^2}{\varepsilon^2}\int_{\mathbb{R}^3} f_\alpha\,dp\,, \tag{2.54a}
$$

$$
\jmath(\mathrm{f}_\alpha)(\mathbf{t},\mathbf{x}) \equiv \jmath^{\rm c}(f_\alpha)(\mathbf{t},\mathbf{x}) := -\,\frac{\mu^2}{\varepsilon}\int_{\mathbb{R}^3}\frac{p}{\langle \varepsilon\, r\rangle}\, f_1\,dp + \sum_{\alpha=2}^{N}\frac{\mu^2}{\varepsilon}\int_{\mathbb{R}^3}\frac{p}{\langle \varepsilon\, r\rangle}\, f_\alpha\,dp\,. \tag{2.54b}
$$

2.8. **Within the framework of geometrical optics.** The plasmas can support a wide variety of wave phenomena. We refer to [10, 11, 25] for an overview. In most cases, these phenomena appear to be interconnected sets of particles and fields which can evolve in a periodically repeating fashion [7]. In order to capture the precise features underlying the propagation of such plasma waves, a good strategy is to start from the dimensionless version of the RVM system which has just been exhibited in Paragraph 2.7, made up of (2.52)-(2.53) together with (2.54). This allows to set the discussion within the coherent framework of geometric optics [26, 30]. The corresponding asymptotic analysis is new for two main reasons. The first, which is well detailed in Sections 1 and 2.5, comes from the spatial variations of the magnetic field; the second is due to the *mesoscopic* precision of our model. It is important here to discuss this second aspect more thoroughly.
Being interested in the propagation of *electromagnetic waves* means to focus on oscillations of the self-consistent field $(E,B)(\cdot)$. Since the function $(E,B)(\cdot)$ depends only on $(\mathbf{t},\mathbf{x})$, a key point is that only *time-space oscillations* can be involved at this level. With this in mind, we can introduce some smooth phase function $\phi \in \mathcal{C}^\infty(M;\mathbb{R})$, which depends on the *macroscopic* variable $(\mathbf{t},\mathbf{x}) \in M$ but certainly not on the *kinetic* variable $p \in \mathbb{R}^3$.

Assumption 2.6. *[non-stationary phase] The function ϕ is such that:*

$$\forall\,(\mathbf{t},\mathbf{x}) \in M\,, \qquad (\partial_{\mathbf{t}}\phi, \nabla_{\mathbf{x}}\phi)(\mathbf{t},\mathbf{x}) \neq 0\,. \tag{2.55}$$

The oscillating behaviour of $(E,B)(\cdot)$ may be viewed as a sum of monophase pieces which can be modelled by:

$$(E,B)(\mathbf{t},\mathbf{x}) \,\equiv\, (E^\varepsilon,B^\varepsilon)(\mathbf{t},\mathbf{x}) \,=\, (\mathscr{E},\mathscr{B})\Big(\mathbf{t},\mathbf{x},\frac{\phi(\mathbf{t},\mathbf{x})}{\varepsilon}\Big)\,, \qquad \varepsilon \in]0,1]\,.$$

Usually, the time evolution of $(E,B)(\cdot)$ is considered in the framework of MHD descriptions, through *fluid* models based on Maxwell's equations, involving the variables $(\mathbf{t},\mathbf{x})$. This has the advantage of simplicity. But this also means various simplifying assumptions which are debatable when dealing with plasma phenomena out of equilibrium. To understand all subtleties induced by the underlying presence of $p \in \mathbb{R}^3$, it is necessary to come back to the original RVM system. To this end, we seek the complete solution u of (2.52)-(2.53) in the form of a basic *monophase* representation implying ϕ through:

$$u(\mathbf{t},\mathbf{y}) \,=\, \begin{pmatrix} f_1(\mathbf{t},\mathbf{y}) \\ \vdots \\ f_N(\mathbf{t},\mathbf{y}) \\ B(\mathbf{t},\mathbf{x}) \\ E(\mathbf{t},\mathbf{x}) \end{pmatrix} \,=\, u^\varepsilon(\mathbf{t},\mathbf{y}) \,=\, \mathscr{U}\Big(\mathbf{t},\mathbf{y},\frac{\phi(\mathbf{t},\mathbf{x})}{\varepsilon}\Big)\,, \qquad \mathbf{y}=(\mathbf{x},\varpi,\omega,r)\,. \tag{2.56}$$

In (2.56), the profile $\mathscr{U}$ is assumed to be periodic in the *fast* variable $\theta \in \mathbb{T} := \mathbb{R}/(2\,\pi\,\mathbb{Z})$. The coordinates inside $(\mathbf{t},\mathbf{y})$ are considered as *slow* variables. When dealing with capital letters like U, the different font styles $\mathscr{U}$, $\mathcal{U}$ and U will be used for expressions depending respectively on the variables $(\mathbf{t},\mathbf{y},\theta)$, $(\mathbf{t},\mathbf{y})$ and $(\mathbf{t},\mathbf{x},\varpi,\omega)$. When studying (2.52)-(2.53), a first stage is to exhibit approximate solutions.

Given $N \in \mathbb{N}^*$, we aim at a precision of the order $O(\varepsilon^{N-1})$ through expansions like:

$$
\begin{aligned}
u_a^\varepsilon(\mathbf{t},\mathbf{y},\mathbf{r}) \,&=\, \begin{pmatrix} f_{a,1}^\varepsilon(\mathbf{t},\mathbf{y}) \\ \vdots \\ f_{a,N}^\varepsilon(\mathbf{t},\mathbf{y}) \\ B_a^\varepsilon(\mathbf{t},\mathbf{x}) \\ E_a^\varepsilon(\mathbf{t},\mathbf{x}) \end{pmatrix} \,=\, \mathscr{U}_a^\varepsilon\Big(\mathbf{t},\mathbf{y},\tfrac{\phi(\mathbf{t},\mathbf{x})}{\varepsilon}\Big) \\
&= \sum_{j=0}^{N} \varepsilon^j\, \mathscr{U}_j\Big(\mathbf{t},\mathbf{y},\frac{\phi(\mathbf{t},\mathbf{x})}{\varepsilon}\Big) \,=\, \sum_{j=0}^{N} \varepsilon^j \begin{pmatrix} \mathscr{F}_{j,1}(\mathbf{t},\mathbf{y},\phi(\mathbf{t},\mathbf{x})/\varepsilon) \\ \vdots \\ \mathscr{F}_{j,N}(\mathbf{t},\mathbf{y},\phi(\mathbf{t},\mathbf{x})/\varepsilon) \\ \mathscr{B}_j(\mathbf{t},\mathbf{x},\phi(\mathbf{t},\mathbf{x})/\varepsilon) \\ \mathscr{E}_j(\mathbf{t},\mathbf{x},\phi(\mathbf{t},\mathbf{x})/\varepsilon) \end{pmatrix}.
\end{aligned}
\tag{2.57}
$$

In (2.57), the profiles $\mathscr{U}_j(\mathbf{t},\mathbf{y},\theta)$ are assumed to be smooth bounded real valued functions:

$$
\mathscr{U}_j = {}^t(\mathscr{F}_{j,1},\cdots,\mathscr{F}_{j,N},\mathscr{B}_j,\mathscr{E}_j) \in \mathcal{C}_b^\infty(M\times\mathbb{T}^2\times\mathbb{R}_+\times\mathbb{T};\mathbb{R}^{N+6})\,, \qquad \forall\, j\in\{0,\cdots,N\}\,,
$$

with Fourier series:

$$
\mathscr{U}_j(\mathbf{t},\mathbf{y},\theta) = \sum_{l\in\mathbb{Z}} \mathcal{U}_j^l(\mathbf{t},\mathbf{y})\; e^{i\,l\,\theta}\,, \qquad \mathcal{U}_j^l = {}^t(\mathcal{F}_{j,1}^l,\cdots,\mathcal{F}_{j,N}^l,B_j^l,E_j^l) \equiv \bar{\mathcal{U}}_j^{-l}\,. \tag{2.58}
$$

It is understood that the function $\mathcal{F}_{j,\alpha}^l(\cdot)$ and its derivatives at all orders satisfy (2.46). Plugg the real valued function $u_a^\varepsilon(\cdot)$ of (2.57) into (2.52)-(2.53) and into (2.54). Collect the contributions having the same power of ε in factor, sorted in increasing order. By this way, we get the condition:

$$
\sum_{j=-1}^{+\infty} \varepsilon^j\, \mathscr{G}_j\Big(\mathbf{t},\mathbf{y},\frac{\phi(t,\mathbf{x})}{\varepsilon}\Big) = 0\,, \qquad \mathscr{G}_j(\mathbf{t},\mathbf{y},\theta) = \sum_{l\in\mathbb{Z}} \mathcal{G}_j^l(\mathbf{t},\mathbf{y})\; e^{i\,l\,\theta}\,, \qquad \mathcal{G}_j^l \equiv \bar{\mathcal{G}}_j^{-l}\,. \tag{2.59}
$$

It turns out that the expressions $\mathscr{G}_j(\cdot)$ depend only on terms $\mathscr{U}_i$ with $i \le j+1$. The approximate solution $u_a^\varepsilon(\cdot)$ can be derived by solving successively the conditions $\mathscr{G}_j \equiv 0$ for $j=-1$, $j=0$, and so on $\cdots$ up to $j=N-1$. The corresponding WKB analysis is rather difficult and imbricated. We must proceed step by step. To begin with, we limit ourselves here to the initialization procedure. We will only consider the preliminary constraint $\mathscr{G}_{-1}\equiv 0$ obtained for $j=-1$. This includes especially the so-called *eikonal equation* which allows to determine ϕ and therefore governs the geometry of the propagation. The study of transport equations (for $j=0$), of weakly nonlinear effects (interaction of waves) and of stability properties is postponed to other articles.

3. Cold plasma dispersion relations

From now on, the matter is to solve the condition $\mathscr{G}_{-1}(\mathscr{U}_0)\equiv 0$, which is inherited from the cold plasma model exposed in Paragraph 2.7. Given $\ell\in\mathbb{N}$, the Fourier coefficient $\mathcal{G}_{-1}^\ell$ depends only on $\mathcal{U}_0^\ell$. There remains:

$$
\mathcal{G}_{-1}^\ell(\mathcal{U}_0^\ell) \equiv 0\,, \qquad \forall\,\ell\in\mathbb{Z}\,. \tag{3.1}
$$

The expressions $\mathcal{G}^\ell_{-1}(\cdot)$ are linear with respect to $\mathcal{U}^l_0$ with coefficients depending on the choice of ϕ. With (2.58) and (2.59), it follows that:

$$\mathcal{G}^\ell_{-1}(\mathcal{U}^\ell_0) = \bar{\mathcal{G}}^{-\ell}_{-1}(\bar{\mathcal{U}}^{-\ell}_0) = \overline{\mathcal{G}^{-\ell}_{-1}(\mathcal{U}^{-\ell}_0)}\,, \qquad \mathcal{G}^\ell_{-1}(0) = 0\,, \qquad \forall\, \ell \in \mathbb{Z}\,. \tag{3.2}$$

The situation under study is very dispersive. After adjusting ϕ in order to obtain $\mathcal{G}^l_{-1} \equiv 0$ (and therefore $\bar{\mathcal{G}}^{-l}_{-1} \equiv 0$) for some $l \in \mathbb{Z}^*$, the other conditions $\mathcal{G}^\ell_{-1} \equiv 0$ (with $\ell \neq |l|$) are in general not verified (except for the trivial choice $\mathcal{U}^\ell_0 \equiv 0$). This is why, at leading order, only one Fourier coefficient will be switched on.

Assumption 3.1. *[presence of a non-trivial monochromatic electromagnetic oscillation] There is some non-zero integer $l \in \mathbb{Z}^*$ such that:*

$$(E^l_0, B^l_0) \equiv (\bar{E}^{-l}_0, \bar{B}^{-l}_0) \not\equiv 0\,, \qquad \mathcal{U}^\ell_0 \equiv 0\,, \qquad \forall\, \ell \in \mathbb{Z} \setminus \{-l, l\}\,. \tag{3.3}$$

Due to (3.2) and (3.3), the conditions inside (3.1) reduce to:

$$\mathcal{G}^l_{-1}(\mathcal{U}^l_0) \equiv 0\,, \qquad \mathcal{U}^l_0 = {}^t(\mathcal{F}^l_{0,1}, \cdots, \mathcal{F}^l_{0,N}, B^l_0, E^l_0)\,. \tag{3.4}$$

This Section 3 is devoted to the analysis of (3.4).

3.1. The first step of the WKB calculus.

With $l \in \mathbb{Z}^*$ as in Assumption 3.1, introduce:

$$\tau := l\, \partial_{\mathbf{t}}\phi(\mathbf{t}, \mathbf{x}) \in \mathbb{R}\,, \qquad \xi := l\ {}^t\!O(\mathbf{x})\, \nabla_{\mathbf{x}}\phi(\mathbf{t}, \mathbf{x}) \in \mathbb{R}^3\,. \tag{3.5}$$

Recall that, due to (2.55), we have $(\tau, \xi) \neq (0, 0)$. From (2.52), knowing that $\varepsilon_1 = -\varepsilon$ and $\varepsilon_\alpha \lesssim 1$ for $\alpha \neq 1$, we can extract:

$$\big[i\,\tau + \mathbf{b}_e\, \partial_\omega\big]\, \mathcal{F}^l_{0,1} = \mathbf{n}^{\mathrm{d}}_1\ \partial_r \mathcal{M}^b_{\theta^{\mathrm{d}}_1}(r)\ r^{-1}\ p \cdot E^l_0\,, \tag{3.6}$$

together with:

$$\forall\, \alpha \in \{2, \cdots, N\}, \qquad i\,\tau\, \mathcal{F}^l_{0,\alpha} = 0\,. \tag{3.7}$$

In view of (3.6), an electric oscillation ($E^l_0 \not\equiv 0$) is correlated with an oscillation of the electron density distribution ($\mathcal{F}^l_{0,1} \not\equiv 0$). On the contrary, the density distributions of ions contain no oscillations (at leading order). In order to satisfy (3.7), we must impose:

$$\forall\, \alpha \in \{2, \cdots, N\}, \qquad \mathcal{F}^l_{0,\alpha} = 0\,. \tag{3.8}$$

With the $f^\varepsilon_{a,\alpha}$ as in (2.57), exploiting (3.8), the charge density ρ and the electric current $\jmath$ which are given by (2.54) can be expanded in powers of $\varepsilon \in\,]0, 1]$ according to:

$$\rho(f^\varepsilon_{a,\alpha})(\mathbf{t}, \mathbf{x}) \;=\; -\,\frac{\mu^2}{\varepsilon^2}\,\Big(\int_{\mathbb{R}^3} \mathcal{F}^l_{0,1}(\mathbf{t}, \mathbf{y})\ dp\Big)\ e^{i\,l\,\phi(\mathbf{t},\mathbf{x})/\varepsilon} \;+\; O\Big(\frac{1}{\varepsilon}\Big)\,, \tag{3.9a}$$

$$\jmath(f^\varepsilon_{a,\alpha})(\mathbf{t}, \mathbf{x}) \;=\; -\,\frac{\mu^2}{\varepsilon}\,\Big(\int_{\mathbb{R}^3} p\ \mathcal{F}^l_{0,1}(\mathbf{t}, \mathbf{y})\ dp\Big)\ e^{i\,l\,\phi(\mathbf{t},\mathbf{x})/\varepsilon} \;+\; O(1)\,. \tag{3.9b}$$

Coming back to (2.52)-(2.53), with the definitions of (2.47), we have to consider:

$$\xi \times E_0^l + \tau\, B_0^l = 0\,. \tag{3.10a}$$

$$\xi \times B_0^l - \tau\, E_0^l = i\,\mu^2\, \mathcal{J}\big(0; \mathcal{F}_{0,1}^l(\mathbf{t},\mathbf{x},\cdot)\big)\,, \tag{3.10b}$$

$$\mathsf{p}\big(\mathcal{F}_{0,1}^l(\mathbf{t},\mathbf{x},\cdot)\big) = 0\,, \qquad \xi \cdot B_0^l = 0\,. \tag{3.10c}$$

The rest of the article is devoted to the study of the system (3.6)-(3.10) on $(\mathcal{F}_{0,1}^l, B_0^l, E_0^l)$. The subscript α is not present at the level of (3.6)-(3.10). Thus, without any possibility of confusion, we can drop the subscript 1 at the level of $\theta_1^{\rm d}$, $\mathbf{n}_1^{\rm d}$ and $\mathcal{F}_{0,1}^l$. From now on, $\theta^{\rm d}$, $\mathbf{n}^{\rm d}$ and $\mathcal{F}_0^l$ stand for $\theta_1^{\rm d}$, $\mathbf{n}_1^{\rm d}$ and $\mathcal{F}_{0,1}^l$.

3.1.1. *Looking for reduced-form equations on the electric part.* The aim here is to extract from (3.6)-(3.10) necessary conditions involving only E_0^l. Let us go step-by-step.

∘ 3.1.1.a) Eliminating the presence of the variable r. The expression $\mathcal{F}_0^l \equiv \mathcal{F}_{0,1}^l$ can always be factored into:

$$\mathcal{F}_0^l(\mathbf{t},\mathbf{y}) = F_0^l(\mathbf{t},\mathbf{x},\varpi,\omega)\ \partial_r \mathcal{M}_{\theta^{\rm d}}^b(r)\,, \qquad F_0^l \in \mathcal{C}^\infty(M\times\mathbb{T}^2;\mathbb{C})\,.$$

This allows to convert (3.6) into:

$$\big[i\,\tau + \mathbf{b}_e\,\partial_\omega\big]\, F_0^l = \mathbf{n}^{\rm d}\ (\cos\omega\,\sin\varpi, \sin\omega\,\sin\varpi, \cos\varpi)\cdot E_0^l\,. \tag{3.11}$$

On the other hand, we have:

$$\begin{aligned}\int_0^{+\infty} r^3\,\partial_r \mathcal{M}_{\theta^{\rm d}}^b(r)\,dr &= -\frac{1}{\pi^{3/2}}\int_0^{+\infty}\Big(\frac{r^2}{(\theta^{\rm d})^2}\Big)^{3/2}\exp\Big(-\frac{r^2}{(\theta^{\rm d})^2}\Big)\,d\Big(\frac{r^2}{(\theta^{\rm d})^2}\Big)\\ &= -\frac{1}{\pi^{3/2}}\,\Gamma\Big(\frac{5}{2}\Big) = -\frac{3}{4\,\pi}\,.\end{aligned}$$

Coming back to (2.47b), it follows that:

$$\mathcal{J}(0;\mathcal{F}_0^l) \equiv \mathcal{J}_0(F_0^l) := -\frac{3}{4\,\pi}\int_0^\pi\!\!\int_{-\pi}^\pi \begin{pmatrix}\cos\omega\,\sin\varpi\\ \sin\omega\,\sin\varpi\\ \cos\varpi\end{pmatrix} F_0^l(\mathbf{t},\mathbf{x},\varpi,\omega)\ \sin\varpi\ d\varpi\,d\omega\,. \tag{3.12}$$

In the same way, we can compute:

$$\mathsf{p}(\mathcal{F}_0^l(\mathbf{t},\mathbf{x},\cdot)) \equiv \mathsf{p}_0(F_0^l) := -\frac{1}{\pi^{3/2}\,\theta^{\rm d}(\mathbf{x})}\int_0^\pi\!\!\int_{-\pi}^\pi F_0^l(\mathbf{t},\mathbf{x},\varpi,\omega)\ \sin\varpi\ d\varpi\,d\omega\,. \tag{3.13}$$

∘ 3.1.1.b) Eliminating the presence of the variable ω. This can be done by a Fourier analysis:

$$F_0^l(\mathbf{t},\mathbf{x},\varpi,\omega) = \sum_{m\in\mathbb{Z}} F_0^{l,m}(\mathbf{t},\mathbf{x},\varpi)\ e^{i\,m\,\omega} = \sum_{(m,n)\in\mathbb{Z}^2} F_{0,n}^{l,m}(\mathbf{t},\mathbf{x})\ e^{i\,(n\,\varpi + m\,\omega)}\,.$$

Then, the condition (3.11) can be declined into:

$$i\ \big[\tau - \mathbf{b}_e(\mathbf{x})\big]\, F_0^{l,-1} = 2^{-1}\,\mathbf{n}^{\rm d}\ (E_0^{l1} + i\,E_0^{l2})\ \sin\varpi\,, \tag{3.14a}$$

$$i\ \tau\ F_0^{l,0} = \mathbf{n}^{\rm d}\ E_0^{l3}\ \cos\varpi\,, \tag{3.14b}$$

$$i\ \big[\tau + \mathbf{b}_e(\mathbf{x})\big]\, F_0^{l,+1} = 2^{-1}\,\mathbf{n}^{\rm d}\ (E_0^{l1} - i\,E_0^{l2})\ \sin\varpi\,, \tag{3.14c}$$

$$i\ \big[\tau + m\,\mathbf{b}_e(\mathbf{x})\big]\, F_0^{l,m} = 0\,, \qquad \forall\, m\in\mathbb{Z}\setminus\{-1,0,1\}\,. \tag{3.14d}$$

On the other hand, we are left with:

$$\mathcal{J}_0(F_0^l) \equiv \mathcal{J}_0(F_0^{l,-1}, F_0^{l,0}, F_0^{l,1}) = -\frac{3}{4}\int_0^\pi \begin{pmatrix} F_0^{l,1}+F_0^{l,-1} \\ i\,(F_0^{l,1}-F_0^{l,-1}) \\ 2\,\mathrm{cotan}\,\varpi\; F_0^{l,0} \end{pmatrix}(\mathbf{t},\mathbf{x},\varpi)\;(\sin\varpi)^2\;d\varpi\,, \tag{3.15}$$

together with:

$$\rho_0(F_0^l) \equiv \rho_0(F_0^{l,0}) = -\frac{2}{\pi^{1/2}\,\theta^{\mathrm{d}}(\mathbf{x})}\int_0^\pi F_0^{l,0}(\mathbf{t},\mathbf{x},\varpi)\;\sin\varpi\;d\varpi\,. \tag{3.16}$$

Now, from (3.14b), we can deduce that:

$$i\;\tau\;\pi^{1/2}\;\theta^{\mathrm{d}}\;\rho_0(F_0^l) \;=\; -2\;\mathbf{n}^{\mathrm{d}}\;E_0^{l3}\int_0^\pi \cos\varpi\;\sin\varpi\;d\varpi \;=\; 0\,. \tag{3.17}$$

Remark 3.1. *For $\tau \neq 0$, the first condition and the second condition inside (3.10c) are obvious consequences of respectively (3.17) and (3.10a). Thus, when $\tau \neq 0$, we can forget the compatibility condition (3.10c).*

∘ 3.1.1.c) Eliminating the presence of the magnetic component B_0^l. Multiply the line (3.10b) by τ. In the expression thus obtained, use (3.10a) to replace $\tau\,B_0^l$. This yields:

$$\xi\times(\xi\times E_0^l)+\tau^2\,E_0^l \;=\; -\,i\;\mu^2\;\tau\;\mathcal{J}_0(F_0^l)\,. \tag{3.18}$$

∘ 3.1.1.d) Eliminating the presence of the density component F_0^l. The idea here is to exploit the equations of (3.14) in order to exhibit a relation between $\mathcal{J}_0(\mathcal{F}_0^l)$ and E_0^l. To begin with, from (3.14), we can extract:

$$\Sigma(\mathbf{x},\tau)\begin{pmatrix} F_0^{l,1}+F_0^{l,-1} \\ i\,(F_0^{l,1}-F_0^{l,-1}) \\ 2\,\mathrm{cotan}\,\varpi\;F_0^{l,0}\end{pmatrix} = \mathbf{n}^{\mathrm{d}}\begin{pmatrix} E_0^{l,1}\sin\varpi \\ E_0^{l,2}\sin\varpi \\ E_0^{l,3}\cos\varpi\end{pmatrix},$$

where we have introduced the skew-Hermitian matrix:

$$\Sigma(\mathbf{x},\tau) := \begin{pmatrix} i\,\tau & +\mathbf{b}_e(\mathbf{x}) & 0 \\ -\mathbf{b}_e(\mathbf{x}) & i\,\tau & 0 \\ 0 & 0 & i\,\tau\end{pmatrix}. \tag{3.19}$$

Multiply this identity by $(\sin\varpi)^2$ and integrate with respect to $d\varpi$. There remains:

$$\Sigma(\mathbf{x},\tau)\;\mathcal{J}_0(F_0^l) = -\,\mathbf{n}^{\mathrm{d}}\,E_0^l\,. \tag{3.20}$$

Then, by applying Σ to (3.18), we get:

$$\mathfrak{N}\,E_0^l = 0\,, \qquad \mathfrak{N}(\mathbf{x},\tau,\xi) := \Sigma(\mathbf{x},\tau)\left(\xi\,{}^t\xi + (\tau^2-|\xi|^2)\,Id\right) - \;i\;\mu^2\,\mathbf{n}^{\mathrm{d}}\,\tau\,Id\,. \tag{3.21}$$

At this stage, we can state that a *necessary condition* to obtain non-trivial solutions $\mathcal{U}_0^l \not\equiv 0$ of the system (3.4), satisfying $E_0^l \not\equiv 0$, is to impose $det\,\mathfrak{N}(\mathbf{x},\tau,\xi) = 0$. The discussion about a *sufficient condition* requires to distinguish between the values of τ.

3.1.2. *The stationary case ($\tau = 0$).* When $\tau = 0$, we simply find $det\, \mathfrak{N}(\mathbf{x}, 0, \xi) = 0$. In fact, the step 3.1.1.c) makes no sense since it removes the information contained in (3.10b). The same applies for the step 3.1.1.d) since the matrix $\Sigma(\mathbf{x}, 0)$ is not invertible. The situation $\tau = 0$ must therefore be handled separately.

Lemma 3.1 (trace of the dispersion relations in the stationary case)**.** *For $\tau = 0$, the system (3.6)-(3.10) has a solution $(\mathcal{F}_0^l, B_0^l, E_0^l)$ satisfying Assumption 3.1 if and only if the position $(\mathbf{x}, \xi) \in T^*(\Omega)$ is such that $\xi^3 = 0$.*

Proof. The matter here is to deal with:

$$\mathbf{b}_e\, \partial_\omega F_0^l = \mathbf{n}^{\rm d}\, (\cos\omega\, \sin\varpi, \sin\omega\, \sin\varpi, \cos\varpi) \cdot E_0^l\,, \tag{3.22a}$$

$$\xi \times E_0^l = 0\,, \tag{3.22b}$$

$$\xi \times B_0^l = i\, \mu^2\, \mathcal{J}_0(F_0^l)\,, \tag{3.22c}$$

$$\rho_0(F_0^l) = 0\,, \qquad \xi \cdot B_0^l = 0\,. \tag{3.22d}$$

The condition (3.22a) - or the condition (3.14) for $\tau = 0$ - is equivalent to:

$$F_0^{l,-1} \;=\; +\,i\, (2\,\mathbf{b}_e)^{-1}\, \mathbf{n}^{\rm d}\, (E_0^{l1} + i\, E_0^{l2})\, \sin\varpi\,, \tag{3.23a}$$

$$F_0^{l,+1} \;=\; -\,i\, (2\,\mathbf{b}_e)^{-1}\, \mathbf{n}^{\rm d}\, (E_0^{l1} - i\, E_0^{l2})\, \sin\varpi\,, \tag{3.23b}$$

together with $F_0^{l,m} = 0$ for all $m \in \mathbb{Z} \setminus \{-1, 0, 1\}$ and $E_0^{l3} = 0$. In the preceding lines, there is no condition on $F_0^{l,0}$. We can always adjust the component $F_0^{l,0}$ so that the first condition of (3.22d) is satisfied, which amounts to impose:

$$\int_0^\pi F_0^{l,0}(\mathbf{t}, \mathbf{x}, \varpi)\, \sin\varpi\, d\varpi \;=\; 0\,.$$

The part (3.22b) says that the direction E_0^l is parallel to ξ. In particular, we have $\xi^3 = 0$. Using (3.15) together with (3.23), we get $\xi \cdot \mathcal{J}_0(F_0^l) = 0$. This is all we need to adjust B_0^l through (3.22c) and the second relation in (3.22d). □

3.1.3. *The electron cyclotron resonance frequencies ($\tau = \pm \mathbf{b}_e(\mathbf{x})$).* The position $\mathbf{x} \in \Omega$ being fixed, the electron cyclotron resonance frequency is given by the value $|\tau| = \mathbf{b}_e(\mathbf{x})$. It plays a crucial role in plasma physics (and also in condensed matter and accelerator physics). When $|\tau| = \mathbf{b}_e(\mathbf{x})$, the difficulty comes from the step 3.1.1.d). The matrix $\Sigma(\mathbf{x}, \mathbf{b}_e(\mathbf{x}))$ is not invertible. This is why this situation must be tackled separately. We will deal here with the case $\tau = +\mathbf{b}_e$ (the other case $\tau = -\mathbf{b}_e$ being very similar).

Lemma 3.2 (trace of the dispersion relations at the resonance frequencies)**.** *For $\tau = \mathbf{b}_e(\mathbf{x})$, the system (3.6)-(3.10) has a solution $(\mathcal{F}_0^l, B_0^l, E_0^l)$ satisfying Assumption 3.1 if and only if the position $(\mathbf{x}, \xi) \in T^*(\Omega)$ is such that $det\, \mathfrak{N}(\mathbf{x}, \mathbf{b}_e(\mathbf{x}), \xi) = 0$.*

Proof. From Paragraph 3.1.1, we know already that the condition $det\, \mathfrak{N}(\mathbf{x}, \mathbf{b}_e(\mathbf{x}), \xi) = 0$ is necessary. To show that it is also sufficient, assume that $det\, \mathfrak{N}(\mathbf{x}, \mathbf{b}_e(\mathbf{x}), \xi) = 0$. Then, there is some $E_0^l \not\equiv 0$ such that:

$$\mathfrak{N}(\mathbf{x}, \mathbf{b}_e(\mathbf{x}), \xi)\, E_0^l \;=\; 0\,. \tag{3.24}$$

From (3.19), we can see that $(1,i,0)\cdot\Sigma(\mathbf{x},\mathbf{b}_e(\mathbf{x}))=0$. Then, looking at $(1,i,0)\cdot\mathfrak{N}\,E_0^l=0$, we can extract $E_0^{l1}+i\,E_0^{l2}=0$. Therefore, the condition (3.14a) with $\tau=\mathbf{b}_e(\mathbf{x})$ is met. On the other hand, the relations (3.14b) and (3.14c) impose:

$$F_0^{l,0} \;=\; -\,i\;\mathbf{b}_e^{-1}\,\mathbf{n}^{\mathrm{d}}\;E_0^{l3}\;\cos\varpi\,, \tag{3.25a}$$

$$F_0^{l,1} \;=\; -\,i\;(2\,\mathbf{b}_e)^{-1}\,\mathbf{n}^{\mathrm{d}}\;E_0^{l1}\;\sin\varpi\,. \tag{3.25b}$$

The constraint (3.14d) implies $F_0^{l,m}=0$ for all $m\in\mathbb{Z}\setminus\{-1,0,1\}$. Adjust B_0^l as indicated in (3.10a), that is in such a way that $B_0^l=-\mathbf{b}_e^{-1}\,\xi\times E_0^l$. In view of Remark 3.1, there remains to look at (3.10b), or equivalently at (3.18). First, with (3.25), we get:

$$-\,\frac{3}{4}\int_0^\pi F_0^{l,1}(\mathbf{t},\mathbf{x},\varpi)\;(\sin\varpi)^2\;d\varpi=\;i\,(2\,\mathbf{b}_e)^{-1}\,\mathbf{n}^{\mathrm{d}}\;E_0^{l1}\,, \tag{3.26a}$$

$$-\,\frac{3}{4}\int_0^\pi 2\;F_0^{l,0}(\mathbf{t},\mathbf{x},\varpi)\;\cos\varpi\;\sin\varpi\;d\varpi=\;i\;\mathbf{b}_e^{-1}\,\mathbf{n}^{\mathrm{d}}\;E_0^{l3}\,. \tag{3.26b}$$

Recalling (3.15), we can define:

$$\mathcal{J}_0^1(F_0^{l,-1}):=\mathcal{J}_0(F_0^{l,-1},0,0)^1=-\,\frac{3}{4}\int_0^\pi F_0^{l,-1}(\mathbf{t},\mathbf{x},\varpi)\;(\sin\varpi)^2\;d\varpi\,.$$

By developing the content of the equation (3.18) with $\tau=\mathbf{b}_e(\mathbf{x})$, and by eliminating E_0^{l2} through the relation $E_0^{l2}=i\,E_0^{l1}$, we get:

$$\Big(|\xi^1|^2+\mathbf{b}_e^2-|\xi|^2+i\,\xi^1\,\xi^2-\frac{\mu^2\,\mathbf{n}^{\mathrm{d}}}{2}\Big)\,E_0^{l1}+\xi^1\,\xi^3\,E_0^{l3}\;=-\,i\,\mu^2\,\mathbf{b}_e\,\mathcal{J}_0^1(F_0^{l,-1})\,, \tag{3.27a}$$

$$\Big(\xi^1\,\xi^2+i\,(|\xi^2\,|^2+\mathbf{b}_e^2-|\xi|^2)-i\,\frac{\mu^2\,\mathbf{n}^{\mathrm{d}}}{2}\Big)\,E_0^{l1}+\xi^2\,\xi^3\,E_0^{l3}\;=-\,\mu^2\,\mathbf{b}_e\,\mathcal{J}_0^1(F_0^{l,-1})\,, \tag{3.27b}$$

$$(\xi^1+i\xi^2)\,\xi^3\,E_0^{l1}+(|\xi^3|^2+\mathbf{b}_e^2-|\xi|^2-\mu^2\,\mathbf{n}^{\mathrm{d}})\,E_0^{l3}\;=\;0\,. \tag{3.27c}$$

The subsystem (3.27a)-(3.27b) is overdetermined. It implies a compatibility condition, which can be exhibited by looking at the combination $i\,(3.27a)+(3.27b)=0$, which is:

$$i\,\Big(2\,\mathbf{b}_e^2-|\xi|^2-|\xi^3|^2-\mu^2\,\mathbf{n}^{\mathrm{d}}\Big)\;E_0^{l1}+(\xi^2+i\,\xi^1)\,\xi^3\,E_0^{l3}=0\,. \tag{3.28}$$

Assuming (3.28), the equations (3.27a) and (3.27b) can be solved by adjusting $\mathcal{J}_0^1(F_0^{l,-1})$ accordingly. It suffices to select adequately some $F_0^{l,-1}(\mathbf{t},\mathbf{x})$ not depending on ϖ. This can be done because no condition on $F_0^{l,-1}(\cdot)$ has been imposed so far.

To conclude, it suffices to observe that the system (3.24) and (3.27c)-(3.28) are equivalent. Indeed, the two first components of (3.24) correspond to the conditions $(1,i,0)\cdot\mathfrak{N}\,E_0^l=0$ and $(i,1,0)\cdot\mathfrak{N}\,E_0^l=0$, and they turn to be $E_0^{l1}+i\,E_0^{l2}=0$ together with (3.28) . On the other hand, the equation (3.27c) is the same as the third component of (3.24). □

Remark 3.2. *The part (E_0^{l1},E_0^{l3}) extracted from the vector $E_0^l\not\equiv 0$ of (3.24) is necessarily such that $(E_0^{l1},E_0^{l3})\not\equiv(0,0)$, and it satisfies (3.27c)-(3.28). This can be achieved if and only if we have:*

$$(|\xi^1|^2+|\xi^2|^2)\;|\xi^3|^2-(2\,\mathbf{b}_e^2-|\xi|^2-|\xi^3|^2-\mu^2\,\mathbf{n}^{\mathrm{d}})\;(\mathbf{b}_e^2-|\xi|^2+|\xi^3|^2-\mu^2\,\mathbf{n}^{\mathrm{d}})=0\,. \tag{3.29}$$

This condition is equivalent to $det\,\mathfrak{N}(\mathbf{x},\mathbf{b}_e(\mathbf{x}),\xi)=0$. *In fact, the left-hand side of (3.29) is exactly* $-i\,\mathbf{b}_e(\mathbf{x})^{-2}\,det\,\mathfrak{N}(\mathbf{x},\mathbf{b}_e(\mathbf{x}),\xi)$.

3.1.4. *The non-singular case* $(\tau\neq 0$ *and* $\tau\neq\pm\mathbf{b}_e(\mathbf{x}))$. This situation is simpler.

Lemma 3.3 (dispersion relations in the non-singular case)**.** *For* $\tau\in\mathbb{R}\setminus\{0,\pm\mathbf{b}_e(\mathbf{x})\}$, *the system (3.6)-(3.10) has a solution* $(\mathcal{F}_0^l,B_0^l,E_0^l)$ *satisfying Assumption 3.1 if and only if the position* $(\mathbf{x},\xi)\in T^*(\Omega)$ *is such that* $det\,\mathfrak{N}(\mathbf{x},\tau,\xi)=0$.

Proof. Remark that:

$$det\;\Sigma(\mathbf{x},\tau)\;=\;i\;\tau\;\left[-\tau^2+\mathbf{b}_e(\mathbf{x})^2\right]. \tag{3.30}$$

A quick look at (3.10) and at the steps 3.1.1⋆) indicates that the condition $det\,\mathfrak{N}(\mathbf{x},\tau,\xi)=0$ is also sufficient to find a solution of (3.4) satisfying Assumption 3.1. □

In the next Paragraph 3.2, we examine more carefully the content of this restriction.

3.2. **The characteristic variety of cold magnetized plasmas.** Readers should refer to the next Paragraph 3.2.1 if there is doubt about notations or definitions. This information will be used repeatedly in what follows. It is also needed when applying Theorem 1.

3.2.1. *Notations and definitions.* With the rescaled version (2.35) of the electron density $\mathbf{n}^d\equiv\mathbf{n}_1^d$ and with $\mu\equiv|\mu_1|$ as in (2.50), introduce:

$$\kappa\equiv\kappa(\mathbf{x}):=\mathbf{n}^{\mathrm{d}}(\mathbf{x})^{1/2}\,\mu\in\mathbb{R}_+^*. \tag{3.31}$$

With $\mathbf{b}_e$ and τ as in (2.27) and (3.5), look at the skew-Hermitian matrix:

$$\Sigma(\mathbf{x},\tau)\;:=\;\begin{pmatrix} i\,\tau & +\mathbf{b}_e(\mathbf{x}) & 0\\ -\mathbf{b}_e(\mathbf{x}) & i\,\tau & 0\\ 0 & 0 & i\,\tau\end{pmatrix},\qquad(\mathbf{x},\tau)\in\Omega\times\mathbb{R}^*. \tag{3.32}$$

With the preceding ingredients, consider the matrix:

$$\mathfrak{N}(\mathbf{x},\tau,\xi):=\Sigma(\mathbf{x},\tau)\,(\,\xi\,{}^t\xi+(\tau^2-|\xi|^2)\,Id\,)-i\,\kappa(\mathbf{x})^2\,\tau\,Id\,. \tag{3.33}$$

As will be seen later, all the values of $(\tau,\xi)\in\mathbb{R}^4\setminus\{0\}$, including the singular cases 3.1.2 and 3.1.3, can be treated together. To this end, however, the variable τ must be factorized from the characteristic polynomial $det\,\mathfrak{N}$. As will be shown in Lemma 3.5, see the definitions (3.50) and (3.51), there exists an explicit function $\chi\in\mathcal{C}^\infty(\Omega\times(\mathbb{R}^4\setminus\{0\}))$ such that:

$$\forall\,(\mathbf{x},\tau,\xi)\in\Omega\times(\mathbb{R}^4\setminus\{0\}),\qquad det\,\mathfrak{N}(\mathbf{x},\tau,{}^tO(\mathbf{x})\,\xi)=\;-i\;\tau\;\chi(\mathbf{x},\tau,\xi). \tag{3.34}$$

The matrix O has been defined at the level of (2.31), while the matrix $\mathfrak{N}$ is given by (3.33) with κ and Σ as in (3.31) and (3.32). For all $\mathbf{x}\in\Omega$, the function $\chi(\mathbf{x},\cdot)$ is polynomial with respect to the dual variables $(\tau,\xi)\in\mathbb{R}^4$. Thus, given $\mathbf{x}\in\Omega$, the zeros of $\chi(\mathbf{x},\cdot)$ define some algebraic variety in $T^*_{(\mathbf{t},\mathbf{x})}M$.

Definition 3.1. *[characteristic variety] The characteristic variety which can be associated with cold magnetized plasmas is the subset* $\mathscr{V}$ *of the cotangent bundle* T^*M *composed of:*

$$\mathscr{V}:=\left\{(\mathbf{t},\mathbf{x},\tau,\xi)\in[0,1]\times\Omega\times(\mathbb{R}^4\setminus\{0\})\,;\,\chi(\mathbf{x},\tau,\xi)=0\right\}. \tag{3.35}$$

The representation (3.35) of $\mathscr{V}$ offers a complete intrinsic vision of the characteristic variety. Now, we can decompose the direction $\xi = {}^tO(\mathbf{x})\,\xi \in \mathbb{R}^3$ of (3.5) in spherical coordinates, as we did for $p \in \mathbb{R}^3$ in Paragraph 2.6.2. With the convention:

$$S_{ph}(r,\omega,\varpi) := {}^t(r\cos\omega\,\sin\varpi\,,\, r\sin\omega\,\sin\varpi\,,\, r\cos\varpi\,)\,, \tag{3.36}$$

we have:

$$\xi = S_{ph}(r,\omega,\varpi)\,, \qquad (r,\omega,\varpi) \in \mathbb{R}_+ \times [0,2\,\pi[\times[0,\pi]\,. \tag{3.37}$$

Note that the couple (ω,ϖ) inside (3.37) differs from the the one of Figure 1. There will be no possible confusion since the decomposition (2.45) of $p \in \mathbb{R}^3$ will no longer be used.

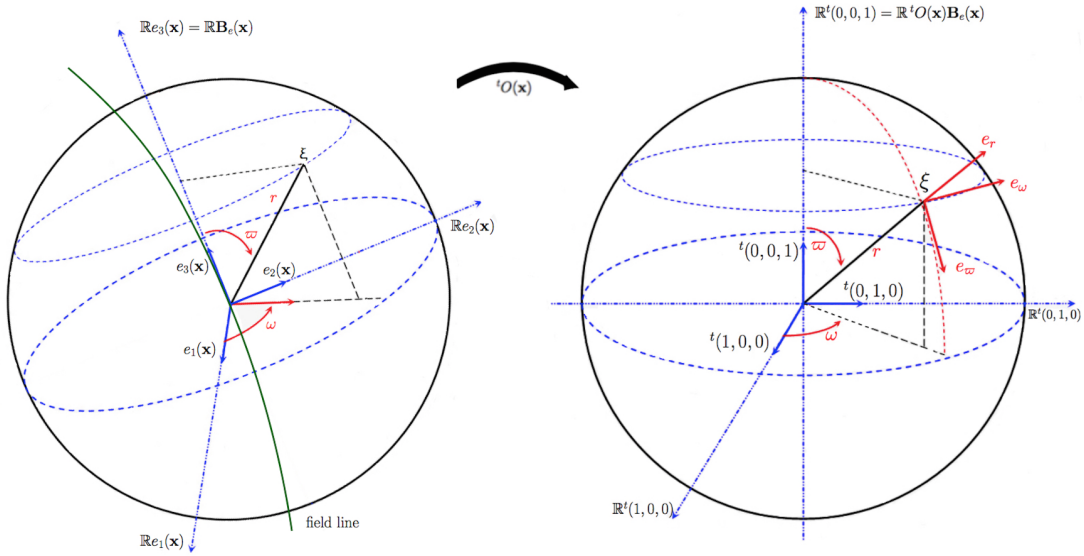

FIGURE 2. Spherical coordinates of $\xi \in \mathbb{R}^3$ after straigntening.

Below, we fix $(\mathbf{t},\mathbf{x}) \in M$ and we introduce useful objects when investigating what happens in the cotangent space $T^*_{(\mathbf{t},\mathbf{x})}M$. According to the forthcoming presentation, the discussion will not directly involve the direction ξ but instead the variable $\xi = {}^tO(\mathbf{x})\,\xi$ through the spherical representation (r,ω,ϖ) of ξ, see the definition (3.36)-(3.37) and Figure 2. In fact, due to some gyrotropic invariance, the angle ω will be almost absent. In particular, the function $\chi(\cdot)$ of Lemma 3.5 does not depend on ω. It remains to deal with (r,ϖ). Now, since the matrix $O(\mathbf{x})$ is orthogonal, there is an obvious link between (r,ϖ) and ξ, namely:

$$r = |\xi| = |\xi|\,, \qquad \varpi = \arctan\Big(\frac{|\xi \times \mathbf{B}_e(\mathbf{x})|}{\xi\cdot\mathbf{B}_e(\mathbf{x})}\Big) = \arctan\Big(\frac{|\xi \times \mathbf{B}_e(\mathbf{x})|}{\xi\cdot\mathbf{B}_e(\mathbf{x})}\Big)\,. \tag{3.38}$$

With (r,ϖ) as in (3.38) and $\chi_{\mathbf{x},\varpi}(\cdot)$ as in (3.50)-(3.51), retain that:

$$\forall\,(\mathbf{x},\tau,\xi) \in \Omega \times (\mathbb{R}^4 \setminus \{0\})\,, \qquad \chi(\mathbf{x},\tau,\xi) = \chi(\mathbf{x},\tau,\xi) = \chi_{\mathbf{x},\varpi}(\tau,r)\,. \tag{3.39}$$

As explained in the introduction, the *characteristic variety* $\mathscr{V}$ can be written:

$$\mathscr{V} := \Big\{ (\mathbf{t},\mathbf{x},\tau,\xi) \in T^*M \,;\, (|\tau|,|\xi|) \in \mathrm{V}(\mathbf{x},\varpi) = \mathrm{V}_o(\mathbf{x},\varpi) \sqcup \mathrm{V}_x(\mathbf{x},\varpi) \Big\}. \tag{3.40}$$

As indicated in (3.40), the subset $\mathrm{V}_o(\mathbf{x},\varpi)$ (for *ordinary* waves) and the subset $\mathrm{V}_x(\mathbf{x},\varpi)$ (for *extraordinary* waves) form some non-trivial partition:

$$\emptyset \subsetneq \mathrm{V}_o(\mathbf{x},\varpi) \subsetneq \mathrm{V}(\mathbf{x},\varpi)\,, \qquad \emptyset \subsetneq \mathrm{V}_x(\mathbf{x},\varpi) \subsetneq \mathrm{V}(\mathbf{x},\varpi)\,, \qquad \mathrm{V}_o(\mathbf{x},\varpi) \cap \mathrm{V}_x(\mathbf{x},\varpi) = \emptyset\,.$$

They can be recovered from Theorem 1 through ingredients $\tau_0^\pm(\cdot)$, $\tau_\infty^\pm(\cdot)$ and $g_\pm(\cdot)$ that are clearly specified in the definitions below.

Definition 3.2. *[cutoff frequencies] The left handed cutoff frequency $\tau_0^-(\cdot)$ and the right handed cutoff frequency $\tau_0^+(\cdot)$ are the two functions $\tau_0^\pm : \Omega \longrightarrow \mathbb{R}_+$ given by:*

$$\tau_0^\pm(\mathbf{x}) := \frac{1}{2}\Big(\pm \mathbf{b}_e(\mathbf{x}) + \sqrt{\mathbf{b}_e(\mathbf{x})^2 + 4\,\kappa(\mathbf{x})^2} \Big)\,, \qquad 0 < \tau_0^- < \tau_0^+\,. \tag{3.41}$$

Definition 3.3. *[resonance frequencies] The lower resonance frequency $\tau_\infty^-(\cdot)$ and the upper resonance frequency $\tau_\infty^+(\cdot)$ are the two functions $\tau_\infty^\pm : \Omega \times [0,\pi] \longrightarrow \mathbb{R}_+$, with $0 \leq \tau_\infty^- \leq \tau_\infty^+$, defined by:*

$$\tau_\infty^\pm(\mathbf{x},\varpi)^2 := \frac{1}{2}\Big(\mathbf{b}_e(\mathbf{x})^2 + \kappa(\mathbf{x})^2 \pm \sqrt{(\mathbf{b}_e(\mathbf{x})^2 + \kappa(\mathbf{x})^2)^2 - 4\,\mathbf{b}_e(\mathbf{x})^2\,\kappa(\mathbf{x})^2\,\cos^2\varpi} \Big)\,. \tag{3.42}$$

Definition 3.4. *[dispersion relations for ordinary waves and extraordinary waves] The links $r^2 = g_\pm(\mathbf{x},\varpi,\tau)$ inside (1.1) involve the (generalized) Appleton-Hartree functions:*

$$g_\pm \,:\, (\Omega \times [0,\pi] \times \mathbb{R}_+) \setminus \{ (\mathbf{x},\varpi,\tau)\,;\, \tau = \tau_\infty^\pm(\mathbf{x},\varpi) \} \longrightarrow \mathbb{R}$$

given by:

$$g_\pm(\mathbf{x},\varpi,\tau) := \frac{\tau^2\ \mathcal{P}(\mathbf{x},\varpi,\tau) \pm \mathbf{b}_e(\mathbf{x})\ \kappa(\mathbf{x})^2\ \sqrt{\mathcal{Q}(\mathbf{x},\varpi,\tau)}}{2\ (\tau^2 - \tau_\infty^+(\mathbf{x},\varpi)^2)\ (\tau^2 - \tau_\infty^-(\mathbf{x},\varpi)^2)}\,, \tag{3.43}$$

where:

$$\begin{aligned} \mathcal{P} &:= ((\tau^2-\kappa^2)^2 - \mathbf{b}_e^2\,\tau^2)\,\sin^2\varpi + (\tau^2-\kappa^2)\,(\tau^2 - \mathbf{b}_e^2 - \kappa^2)\,(1+\cos^2\varpi) \\ &= 2\,(\tau^2-\kappa^2)\,(\tau^2-\kappa^2-\mathbf{b}_e^2) - \mathbf{b}_e^2\,\kappa^2\,\sin^2\varpi\,, \end{aligned} \tag{3.44a}$$

$$\mathcal{Q} := \mathbf{b}_e^2\ \sin^4\varpi\ \tau^4 + 4\,\tau^2\,(\tau^2-\kappa^2)^2\,\cos^2\varpi\,. \tag{3.44b}$$

Retain that all the expressions inside Definitions 3.3 and 3.4 can be interpreted as depending on ξ or ξ. It suffices to exploit (3.38).

3.2.2. *The characteristic variety from the physical viewpoint.* In what follows, we will work in the non-singular case, with $\tau \neq 0$ and with $|\tau| \neq \mathbf{b}_e(\mathbf{x})$. Introduce:

$$\mathfrak{n} := \frac{\xi}{\tau} \in \mathbb{R}^3\,, \qquad \varsigma := \frac{\kappa(\mathbf{x})^2}{\tau^2 - \mathbf{b}_e(\mathbf{x})^2} \in \mathbb{R}\,, \qquad \gamma := \frac{\mathbf{b}_e(\mathbf{x})}{\tau} \in \mathbb{R}^*\,. \tag{3.45}$$

In optics, the following basic notions often come into play.

Definition 3.5. *The refractive index is the vector $\mathfrak{n} \in \mathbb{R}^3$ given by (3.45).*

Definition 3.6. *With ς and γ as in (3.45), the conductivity tensor $\sigma(\cdot)$ is the skew-Hermitian invertible matrix:*

$$\sigma(\mathbf{x},\tau) := -\,\kappa(\mathbf{x})^2\,\Sigma(\mathbf{x},\tau)^{-1} = \begin{pmatrix} i\,\varsigma\,\tau & -\,\gamma\,\varsigma\,\tau & 0 \\ +\,\gamma\,\varsigma\,\tau & i\,\varsigma\,\tau & 0 \\ 0 & 0 & i\,\kappa^2\,\tau^{-1} \end{pmatrix}, \qquad (\mathbf{x},\tau) \in \Omega\times(\mathbb{R}\backslash\{0,\pm\mathbf{b}_e(\mathbf{x})\}).$$

Convections currents resulting from the plasma electrons and ions are usually accounted for the derivation of some *dielectric tensor*.

Definition 3.7. *The relative permittivity $D(\mathbf{x},\tau)$, called sometimes the dielectric tensor, is the Hermitian matrix:*

$$D(\mathbf{x},\tau) \,:=\, Id + i\,\tau^{-1}\,\sigma(\mathbf{x},\tau)\,.$$

In most plasma physics books [11, 27, 33], the presentation of $\mathscr{V}$ is achieved in a way that differs from (3.35). There, the construction of $\mathscr{V}$ is based on the Definitions 3.5, 3.6 and 3.7. Now, to recover (3.35) from $\mathfrak{n}$, σ and D, we can proceed as follows.

Lemma 3.4. *For $\tau \in \mathbb{R} \setminus \{0,\pm\mathbf{b}_e(\mathbf{x})\}$, the condition $(\mathbf{t},\mathbf{x},\tau,\xi) \in \mathscr{V}$ is equivalent to the restriction $det\,\mathfrak{M}(\mathbf{x},\tau,{}^tO(\mathbf{x})\,\xi) = 0$ where:*

$$\mathfrak{M}(\mathbf{x},\tau,\xi) := \mathfrak{n}\,{}^t\mathfrak{n} + (1-|\mathfrak{n}|^2)\,Id + i\,\tau^{-1}\,\sigma(\mathbf{x},\tau) = \mathfrak{n}\,{}^t\mathfrak{n} - |\mathfrak{n}|^2\,Id + D(\mathbf{x},\tau)\,. \tag{3.46}$$

Proof. Let us start by computing the determinant:

$$det\,\Sigma(\mathbf{x},\tau) \;=\; i\;\tau\;\left[-\,\tau^2 + \mathbf{b}_e(\mathbf{x})^2\right]. \tag{3.47}$$

Thus, for $\tau \in \mathbb{R} \setminus \{0,\pm\mathbf{b}_e(\mathbf{x})\}$, the matrix $\Sigma(\mathbf{x},\tau)$ is invertible. By construction, we have:

$$\mathfrak{N}(\mathbf{x},\tau,\xi) = \tau^2\;\Sigma(\mathbf{x},\tau)\;\mathfrak{M}(\mathbf{x},\tau,\xi)\,. \tag{3.48}$$

Combining (3.34), (3.35) and (3.47), this explains the result. □

The function $\mathfrak{M}(\cdot)$ of physicists is clearly not defined for the values $\tau = 0$ and $\tau = \pm\mathbf{b}_e(\mathbf{x})$. By contrast, the function $\chi(\cdot)$ is defined and smooth everywhere, while containing as much information. That is why the use of $\chi(\cdot)$ is mathematically more suitable.

Lemma 3.5. *There exists a function $\chi(\cdot) \in \mathcal{C}^\infty(\Omega \times (\mathbb{R}^4 \setminus \{0\}))$ such that:*

$$det\,\mathfrak{M}(\mathbf{x},\tau,\xi) = \frac{\chi(\mathbf{x},\tau,\xi)}{\tau^6\,(\tau^2 - \mathbf{b}_e(\mathbf{x})^2)}\,. \tag{3.49}$$

The function $\chi(\cdot)$ does not depend on the angle $\omega \in [0, 2\,\pi[$. Given $(\mathbf{x},\varpi) \in \Omega \times [0,\pi]$, it can be put in the form $\chi(\mathbf{x},\tau,\xi) = \chi_{\mathbf{x},\varpi}(\tau,|\xi|)$, where $\chi(\mathbf{x},\cdot)$ is polynomial in (τ,ξ) whereas $\chi_{\mathbf{x},\varpi}(\cdot)$ is a bivariate polynomial in $(\tau,|\xi|)$. More precisely, written as a polynomial in $|\xi|$, the function $\chi_{\mathbf{x},\varpi}(\tau,\cdot)$ is biquadrattic:

$$\chi_{\mathbf{x},\varpi}(\tau,|\xi|) = \mathcal{A}_{\mathbf{x},\varpi}(\tau)\;|\xi|^4 - \mathcal{B}_{\mathbf{x},\varpi}(\tau)\;|\xi|^2 + \mathcal{C}_{\mathbf{x}}(\tau)\,. \tag{3.50}$$

The coefficients $\mathcal{A}_{\mathbf{x},\varpi}(\cdot)$, $\mathcal{B}_{\mathbf{x},\varpi}(\cdot)$ and $\mathcal{C}_{\mathbf{x}}(\cdot)$ are in $\mathbb{R}[\tau]$, given by the explicit formulas:

$$\mathcal{A}_{\mathbf{x},\varpi}(\tau) := \tau^4 - \tau^2\ \big(\mathbf{b}_e(\mathbf{x})^2 + \kappa(\mathbf{x})^2\big) + \mathbf{b}_e(\mathbf{x})^2\ \kappa(\mathbf{x})^2\ \cos^2\varpi \tag{3.51a}$$
$$= (\tau^2 - \kappa(\mathbf{x})^2)\ (\tau^2 - \mathbf{b}_e(\mathbf{x})^2) - \mathbf{b}_e(\mathbf{x})^2\ \kappa(\mathbf{x})^2\ \sin^2\varpi\,,$$

$$\mathcal{B}_{\mathbf{x},\varpi}(\tau) := \tau^2\ \Big[\big((\tau^2 - \kappa(\mathbf{x})^2)^2 - \mathbf{b}_e(\mathbf{x})^2\ \tau^2\big)\ \sin^2\varpi \tag{3.51b}$$
$$+ (\tau^2 - \kappa(\mathbf{x})^2)\ (\tau^2 - \mathbf{b}_e(\mathbf{x})^2 - \kappa(\mathbf{x})^2)(1 + \cos^2\varpi)\Big] = \tau^2\,\mathcal{P}\,,$$

$$\mathcal{C}_{\mathbf{x}}(\tau) := \tau^2\ (\tau^2 - \kappa(\mathbf{x})^2)\,\big((\tau^2 - \kappa(\mathbf{x})^2)^2 - \mathbf{b}_e(\mathbf{x})^2\ \tau^2\big)\,. \tag{3.51c}$$

Proof. First, note that:

$$\gamma^2\,\varsigma + 1 - \varsigma = \frac{\tau^2 - \kappa^2}{\tau^2}\,, \qquad (1-\varsigma)^2 - \gamma^2\,\varsigma^2 = \frac{(\tau^2 - \kappa^2)^2 - \mathbf{b}_e^2\ \tau^2}{\tau^2\,(\tau^2 - \mathbf{b}_e^2)}\,. \tag{3.52}$$

The computation of $det\,\mathfrak{M}(\mathbf{x},\tau,\xi)$ is completely similar to the calculus of R. Fitzpatrick, see the line (4.43) at page 94 of [11]:

$$det\,\mathfrak{M}(\mathbf{x},\tau,\xi) = \mathfrak{a}_{\mathbf{x},\varpi}(\tau)\ |\mathfrak{n}|^4 - \mathfrak{b}_{\mathbf{x},\varpi}(\tau)\ |\mathfrak{n}|^2 + \mathfrak{c}_{\mathbf{x}}(\tau)\,, \tag{3.53}$$

where:

$$\mathfrak{a}_{\mathbf{x},\varpi} := (1-\varsigma)\,\sin^2\varpi + (\gamma^2\,\varsigma + 1 - \varsigma)\,\cos^2\varpi\,, \tag{3.54a}$$
$$\mathfrak{b}_{\mathbf{x},\varpi} := \big((1-\varsigma)^2 - \gamma^2\,\varsigma^2\big)\,\sin^2\varpi + (1-\varsigma)\ (\gamma^2\,\varsigma + 1 - \varsigma)\,(1 + \cos^2\varpi)\,, \tag{3.54b}$$
$$\mathfrak{c}_{\mathbf{x}} := (\gamma^2\,\varsigma + 1 - \varsigma)\,\big((1-\varsigma)^2 - \gamma^2\,\varsigma^2\big)\,. \tag{3.54c}$$

Then, with (3.52) and the definitions of $\mathfrak{n}$, γ and ς from (3.45), it suffices to write (3.53) as a rational fraction in powers of τ to get the result from Lemma 3.5. □

The restriction $\chi_{\mathbf{x},\varpi}(\tau,|\xi|) = 0$ inside (3.35) can be handled as a quadratic equation to be solved for $|\xi|^2$, with discriminant $\Delta := \mathcal{B}^2 - 4\,\mathcal{A}\,\mathcal{C}$. As a consequence of Lemma 3.6 below, the corresponding roots prove to be (positive, negative or zero) *real* numbers.

Lemma 3.6. *The discriminant*

$$\Delta(\mathbf{x},\varpi,\tau) := \mathcal{B}_{\mathbf{x},\varpi}(\tau)^2 - 4\,\mathcal{A}_{\mathbf{x},\varpi}(\tau)\,\mathcal{C}_{\mathbf{x}}(\tau)\,, \tag{3.55}$$

can be put in the form:

$$\Delta = \mathbf{b}_e^2\ \kappa^4\ \mathcal{Q}\,, \qquad \mathcal{Q} := \tau^2\ \big[\,4\,(\tau^2 - \kappa^2)^2\ \cos^2\varpi + \tau^2\ \mathbf{b}_e^2\ \sin^4\varpi\,\big]\,. \tag{3.56}$$

The function $\mathcal{Q}(\cdot)$ is defined as in (3.44b). It is clearly non-negative. It vanishes if and only if $\tau = 0$ or if $(\tau,\varpi) = (\kappa, 0)$.

Proof. It follows from the second formulas listed in (3.51). When computing Δ, it suffices to identify the terms which are in factor of the different powers of $\sin^2\varpi$. □

3.2.3. *The physical motivations behind the study of the characteristic variety.* Looking at the set $\mathscr{V} \subset T^*M$ is interesting because we can send or receive information only by using points (τ, ξ) in the phase space T^*M which are microlocalized inside $\mathscr{V}$.

Lemma 3.7. *A necessary and sufficient condition to find solutions $\mathcal{U}_0^l$ to the system (3.4), with some non-trivial electromagnetic part $(E_0^l, B_0^l) \not\equiv 0$ satisfying Assumption 3.1, is to impose the eikonal equation:*

$$(\mathbf{t}, \mathbf{x}, l\,\partial_{\mathbf{t}}\phi(\mathbf{t}, \mathbf{x}), l\,\nabla_{\mathbf{x}}\phi(\mathbf{t}, \mathbf{x})) \in \mathscr{V}, \qquad \forall\,(\mathbf{t}, \mathbf{x}) \in M\,. \tag{3.57}$$

Proof. When $\tau \in \mathbb{R}^*$, in view of (3.34), the condition (3.57) is equivalent to:

$$det\,\mathfrak{N}(\mathbf{x}, l\,\partial_{\mathbf{t}}\phi(\mathbf{t}, \mathbf{x}), l\,{}^tO(\mathbf{x})\,\nabla_{\mathbf{x}}\phi(\mathbf{t}, \mathbf{x})) = 0\,. \tag{3.58}$$

Now, from Paragraphs 3.1.4 and 3.1.3, we know that (3.58) is a NSC.

In the stationary case, when $\tau = 0$, Paragraph 3.1.2 says that $\xi^3 = 0$ or equivalently that $\varpi = \pi/2$ is a NSC. Thus, it suffices to show that the restriction (3.35), that is:

$$\chi(\mathbf{x}, 0, \xi) = \chi(\mathbf{x}, 0, l\,\nabla_{\mathbf{x}}\phi(\mathbf{t}, \mathbf{x})) = \chi_{\mathbf{x},\varpi}(0, |\xi|) = 0 \tag{3.59}$$

can be realized if and only if $\varpi = \pi/2$. With (3.51), just remark that:

$$\mathcal{A}_{\mathbf{x},\varpi}(0) = \mathbf{b}_e(\mathbf{x})^2\ \kappa(\mathbf{x})^2\ \cos^2\varpi\,, \qquad \mathcal{B}_{\mathbf{x},\varpi}(0) = 0\,, \qquad \mathcal{C}_{\mathbf{x}}(0) = 0\,,$$

so that:

$$\chi_{\mathbf{x},\varpi}(0, |\xi|) = \mathbf{b}_e(\mathbf{x})^2\ \kappa(\mathbf{x})^2\ \cos^2\varpi\ |\xi|^4\,.$$

Since $|\xi| \neq 0$, we must have $\cos\varpi = 0$, that is $\varpi = \pi/2$ as required.

□

3.2.4. *Some geometrical interpretation of the characteristic variety.* Consider the cone:

$$\mathscr{C}(\varpi) := \{\, r\ {}^t(\cos\omega\,\sin\varpi, \sin\omega\,\sin\varpi, \cos\varpi)\,;\,(r, \omega) \in \mathbb{R}_+ \times [0, 2\,\pi]\,\}\,.$$

The set $\mathscr{V}$ can be viewed as the union of disjoint subsets:

$$\mathscr{V} = \cup\,\{(\mathbf{t}, \mathbf{x}, \mathscr{V}_{\mathbf{x}}^*)\,;\,(\mathbf{t}, \mathbf{x}) \in M\}\,, \qquad \mathscr{V}_{\mathbf{x}}^* := \cup\,\{\mathscr{V}^*(\mathbf{x}, \varpi)\,;\,\varpi \in [0, \pi]\} \subset T^*_{(\mathbf{t},\mathbf{x})}M\,.$$

Thereby, the set $\mathscr{V}_{\mathbf{x}}^*$ is the section above the position $(\mathbf{t}, \mathbf{x}) \in M$ of the characteristic variety $\mathscr{V}$. It is contained in the four dimensional cotangent fiber $T^*_{(\mathbf{t},\mathbf{x})}M \equiv \mathbb{R}^4$. Its form does not depend on $\mathbf{t} \in [0, 1]$. Now, the refined subset $\mathscr{V}^*(\mathbf{x}, \varpi)$ is obtained by further fixing ϖ, namely:

$$\mathscr{V}^*(\mathbf{x}, \varpi) := \{(\tau, \xi) \in \mathbb{R}^4 \setminus \{0\}\,;\,(\tau, \xi) \in \mathscr{V}_{\mathbf{x}}^*\,,\ \xi \in \mathscr{C}(\varpi)\} \subset T^*_{(\mathbf{t},\mathbf{x})}M\,.$$

With S_{ph} as in (3.36), we can fix $(\mathbf{x}, \varpi) \in \Omega \times [0, \pi]$, and define(we will do not mark the star $*$ at the level of V):

$$\mathrm{V}(\mathbf{x}, \varpi) := \{(\tau, r) \in \mathbb{R}_+ \times \mathbb{R}_+\,;\,(\tau, S_p(r, 0, \varpi)) \in \mathscr{V}^*(\mathbf{x}, \varpi)\}\,. \tag{3.60}$$

With ξ as in (3.37), the coefficients $\mathcal{A}$, $\mathcal{B}$ and $\mathcal{C}$ depend only on $\mathbf{x}$, τ^2 and ϖ. Thus, starting from $\mathrm{V}(\mathbf{x}, \varpi)$, we can recover the whole section $\mathscr{V}^*(\mathbf{x}, \varpi)$ by rotations:

$$\mathscr{V}^*(\mathbf{x}, \varpi) = \{(\tau, S_p(r, \omega, \varpi))\,;\,(|\tau|, r) \in \mathrm{V}(\mathbf{x}, \varpi)\,,\ \omega \in [0, 2\,\pi[\,\}\,. \tag{3.61}$$

This rotational invariance can be clearly seen in Figures 10, 11, 12 and 13. By this way, the issue reduces to the study of $\mathrm{V}(\mathbf{x},\varpi)$, which is generically a one-dimensional subset of the quadrant $\mathbb{R}_+\times\mathbb{R}_+$. Note also that the coefficients $\mathcal{A}$ and $\mathcal{B}$ satisfy:

$$\mathcal{A}_{\mathbf{x},\varpi}(\tau)=\mathcal{A}_{\mathbf{x},\pi-\varpi}(\tau)\,,\qquad \mathcal{B}_{\mathbf{x},\varpi}(\tau)=\mathcal{B}_{\mathbf{x},\pi-\varpi}(\tau)\,,\qquad \forall\,(\mathbf{x},\tau,\varpi)\in\Omega\times\mathbb{R}\times[0,\pi[\,.$$

This brief discussion can be summarized in a remark.

Remark 3.3. *All the geometrical information is provided by the intersection of $\mathscr{V}^*_{\mathbf{x}}$ with the quadrant of an hyperplane. More precisely, we can focus on:*

$$\mathscr{V}^*_{\mathbf{x}}\cap\big\{\,(\tau,\xi)\in\mathbb{R}^4\,;\,0<\tau\,,\,\xi^1=0\,,\,0<\xi^3\,\big\}\subset T^*_{(\mathbf{t},\mathbf{x})}M\,,$$

and then recover the whole set $\mathscr{V}^*_{\mathbf{x}}$ by changing $\tau\in\mathbb{R}_+$ into $-\tau$, by replacing $\xi^3\in\mathbb{R}_+$ by $-\xi^3$, and by applying rotations with axis $\mathbb{R}\,^t(0,0,1)$ and angles $\omega\in[0,2\,\pi[$. This means also that, in practice, we can restrict our attention to the case $(\tau,\varpi)\in\mathbb{R}_+\times[0,\pi/2]$.

Lemma 3.6 indicates that the situation $\varpi=0$ (existence of a double root when $\tau=\kappa$) and the other cases $\varpi\in]0,\frac{\pi}{2}]$ must be distinguished. In plasma physics books, the two values $\varpi=0$ and $\varpi=\frac{\pi}{2}$ are usually studied separately, and they are exploited to obtain a classification of waves. However, this viewpoint does not give access to a complete vision of the characteristic variety $\mathscr{V}$. In what follows, we will rather consider that the generic situation is when $\varpi\in]0,\frac{\pi}{2}[$, while the two cases $\varpi=0$ and $\varpi=\frac{\pi}{2}$ can be recovered as (very special) endpoints.

3.3. **Parallel, oblique and perpendicular propagation.** In the next Paragraph 3.3.1, we recall what happens when dealing with the case of *parallel* ($\varpi=0(\pi)$) *non-resonant* ($|\tau|\neq\mathbf{b}_e(\mathbf{x})$) propagation. The general situation of *oblique* ($\varpi\neq0(\pi)$) propagation is detailed after, in Paragraph 3.3.2. Then, we will come back to the parallel case $\varpi=0$ (in Paragraph 3.3.3) and to the *perpendicular* case $\varpi=\frac{\pi}{2}$ (in Paragraph 3.3.4). Finally, there are different ways to describe $\mathscr{V}^*_{\mathbf{x}}$. We can either study what occurs for a fixed value of $\varpi\in[0,\frac{\pi}{2}]$, as above when involving $\mathscr{V}^*(\mathbf{x},\varpi)$,. Or we can set the value of $\xi\in\mathbb{R}^3$ (see Paragraph 3.4.3) or of $\tau\in\mathbb{R}$ (see Paragraph 3.4.2).

3.3.1. *Parallel* ($\varpi=0(\pi)$) *non-singular* ($\tau\in\mathbb{R}^*_+\setminus\{\mathbf{b}_e(\mathbf{x})\}$) *propagation.* The matter here is to study the equation $\chi_{\mathbf{x},0}(\tau,|\xi|)=0$, which is simply:

$$\begin{aligned}(\tau^2-\kappa^2)\,\Big[(\tau^2-\mathbf{b}_e^2)\,|\xi|^4-2\,\tau^2\,(\tau^2-\mathbf{b}_e^2-\kappa^2)\,|\xi|^2\\ +\tau^2\,\big((\tau^2-\kappa^2)^2-\mathbf{b}_e^2\,\tau^2\big)\Big]\;=\;0\,.\end{aligned}\tag{3.62}$$

Either we have $\tau^2-\kappa^2=0$ or $Z=|\xi|^2$ must be subjected to:

$$(\tau^2-\mathbf{b}_e^2)\,Z^2-2\,\tau^2\,(\tau^2-\mathbf{b}_e^2-\kappa^2)\,Z+\tau^2\,\big((\tau^2-\kappa^2)^2-\mathbf{b}_e^2\,\tau^2\big)=0\,.$$

Since $|\tau|\neq\mathbf{b}_e(\mathbf{x})$, this quadratic equation has two roots $Z_1(\mathbf{x},\tau)$ and $Z_2(\mathbf{x},\tau)$ given by:

$$Z_1(\mathbf{x},\tau):=\frac{\tau^2\,(\tau^2-\mathbf{b}_e^2-\kappa^2)+\mathbf{b}_e\,\kappa^2\,\tau}{\tau^2-\mathbf{b}_e^2}\,,\qquad Z_2(\mathbf{x},\tau):=\frac{\tau^2\,(\tau^2-\mathbf{b}_e^2-\kappa^2)-\mathbf{b}_e\,\kappa^2\,\tau}{\tau^2-\mathbf{b}_e^2}\,.$$

The set $\mathrm{V}(\mathbf{x},0)$ is usually (see for instance [11]-chapter 4) separated into connected parts, corresponding to the different possibilities marked above.

a) Parallel *left-handed* circularly polarized wave ($|\xi|^2 = Z_1(\mathbf{x},\tau)$). Knowing that $\tau \in \mathbb{R}_+^*$, this can be achieved for some $|\xi| \in \mathbb{R}_+$ if and only if:

$$0 \le Z_1(\mathbf{x},\tau) = \frac{\tau\,(\tau^2 + \mathbf{b}_e\,\tau - \kappa^2)}{\tau + \mathbf{b}_e} \quad \Longleftrightarrow \quad \tau_0^-(\mathbf{x}) \le \tau\,. \tag{3.63}$$

We find only one connected component:

$$\mathrm{V}_l(\mathbf{x},0) \;=\; \Big\{\,(\tau,r) \in \mathbb{R}_+ \times \mathbb{R}_+\,;\,\tau_0^- \le \tau\,,\; r^2 = \tau^2 - \kappa(\mathbf{x})^2\,\tau/(\tau + \mathbf{b}_e(\mathbf{x}))\,\Big\}\,. \tag{3.64}$$

b) Parallel *right-handed* circularly polarized wave ($|\xi|^2 = Z_2(\mathbf{x},\tau)$). Knowing that $\tau \in \mathbb{R}_+^*$, this can be achieved for some $|\xi| \in \mathbb{R}_+$ if and only if:

$$0 \le Z_2(\mathbf{x},\tau) = \frac{\tau\,(\tau^2 - \mathbf{b}_e\,\tau - \kappa^2)}{\tau - \mathbf{b}_e} \quad \Longleftrightarrow \quad 0 < \tau < \mathbf{b}_e \;\text{ or }\; \tau_0^+(\mathbf{x}) \le \tau\,. \tag{3.65}$$

Accordingly, the set $\mathrm{V}_r(\mathbf{x},0)$ can be split into two connected parts $\mathrm{V}_r^-(\mathbf{x},0)$ and $\mathrm{V}_r^+(\mathbf{x},0)$ which are distinguished below.

b.1) The first part $\mathrm{V}_r^-(\mathbf{x},0)$ contains both the dispersion relation for *Alfvèn* waves (values of τ such that $0 \lesssim \tau$) and the dispersion relation for *whistler* (or *electron cyclotron*) waves (values of τ such that $\tau \lesssim \mathbf{b}_e$):

$$\mathrm{V}_r^-(\mathbf{x},0) := \Big\{(\tau,r)\,;\,0 < \tau < \mathbf{b}_e(\mathbf{x})\,,\;0 < r\,,\;r^2 = \tau^2 - \kappa(\mathbf{x})^2\,\tau/(\tau - \mathbf{b}_e(\mathbf{x}))\,\Big\}\,. \tag{3.66}$$

b.2) The second is the standard right-handed circularly polarized wave:

$$\mathrm{V}_r^+(\mathbf{x},0) := \Big\{(\tau,r)\,;\,\tau_0^+(\mathbf{x}) \le \tau\,,\;0 < r\,,\;r^2 = \tau^2 - \kappa(\mathbf{x})^2\,\tau/(\tau - \mathbf{b}_e(\mathbf{x}))\,\Big\}\,. \tag{3.67}$$

c) Parallel longitudinal wave or *electrostatic* plasma wave ($\tau = \kappa$). With κ as in (3.31), this means a link between τ and $\mathbf{x}$, whereas no condition is imposed on $|\xi|$. We find the vertical half-line $\mathrm{V}_0(\mathbf{x},0) := \{(\kappa,r)\,;\,r \in \mathbb{R}_+\,\}$.

Briefly, retain that:

$$\mathrm{V}(\mathbf{x},0) = \mathrm{V}_l(\mathbf{x},0) \cup \mathrm{V}_r^-(\mathbf{x},0) \cup \mathrm{V}_r^+(\mathbf{x},0) \cup \mathrm{V}_0(\mathbf{x},0)\,. \tag{3.68}$$

The corresponding curves are represented on Figure 3 below:

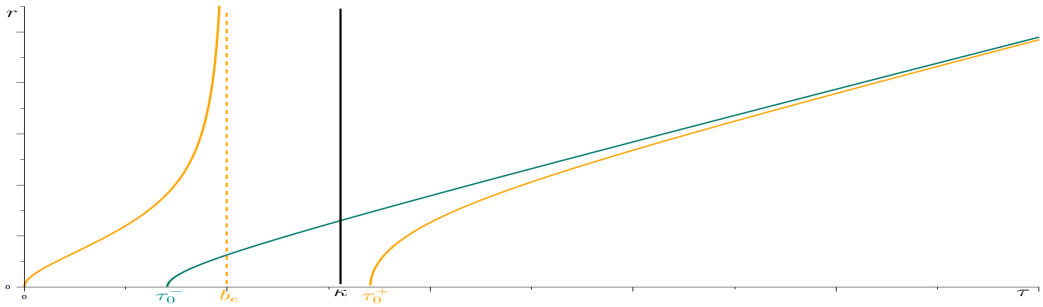

FIGURE 3. Parallel propagation ($\varpi = 0$). Standard nomenclature.
$\mathrm{V}_r(\mathbf{x},0)$ (in orange), $\mathrm{V}_l(\mathbf{x},0)$ (in blue-green) and $\mathrm{V}_0(\mathbf{x},0)$ (in black).

3.3.2. *Oblique ($\varpi \in]0, \frac{\pi}{2}]$) non-singular ($\tau \in \mathbb{R}_+^* \setminus \{\mathbf{b}_e(\mathbf{x})\}$) propagation.* We first study the coefficient $\mathcal{A}$ which is in factor of $|\xi|^4$ in the equation $\chi_{\mathbf{x},\varpi}(\tau, |\xi|) = 0$.

Lemma 3.8. *With $\tau_\infty^\pm(\cdot)$ as in (3.42), we have:*

$$\mathcal{A}_{\mathbf{x},\varpi}(\tau) = (\tau^2 - \tau_\infty^-(\mathbf{x},\varpi)^2)\ (\tau^2 - \tau_\infty^+(\mathbf{x},\varpi)^2)\,. \tag{3.69}$$

Proof. This follows from direct calculations. □

For $\tau \neq \tau_\infty^\pm$, as a consequence of Lemma 3.6, the equation $\chi_{\mathbf{x},\varpi}(\tau, |\xi|) = 0$ has two distinct real solutions which can be described by:

$$|\xi|^2 = g_\pm(\mathbf{x},\varpi,\tau) = \frac{\mathcal{B} \pm \mathbf{b}_e\, \kappa^2\, \sqrt{\mathcal{Q}}}{2\ \mathcal{A}} = \frac{2\ \mathcal{C}}{\mathcal{B} \mp \mathbf{b}_e\, \kappa^2\, \sqrt{\mathcal{Q}}}\,. \tag{3.70}$$

When $g_\pm(\mathbf{x},\varpi,\tau) < 0$, there is no mathematical solution. The associated waves are usually considered to be evanescent. On the contrary, when $0 \leq g_\pm(\mathbf{x},\varpi,\tau)$, the condition (3.70) is achieved for some $|\xi| \in \mathbb{R}_+$. This means that a wave can be propagated. To distinguish between these two situations, we have to study the functions $g_\pm(\mathbf{x},\varpi,\cdot)$. To illustrate the following discussion, we can directly plot the graphs of the functions $g_\pm(\mathbf{x},\varpi,\cdot)$. The content of Figures 4 and 5 is justified below.

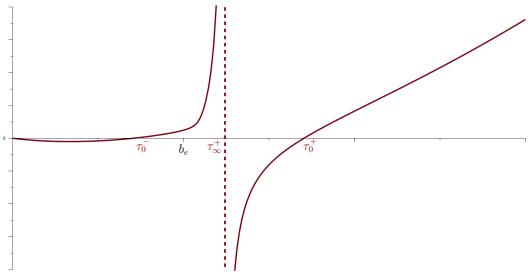

FIGURE 4. Graph of $g_-(\mathbf{x},\varpi,\cdot)$.

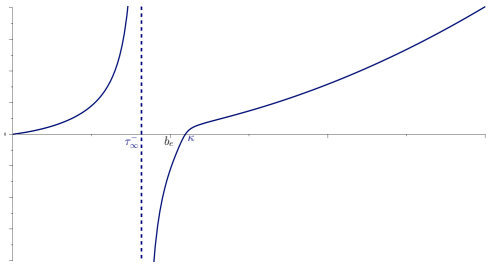

FIGURE 5. Graph of $g_+(\mathbf{x},\varpi,\cdot)$.

Lemma 3.9. *[properties of the functions $\tau_\infty^\pm(\mathbf{x},\cdot)$] For all $\mathbf{x} \in \Omega$, the function $\tau_\infty^+(\mathbf{x},\cdot)$ is strictly increasing on the interval $[0,\pi/2]$, and it satisfies:*

$$\tau_\infty^+(\mathbf{x},0) = \max\big(\,\mathbf{b}_e(\mathbf{x})\,;\,\kappa(\mathbf{x})\,\big)\,, \qquad \tau_\infty^+(\mathbf{x},\pi/2) = \sqrt{\mathbf{b}_e(\mathbf{x})^2 + \kappa(\mathbf{x})^2}\,. \tag{3.71}$$

For all $\mathbf{x} \in \Omega$, the function $\tau_\infty^-(\mathbf{x},\cdot)$ is strictly decreasing on $[0,\pi/2]$, with:

$$\tau_\infty^-(\mathbf{x},0) = \min\big(\,\mathbf{b}_e(\mathbf{x})\,;\,\kappa(\mathbf{x})\,\big)\,, \qquad \tau_\infty^-(\mathbf{x},\pi/2) = 0\,. \tag{3.72}$$

Proof. By direct calculation. □

Lemma 3.10. *[comparison of resonance and cutoff frequencies] If $\sqrt{2}\ \mathbf{b}_e(\mathbf{x}) < \kappa(\mathbf{x})$, we have:*

$$\tau_\infty^-(\mathbf{x},\varpi) < \tau_0^-(\mathbf{x})\,, \qquad \forall\,(\mathbf{x},\varpi) \in \Omega \times [0,\pi]\,. \tag{3.73}$$

If $\kappa(\mathbf{x}) < \sqrt{2}\ \mathbf{b}_e(\mathbf{x})$, we have $\tau_0^-(\mathbf{x}) < \mathbf{b}_e(\mathbf{x})$ and $\tau_0^-(\mathbf{x}) < \tau_\infty^-(\mathbf{x},0)$. Moreover:

$$\tau_0^-(\mathbf{x}) < \tau_\infty^+(\mathbf{x},\varpi) < \tau_0^+(\mathbf{x})\,, \qquad \forall\,(\mathbf{x},\varpi) \in \Omega \times [0,\pi]\,. \tag{3.74}$$

Proof. Assume that $\sqrt{2}\ \mathbf{b}_e(\mathbf{x}) < \kappa(\mathbf{x})$. In view of (3.72), to get (3.73), it suffices to note that:

$$\tau_\infty^-(\mathbf{x},0) = \frac{1}{2}\Big(-\mathbf{b}_e + \sqrt{\mathbf{b}_e^2 + 8\,\mathbf{b}_e^2}\Big) < \frac{1}{2}\Big(-\mathbf{b}_e + \sqrt{\mathbf{b}_e^2 + 4\,\kappa^2}\Big) = \tau_0^-(\mathbf{x})\,.$$

The other comparisons follow from straightforward computations. □

Lemma 3.11. *Fix $(\mathbf{x},\varpi) \in \Omega \times [0,\frac{\pi}{2}]$. The functions $g_+(\mathbf{x},\varpi,\cdot)$ and $g_-(\mathbf{x},\varpi,\cdot)$ of (3.43) are of class C^∞ respectively on the domains $\mathbb{R}_+ \setminus \{\tau_\infty^-(\mathbf{x},\varpi)\}$ and $\mathbb{R}_+ \setminus \{\tau_\infty^+(\mathbf{x},\varpi)\}$.*

Proof. With the expressions given in Definition 3.4, the functions $g_\pm(\mathbf{x},\varpi,\cdot)$ are clearly of class C^∞ on $\mathbb{R}_+ \setminus \{\tau_\infty^+(\mathbf{x},\varpi), \tau_\infty^-(\mathbf{x},\varpi)\}$. Moreover, using the right part of (3.70), they can be written in the form:

$$g_\pm(\mathbf{x},\varpi,\tau) = \frac{2\ \tau^2\ (\tau^2-\kappa^2)\ ((\tau^2-\kappa^2)^2 - \mathbf{b}_e^2\,\tau^2)}{\tau^2\,\mathcal{P}(\varpi,\tau) \mp \sqrt{\mathbf{b}_e^2\,\kappa^4\,\mathcal{Q}(\varpi,\tau)}}\,. \tag{3.75}$$

The difficulty is to show that $g_\pm(\mathbf{x},\varpi,\cdot)$ is well defined and smooth near $\tau_\infty^\pm(\mathbf{x},\varpi)$. To this end, we have to examine more precisely the denominator in (3.75). First, combining (3.51b), (3.51c) and (3.69), the term $\Delta = \mathbf{b}_e^2\,\kappa^4\,\mathcal{Q}$ of (3.56) can be written in the form:

$$\Delta = \tau^4\ \mathcal{P}^2 - 4\ \tau^2\ (\tau^2 - (\tau_\infty^+)^2)\ (\tau^2 - (\tau_\infty^-)^2)\ (\tau^2-\kappa^2)\ ((\tau^2-\kappa^2)^2 - \mathbf{b}_e^2\,\tau^2)\,.$$

For $\tau = \tau_\infty^\pm$, it follows that:

$$(\tau_\infty^\pm)^2\ \mathcal{P}(\mathbf{x},\varpi,\tau_\infty^\pm) \mp \sqrt{\mathbf{b}_e^2\,\kappa^4\,\mathcal{Q}(\mathbf{x},\varpi,\tau_\infty^\pm)} = (\tau_\infty^\pm)^2\,(\mathcal{P}(\mathbf{x},\varpi,\tau_\infty^\pm) \mp |\mathcal{P}(\mathbf{x},\varpi,\tau_\infty^\pm)|)\,.$$

In view of the second formulas in (3.44a) and (3.51a), we have:

$$\begin{aligned}\mathcal{P}(\mathbf{x},\varpi,\tau) &= \mathcal{A} + (\tau^2-\kappa^2)\,(\tau^2 - \mathbf{b}_e^2 - 2\,\kappa^2)\\ &= (\tau^2-(\tau_\infty^+)^2)\,(\tau^2-(\tau_\infty^-)^2) + (\tau^2-\kappa^2)\,(\tau^2-\mathbf{b}_e^2-2\,\kappa^2)\,.\end{aligned} \tag{3.76}$$

From (3.76) and Lemma 3.9, we can easily deduce that:

$$\mathcal{P}(\mathbf{x},\varpi,\tau_\infty^+) = ((\tau_\infty^+)^2-\kappa^2)\,((\tau_\infty^+)^2 - (\mathbf{b}_e^2+2\,\kappa^2)) < 0\,, \tag{3.77a}$$

$$\mathcal{P}(\mathbf{x},\varpi,\tau_\infty^-) = ((\tau_\infty^-)^2-\kappa^2)\,((\tau_\infty^-)^2 - (\mathbf{b}_e^2+2\kappa^2)) > 0\,. \tag{3.77b}$$

And therefore:

$$(\tau_\infty^+)^2\ \mathcal{P}(\mathbf{x},\varpi,\tau_\infty^+) - \sqrt{\mathbf{b}_e^2\,\kappa^4\,\mathcal{Q}(\mathbf{x},\varpi,\tau_\infty^+)} = 2\ (\tau_\infty^+)^2\ \mathcal{P}(\mathbf{x},\varpi,\tau_\infty^+) < 0\,, \tag{3.78a}$$

$$(\tau_\infty^-)^2\ \mathcal{P}(\mathbf{x},\varpi,\tau_\infty^-) + \sqrt{\mathbf{b}_e^2\,\kappa^4\,\mathcal{Q}(\mathbf{x},\varpi,\tau_\infty^-)} = 2\ (\tau_\infty^-)^2\ \mathcal{P}(\mathbf{x},\varpi,\tau_\infty^-) > 0\,. \tag{3.78b}$$

This means that the denominator of (3.75) does not vanish. This gives the conclusion. □

Lemma 3.12. *[zeros of the functions $g_\pm(\mathbf{x},\varpi,\cdot) : \mathbb{R}_+ \setminus \{\tau_\infty^\mp(\mathbf{x},\varpi)\} \longrightarrow \mathbb{R}$]*

$$\{\tau \in \mathbb{R}_+ \setminus \{\tau_\infty^-(\mathbf{x},\varpi)\}\,;\ g_+(\mathbf{x},\varpi,\tau) = 0\} \ = \ \{0, \kappa(\mathbf{x})\}\,, \tag{3.79a}$$

$$\{\tau \in \mathbb{R}_+ \setminus \{\tau_\infty^+(\mathbf{x},\varpi)\}\,;\ g_-(\mathbf{x},\varpi,\tau) = 0\} \ = \ \{0, \tau_0^-(\mathbf{x}), \tau_0^+(\mathbf{x})\}\,. \tag{3.79b}$$

Proof. From (3.43) and (3.44b), we get easily $g_\pm(\mathbf{x},\varpi,0) = 0$. Now, when $g_\pm(\mathbf{x},\varpi,\tau) = 0$, by definition, the value $|\xi| = 0$ must be a solution to the equation $\chi_{\mathbf{x},\varpi}(\tau,|\xi|) = 0$. In view of (3.50), this implies $\mathcal{C}(\tau) = 0$. Recalling the discussion in Paragraph 3.3.1, we find that:

$$\{\tau \in \mathbb{R}_+^*\,;\ \mathcal{C}_{\mathbf{x}}(\tau) = 0\} = \{\kappa(\mathbf{x}), \tau_0^-(\mathbf{x}), \tau_0^+(\mathbf{x})\}\,.$$

Now, using (3.43) and (3.44), we can directly check that:

$$g_+(\mathbf{x},\varpi,\kappa(\mathbf{x}))=0\,,\qquad g_-(\mathbf{x},\varpi,\kappa(\mathbf{x}))\neq 0\,. \tag{3.80}$$

On the other hand, the choice $\tau=\tau_0^\pm$ corresponds to $\tau^2-\kappa^2=\mp\mathbf{b}_e\,\tau$. With (3.51b), this gives rise to:

$$\mathcal{B}(\tau_0^\pm)=(\tau_0^\pm)^2((\tau_0^\pm)^2-\kappa^2)((\tau_0^\pm)^2-\mathbf{b}_e^2-\kappa^2)(1+\cos^2\varpi)\,,\ \ \mathcal{C}(\tau_0^\pm)=0\,,\ \ \Delta(\tau_0^\pm)=\mathcal{B}(\tau_0^\pm)^2\,.$$

Coming back to (3.70), we see that $g_\pm(\mathbf{x},\varpi,\tau_0^\pm)=0$ if and only if $(\mathcal{B}\pm|\mathcal{B}|)(\tau_0^\pm)=0$. From (3.41), we can infer that:

$$\kappa^2<\kappa^2+\mathbf{b}_e^2<(\tau_0^+)^2=\kappa^2+\frac{1}{2}\,\mathbf{b}_e\,\big[\mathbf{b}_e+\sqrt{\mathbf{b}_e^2+4\,\kappa^2}\big]\quad\Longrightarrow\quad 0<\mathcal{B}(\tau_0^+)\,, \tag{3.81}$$

so that:

$$g_+\big(\mathbf{x},\varpi,\tau_0^+(\mathbf{x})\big)\neq 0\,,\qquad g_-\big(\mathbf{x},\varpi,\tau_0^+(\mathbf{x})\big)=0\,. \tag{3.82}$$

Similarly, from (3.41), we can obtain:

$$(\tau_0^-)^2=\kappa^2+\frac{1}{2}\,\mathbf{b}_e\,\big[\mathbf{b}_e-\sqrt{\mathbf{b}_e^2+4\,\kappa^2}\big]<\kappa^2<\kappa^2+\mathbf{b}_e^2\quad\Longrightarrow\quad 0<\mathcal{B}(\tau_0^-)\,. \tag{3.83}$$

It follows that:

$$g_+\big(\mathbf{x},\varpi,\tau_0^-(\mathbf{x})\big)\neq 0\,,\qquad g_-\big(\mathbf{x},\varpi,\tau_0^-(\mathbf{x})\big)=0\,. \tag{3.84}$$

Combining (3.80), (3.82) and (3.84), we can deduce (3.79a) and (3.79b). □

Lemma 3.13. *[asymptotic behaviors near the resonance frequencies]*

$$\lim_{\tau\to(\tau_\infty^-)^-} g_+(\mathbf{x},\varpi,\tau)=+\infty\,,\qquad \lim_{\tau\to(\tau_\infty^-)^+} g_+(\mathbf{x},\varpi,\tau)=-\infty\,, \tag{3.85a}$$

$$\lim_{\tau\to(\tau_\infty^+)^-} g_-(\mathbf{x},\varpi,\tau)=+\infty\,,\qquad \lim_{\tau\to(\tau_\infty^+)^+} g_-(\mathbf{x},\varpi,\tau)=-\infty\,. \tag{3.85b}$$

Proof. In view of (3.69) and (3.70), to obtain (3.85a) and (3.85b), it suffices to show that:

$$\frac{(\tau_\infty^-)^2\,\mathcal{P}(\varpi,\tau_\infty^-)+\mathbf{b}_e\,\kappa^2\,\sqrt{\mathcal{Q}(\varpi,\tau_\infty^-)}}{2\,\big((\tau_\infty^-)^2-(\tau_\infty^+)^2\big)}<0\,, \tag{3.86a}$$

$$\frac{(\tau_\infty^+)^2\,\mathcal{P}(\varpi,\tau_\infty^+)-\mathbf{b}_e\,\kappa^2\,\sqrt{\mathcal{Q}(\varpi,\tau_\infty^+)}}{2\,\big((\tau_\infty^+)^2-(\tau_\infty^-)^2\big)}<0\,. \tag{3.86b}$$

Taking into account Lemma 3.9, we have $\tau_\infty^-\leq\kappa\leq\tau_\infty^+$, as well as $\tau_\infty^-<\tau_\infty^+$. Applying (3.77b), we find (3.86a). Similarly, (3.86b) comes from (3.77a). □

We are now able to distinguish between the different regions of wave propagation. This can be done by selecting the connected parts of $\mathrm{V}(\mathbf{x},\varpi)$. This means to isolate where the functions $g_-(\mathbf{x},\varpi,\cdot)$ and $g_+(\mathbf{x},\varpi,\cdot)$ are positive. We will adopt the following classification.

a) Oblique *ordinary* wave ($|\xi|^2=g_+(\mathbf{x},\varpi,\tau)\geq 0$). With Lemmas 3.11 and 3.13, together with the intermediate value theorem, we get:

$$g_+(\mathbf{x},\varpi,\tau)\geq 0\iff\tau\in[0,\tau_\infty^-(\mathbf{x},\varpi)[\,\cup[\kappa(\mathbf{x}),+\infty[\,. \tag{3.87}$$

The set $\mathrm{V}_o(\mathbf{x},\varpi)$ consists of two connnected parts $\mathrm{V}_o^-(\mathbf{x},\varpi)$ and $\mathrm{V}_o^+(\mathbf{x},\varpi)$ which are defined by:

$$\mathrm{V}_o^-(\mathbf{x},\varpi) := \{(\tau,r)\,;\, 0<\tau<\tau_\infty^-(\mathbf{x},\varpi)\,,\, 0\le r\,,\, r^2=g_+(\mathbf{x},\varpi,\tau)\}\,, \tag{3.88a}$$

$$\mathrm{V}_o^+(\mathbf{x},\varpi) := \{(\tau,r)\,;\, \kappa(\mathbf{x})\le\tau\,,\, 0\le r\,,\, r^2=g_+(\mathbf{x},\varpi,\tau)\}\,. \tag{3.88b}$$

The part of $\mathrm{V}_o^-(\mathbf{x},\varpi)$ with $0\lesssim\tau$ gives the dispersion relation for *Alfvèn* waves. The part of $\mathrm{V}_o^-(\mathbf{x},\varpi)$ with $\tau\lesssim\tau_\infty^-(\mathbf{x},\varpi)$ determines the dispersion relation for *whistler* waves.

b) Oblique *extraordinary* wave ($|\xi|^2=g_-(\mathbf{x},\varpi,\tau)\ge 0$). The set $\mathrm{V}_x(\mathbf{x},\varpi)$ is also composed of two connected parts $\mathrm{V}_x^-(\mathbf{x},\varpi)$ and $\mathrm{V}_x^+(\mathbf{x},\varpi)$ which are defined by:

$$\mathrm{V}_x^-(\mathbf{x},\varpi) := \{(\tau,r)\,;\, \tau_0^-(\mathbf{x})\le\tau<\tau_\infty^+(\mathbf{x},\varpi)\,,\, 0\le r\,,\, r^2=g_-(\mathbf{x},\varpi,\tau)\}\,, \tag{3.89a}$$

$$\mathrm{V}_x^+(\mathbf{x},\varpi) := \{(\tau,r)\,;\, \tau_0^+(\mathbf{x})\le\tau\,,\, 0\le r\,,\, r^2=g_-(\mathbf{x},\varpi,\tau)\}\,. \tag{3.89b}$$

Retain that:

$$\mathrm{V}(\mathbf{x},\varpi)=\mathrm{V}_o^-(\mathbf{x},\varpi)\sqcup\mathrm{V}_o^+(\mathbf{x},\varpi)\sqcup\mathrm{V}_x^-(\mathbf{x},\varpi)\sqcup\mathrm{V}_x^+(\mathbf{x},\varpi)\,. \tag{3.90}$$

The case of perpendicular propagation ($\varpi=\pi/2$) can be incorporated within the general framework of oblique propagation. However, using (3.42), we get $\tau_\infty^-(\mathbf{x},\pi/2)=0$. It follows that $\mathrm{V}_o^-(\mathbf{x},\pi/2)=\{(0,r)\,;\, r\in\mathbb{R}_+\}$. Thus, the set $\mathrm{V}_o(\mathbf{x},\pi/2)$ reduces to the vertical half-line $\{\tau=0\}$ together with the connected component $\mathrm{V}_o^+(\mathbf{x},\pi/2)$ which is associated to what physicists call *ordinary* waves. On the other hand, the set $\mathrm{V}_x(\mathbf{x},\pi/2)$ is still composed of two disjoint connected parts $\mathrm{V}_x^-(\mathbf{x},\pi/2)$ and $\mathrm{V}_x^+(\mathbf{x},\pi/2)$ which correspond to *extraordinary* waves. Some sets $\mathrm{V}_o(\mathbf{x},\varpi)$ and $\mathrm{V}_x(\mathbf{x},\varpi)$ are represented on Figure 6 below.

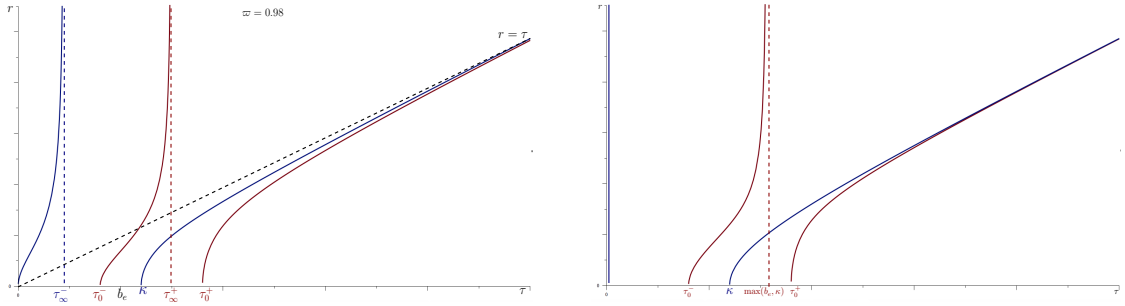

(a) General case ($\varpi=0.98$). (b) Perpendicular case ($\varpi=\pi/2$).

FIGURE 6. Oblique propagation for angles $\varpi\in]0,\pi/2]$:
- Ordinary waves $\mathrm{V}_o(\mathbf{x},\varpi)=\mathrm{V}_o^-(\mathbf{x},\varpi)\sqcup\mathrm{V}_o^+(\mathbf{x},\varpi)$ in blue;
- Extraordinary waves $\mathrm{V}_x(\mathbf{x},\varpi)=\mathrm{V}_x^-(\mathbf{x},\varpi)\sqcup\mathrm{V}_x^+(\mathbf{x},\varpi)$ in red.

3.3.3. *Come back to parallel propagation.* In this Paragraph 3.3.3, we examine again the case of parallel propagation. But, to this end, we follow the approach of (3.88) and (3.89). This allows to provide a fresh perspective on what happens when $\varpi = 0$. When $\varpi = 0$, the formula (3.43) yields:

$$g_\pm(\mathbf{x}, 0, \tau) = \tau^2 - \frac{\kappa(\mathbf{x})^2\,\tau}{\tau \pm sgn(\tau - \kappa(\mathbf{x}))\ \mathbf{b}_e(\mathbf{x})}\,. \tag{3.91}$$

Recall (3.81) which guarantees that $\kappa < \tau_0^+$. As a consequence of (3.91), the definitions (3.67) of $\mathrm{V}_r^+(\mathbf{x}, 0)$ and (3.89b) of $\mathrm{V}_x^+(\mathbf{x}, 0)$ coincide. The function $g_\pm(\mathbf{x}, 0, \cdot)$ is not suitable for the description of the other components of $\mathrm{V}(\mathbf{x}, 0)$. This is because $g_\pm(\mathbf{x}, 0, \cdot)$ is not continuous at the point $\tau = \kappa$.

Definition 3.8. *[overdense and underdense plasmas] The plasma is said <u>overdense</u> at the spatial position* $\mathbf{x}$ *if* $\mathbf{b}_e(\mathbf{x}) < \kappa$. *Otherwise, it is said <u>underdense</u>.*

For $\varpi = 0$, the identity (3.42) gives rise to:

$$\tau_\infty^-(\mathbf{x}, 0) = \begin{cases} \kappa(\mathbf{x}) & \text{if} \quad \kappa(\mathbf{x}) < \mathbf{b}_e(\mathbf{x})\,, \\ \mathbf{b}_e(\mathbf{x}) & \text{if} \quad \mathbf{b}_e(\mathbf{x}) < \kappa(\mathbf{x})\,, \end{cases} \qquad \tau_\infty^+(\mathbf{x}, 0) = \begin{cases} \kappa(\mathbf{x}) & \text{if} \quad \mathbf{b}_e(\mathbf{x}) < \kappa(\mathbf{x})\,, \\ \mathbf{b}_e(\mathbf{x}) & \text{if} \quad \kappa(\mathbf{x}) < \mathbf{b}_e(\mathbf{x})\,. \end{cases}$$

Under the overdense condition, we find:

$$\mathrm{V}_o^-(\mathbf{x}, 0) \equiv \mathrm{V}_r^-(\mathbf{x}, 0)\,, \qquad \mathrm{V}_x^-(\mathbf{x}, 0) \cup \mathrm{V}_o^+(\mathbf{x}, 0) \equiv \mathrm{V}_l(\mathbf{x}, 0)\,.$$

Under the underdense condition, we can further decompose $\mathrm{V}_x^-(\mathbf{x}, 0)$ into the disjoint union of $\mathrm{V}_x^{--}(\mathbf{x}, 0)$ and $\mathrm{V}_x^{-+}(\mathbf{x}, 0)$, with:

$$\mathrm{V}_x^{--}(\mathbf{x}, 0) := \big\{\tau_0^- < \tau < \kappa(\mathbf{x})\,;\ 0 \le r\,,\ r^2 = \tau^2 - \kappa(\mathbf{x})^2\,\tau\,\big(\tau + \mathbf{b}_e(\mathbf{x})\big)^{-1}\big\}\,,$$

$$\mathrm{V}_x^{-+}(\mathbf{x}, 0) := \big\{\kappa(\mathbf{x}) \le \tau < \mathbf{b}_e(\mathbf{x})\,;\ 0 \le r\,,\ r^2 = \tau^2 - \kappa(\mathbf{x})^2\,\tau\,\big(\tau - \mathbf{b}_e(\mathbf{x})\big)^{-1}\big\}\,.$$

Then, we can recover:

$$\mathrm{V}_o^-(\mathbf{x}, 0) \cup \mathrm{V}_x^{-+}(\mathbf{x}, 0) \equiv \mathrm{V}_r^-(\mathbf{x}, 0)\,, \qquad \mathrm{V}_x^{--}(\mathbf{x}, 0) \cup \mathrm{V}_o^+(\mathbf{x}, 0) \equiv \mathrm{V}_l(\mathbf{x}, 0)\,.$$

Finally, due to the disontinuity of the functions $g_\pm(\mathbf{x}, 0, \cdot)$, the case $\tau = \kappa$ has to be treated separetely. In fact, the corresponding study is exactly the same as in Paragraph 3.3.1 *c)*. We recover the case of parallel longitudinal waves. These considerations together with Figures 3, 7 and 8 clarify the connections between the physical approach of Paragraph 3.3.1 and the mathematical presentation of the actual Paragraph 3.3.3.

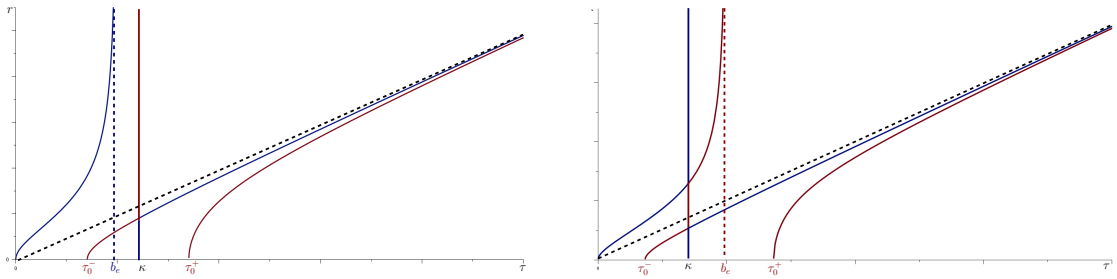

(a) Overdense case. (b) Underdense case.

FIGURE 7. Parallel propagation ($\varpi = 0$). Mixing of $\mathrm{V}_x(\mathbf{x}, 0)$ and $\mathrm{V}_o(\mathbf{x}, 0)$.

3.3.4. *Parallel and perpendicular propagation viewed as limited cases.* When $\varpi \in]0, \pi/2[$, the set $\mathrm{V}(\mathbf{x}, \varpi)$ has two resonances which are located at $\tau = \tau_\infty^-(\mathbf{x}, \varpi)$ and at $\tau = \tau_\infty^+(\mathbf{x}, \varpi)$. On the contrary, the two extreme cases $\varpi = 0$ and $\varpi = \pi/2$ are often presented as having only one resonance each. This would suggest a change in the type of representation. But this is illusive. Indeed, one of the two oblique resonances degenerates into a vertical half-line when ϖ goes to 0 or $\pi/2$. More precisely, the resonance $\tau_\infty^+(\mathbf{x}, \varpi)$ gives rise to the electrostatic plasma waves when $\varpi \to 0$, while $\tau_\infty^-(\mathbf{x}, \varpi)$ evolves into the vertical half-line $\{\tau = 0\}$ when $\varpi \to \pi/2$. This behaviour is illustrated on Figure 8.

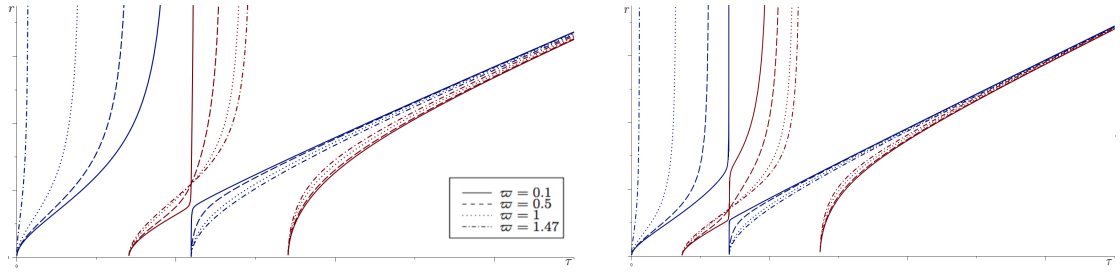

(a) Overdense case. (b) Underdense case.

FIGURE 8. Evolution of $\mathrm{V}_x(\mathbf{x}, \varpi)$ and $\mathrm{V}_o(\mathbf{x}, \varpi)$ in function of ϖ.
Asymptotic behaviour when $\varpi \to 0$ (see $\varpi = 0.1 \sim 0$) and $\varpi \to \pi/2$ (see $\varpi = 1.47 \sim \pi/2$).

3.4. **Other parametrizations of the characteristic variety.** Until now, to describe the set $\mathscr{V}$, we have looked at the direction $\xi \in \mathbb{R}^3$ (in fact at $|\xi| \in \mathbb{R}_+^*$ for a given $\varpi \in [0, \pi]$) as a function of the frequency $\tau \in \mathbb{R}_+^*$, with τ selected in convenient subdomains. The aim of this Section 3.4 is to investigate the other ways to proceed.

3.4.1. *The characteristic variety at a fixed value of ω.* The description of $\mathscr{V}_\mathbf{x}^*$ through the functions $g_\pm(\cdot)$ does not involve ω and the sign of τ. As observed in Paragraph 3.2.4, this means that $\mathscr{V}_\mathbf{x}^*$ is invariant under rotations with axis $\mathbb{R}\,^t(0, 0, 1)$ and angles $\omega \in [0, 2\,\pi[$. Since we can recover the case $\omega \neq 0$ from the case $\omega = 0$ by such rotations, it suffices to consider the case $\omega = 0$. To this end, as pointed in Remark 3.3, we can cut $\mathscr{V}_\mathbf{x}^*$ with a well-chosen quadrant of an hyperplane. Moreover, we can consider $\varpi \in [0, \pi]$ as a variable rather than as a parameter (like we did before in Paragraph 3.3.2). By doing so, we get a three dimensional representation of $\mathscr{V}_\mathbf{x}^*$, which could be materialized through:

$$\mathcal{V}_\mathbf{x}^* := \{(\varpi, \tau, r) \in [0, \pi] \times \mathbb{R}_+^2 \,;\, (\tau, S_p(r, 0, \varpi)) \in \mathscr{V}_\mathbf{x}^*\}\,.$$

In accordance with the classification of Paragraph 3.3.2 into the categories *a)* and *b)*, the set $\mathcal{V}_\mathbf{x}^*$ can be separated into connected parts:

$$\mathcal{V}_\mathbf{x}^* = \mathcal{V}_o^-(\mathbf{x}) \cup \mathcal{V}_o^+(\mathbf{x}) \cup \mathcal{V}_x^-(\mathbf{x}) \cup \mathcal{V}_x^+(\mathbf{x}) \subset [0, \pi] \times \mathbb{R}_+^2\,.$$

With $(\varpi, r) \in [0, \pi] \times \mathbb{R}_+$, these components are defined by:

$$\mathcal{V}_o^-(\mathbf{x}) := \{(\varpi, \tau, r)\,;\, 0 \leq \tau < \tau_\infty^-(\mathbf{x}, \varpi)\,,\, r^2 = g_+(\mathbf{x}, \varpi, \tau)\}\,, \tag{3.92a}$$

$$\mathcal{V}_o^+(\mathbf{x}) := \{(\varpi, \tau, r)\,;\, \kappa(\mathbf{x}) \leq \tau\,,\, r^2 = g_+(\mathbf{x}, \varpi, \tau)\}\,, \tag{3.92b}$$

$$\mathcal{V}_x^-(\mathbf{x}) := \{(\varpi, \tau, r)\,;\, \tau_0^-(\mathbf{x}) \leq \tau < \tau_\infty^+(\mathbf{x}, \varpi)\,,\, r^2 = g_-(\mathbf{x}, \varpi, \tau)\}\,, \tag{3.92c}$$

$$\mathcal{V}_x^+(\mathbf{x}) := \{(\varpi, \tau, r)\,;\, \tau_0^+(\mathbf{x}) \leq \tau\,,\, r^2 = g_-(\mathbf{x}, \varpi, \tau)\}\,. \tag{3.92d}$$

The sets $\mathcal{V}_o^{\pm}(\mathbf{x})$ and $\mathcal{V}_x^{\pm}(\mathbf{x})$ are drawn on Figure 9. We also include (in the plane $r = 0$) the graphs of the functions $\tau_\infty^{\pm}(\mathbf{x}, \cdot) : [0, \pi/2] \longrightarrow \mathbb{R}_+$.

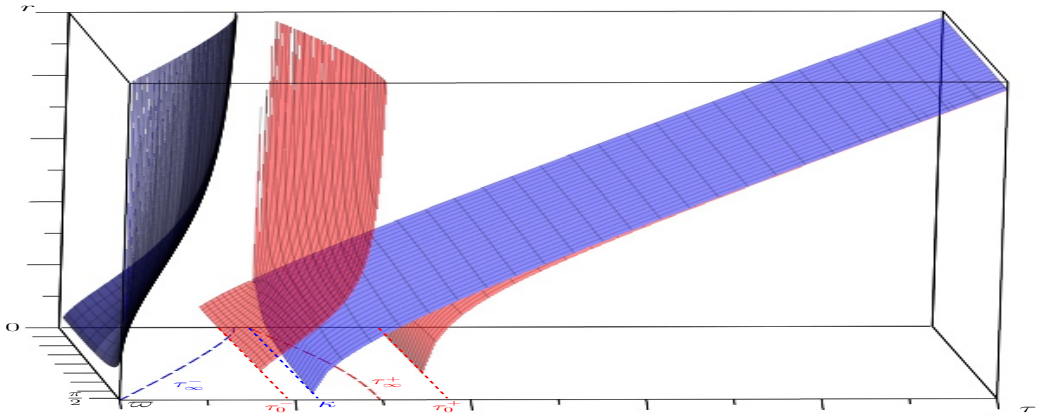

FIGURE 9. The characteristic variety in the variables (τ, ϖ, r).
From left to right: $\mathcal{V}_o^-(\mathbf{x})$, $\mathcal{V}_x^-(\mathbf{x})$, $\mathcal{V}_o^+(\mathbf{x})$ and $\mathcal{V}_x^+(\mathbf{x})$.

3.4.2. *The characteristic variety at a fixed value of τ.* Our purpose here is to give a detailed description of the following set:

$$\boldsymbol{\mathcal{V}}(\mathbf{x}, \tau) := \{\, \xi \in \mathbb{R}^3 \,;\, (\tau, \xi) \in \mathscr{V}_{\mathbf{x}}^* \,\}\,.$$

For a given $\xi \in \mathbb{R}^3$, we use the notation $\xi = S_{ph}(|\xi|, \omega_\xi, \varpi_\xi)$ which comes from the convention of Figure 2 to represent ξ. In connection with what has been done in Paragraph 3.3.2, the set $\boldsymbol{\mathcal{V}}(\mathbf{x}, \tau)$ can be decomposed into $\boldsymbol{\mathcal{V}}(\mathbf{x}, \tau) = \boldsymbol{\mathcal{V}}_o(\mathbf{x}, \tau) \cup \boldsymbol{\mathcal{V}}_x(\mathbf{x}, \tau)$ with:

$$\boldsymbol{\mathcal{V}}_o(\mathbf{x}, \tau) := \{\, \xi \in \mathbb{R}^3 \,;\, (\tau, |\xi|) \in \ \mathrm{V}_o(\mathbf{x}, \varpi_\xi)\}\,, \tag{3.93a}$$

$$\boldsymbol{\mathcal{V}}_x(\mathbf{x}, \tau) := \{\, \xi \in \mathbb{R}^3 \,;\, (\tau, |\xi|) \in \ \mathrm{V}_x(\mathbf{x}, \varpi_\xi)\}\,. \tag{3.93b}$$

The access to $\boldsymbol{\mathcal{V}}$ is achieved through the functions $g_\pm(\cdot)$. Now, given $(\mathbf{x}, \tau) \in \Omega \times \mathbb{R}_+$, the domain of definition, the sign, the regularity and the behaviour of $g_\pm(\mathbf{x}, \cdot, \tau) : [0, \pi/2] \longrightarrow \mathbb{R}$ depend strongly on the choice of τ. Recall that we have to deal with the additional condition $|\xi|^2 = g_\pm(\mathbf{x}, \varpi, \tau) \geq 0$. Thus, of particular interest are the intervals where $g_\pm(\mathbf{x}, \cdot, \tau)$ is non-negative. We can first deal with the case of $g_+(\cdot)$.

Lemma 3.14. *[study of the function $g_+(\mathbf{x}, \cdot, \tau)$] Two situations must be distinguished.*
i) Case $\tau \in \tau_\infty^-(\mathbf{x}, [0, \pi/2]) = [0, \min(\mathbf{b}_e(\mathbf{x}), \kappa(\mathbf{x}))]$. There exists a unique $\varpi_\infty^-(\mathbf{x}, \tau) \in [0, \pi/2]$ such that the function $g_+(\mathbf{x}, \cdot, \tau)$ is defined and continuous on the domain $[0, \pi/2] \setminus \{\varpi_\infty^-(\mathbf{x}, \tau)\}$. It is non-negative if and only if $\varpi \in [0, \varpi_\infty^-(\mathbf{x}, \tau)[$. Moreover, we have:

$$\lim_{\varpi \to (\varpi_\infty^-(\mathbf{x}, \tau))^-} g_+(\mathbf{x}, \varpi, \tau) \ = \ +\infty\,. \tag{3.94}$$

ii) Case $\tau \in \mathbb{R}_+ \setminus \tau_\infty^-(\mathbf{x}, [0, \pi/2]) =]\min(\mathbf{b}_e(\mathbf{x}), \kappa(\mathbf{x})), +\infty[$. The function $g_+(\mathbf{x}, \cdot, \tau)$ is defined and continuous on the whole interval $[0, \pi/2]$. It is non-negative if and only if $\tau \geq \kappa(\mathbf{x})$.

Proof. From the proof of Lemma 3.11, we know that $g_+(\mathbf{x},\cdot,\tau)$ is defined and continuous except if $\tau = \tau_\infty^-(\mathbf{x},\varpi)$. Given $\tau \in \mathbb{R}_+$, from Lemma 3.9, this can happen for some angle $\varpi_\infty^-(\mathbf{x},\tau) \in [0,\pi/2]$ if and only if we are in case *i)*. Now, assuming *i)*, we have:

$$\tau < \tau_\infty^-(\mathbf{x},\varpi) \le \tau_\infty^+(\mathbf{x},\varpi) \quad \Longleftrightarrow \quad \varpi \in \big[0,\varpi_\infty^-(\mathbf{x},\tau)\big[\,. \tag{3.95}$$

Then, coming back to the expression (3.43) and using the information (3.95), we can identify as in *i)* the interval where $g_+(\mathbf{x},\cdot,\tau)$ is non-negative, as well as the asymptotic behaviour (3.94). In fact, to get both *i)* and *ii)*, it suffices to look at Figure 5. □

Similarly, we can consider $g_-(\mathbf{x},\cdot,\tau)$.

Lemma 3.15. *[study of the function $g_-(\mathbf{x},\cdot,\tau)$] Two situations must be distinguished.*

i) Case $\tau \in \tau_\infty^+(\mathbf{x},[0,\pi/2]) = \big[\max(\mathbf{b}_e(\mathbf{x}),\kappa(\mathbf{x})),\sqrt{\mathbf{b}_e(\mathbf{x})^2+\kappa(\mathbf{x})^2}\big]$. There exists some (unique) angle $\varpi_\infty^+(\mathbf{x},\tau) \in [0,\pi/2]$ such that the function $g_-(\mathbf{x},\cdot,\tau)$ is defined and continuous on the domain $[0,\pi/2] \setminus \{\varpi_\infty^+(\mathbf{x},\tau)\}$. It is non-negative if and only if $\varpi \in \big[\varpi_\infty^+(\mathbf{x},\tau),\pi/2\big]$. Moreover, we have:

$$\lim_{\varpi \to (\varpi_\infty^+(\mathbf{x},\tau))^+} g_-(\mathbf{x},\varpi,\tau) \,=\, +\infty\,. \tag{3.96}$$

ii) Case $\tau \in \mathbb{R}_+ \setminus \tau_\infty^+(\mathbf{x},[0,\pi/2])$. The function $g_-(\mathbf{x},\cdot,\tau)$ is defined and continuous on the whole interval $[0,\pi/2]$. It is non-negative if and only if we have either $\tau \in \big[\tau_0^+(\mathbf{x}),+\infty\big[$ or $\tau \in \big[\tau_0^-(\mathbf{x}),\max\big(\,\mathbf{b}_e(\mathbf{x})\,;\,\kappa(\mathbf{x})\,\big)\big]$.

Proof. From the proof of Lemma 3.11, we know that $g_-(\mathbf{x},\cdot,\tau)$ is defined and continuous except if $\tau = \tau_\infty^+(\mathbf{x},\varpi)$. Given $\tau \in \mathbb{R}_+$, from Lemma 3.9, this can happen for some angle $\varpi_\infty^+(\mathbf{x},\tau) \in [0,\pi/2]$ if and only if we are in case *i)*. Now, assuming *i)*, we have:

$$\tau \in \big]\tau_\infty^+(\mathbf{x},\varpi),\sqrt{\mathbf{b}_e(\mathbf{x})^2+\kappa(\mathbf{x})^2}\big] \quad \Longleftrightarrow \quad \varpi \in \big[0,\varpi_\infty^+(\mathbf{x},\tau)\big[\,. \tag{3.97}$$

Then, using (3.43), (3.78a) and (3.97), we can deduce (3.96). To see where $g_-(\mathbf{x},\cdot,\tau)$ is non-negative, simply exploit Figure 4. □

The wave equation describes the propagation of electromagnetic waves in a *vacuum*. In its dimensionless version, it takes the form:

$$\partial_{\mathbf{tt}}^2 E - \Delta_{\mathbf{xx}} E = 0\,, \qquad \partial_{\mathbf{tt}}^2 B - \Delta_{\mathbf{xx}} B = 0\,.$$

The characteristic varieties associated with these two equations (on E and B) are the same. They are simply given by the light cone:

$$\mathscr{V}_l := \big\{\,(\mathbf{t},\mathbf{x},\tau,\xi) \in T^*M\,;\;\tau^2 - |\xi|^2 = 0\,\big\}\,. \tag{3.98}$$

Then, given $\tau \in \mathbb{R}_+^*$, we recover the *sphere* of radius τ:

$$\boldsymbol{\mathcal{V}}_l(\mathbf{x},\tau) \equiv \boldsymbol{\mathcal{V}}_l(\tau) := \big\{\,\xi \in \mathbb{R}^3\,;\;|\xi| = \tau\,\big\}\,. \tag{3.99}$$

Now, in the presence of an exterior magnetic field, the picture (3.99) is strongly affected. The first effect, already encoded within (3.93), is the well-known separation of $\boldsymbol{\mathcal{V}}$ into the two parts $\boldsymbol{\mathcal{V}}_o$ and $\boldsymbol{\mathcal{V}}_x$ corresponding to *ordinary* and *extraordinary* waves. The second impact is a disappearance of $\boldsymbol{\mathcal{V}}_o(\mathbf{x},\tau)$ and $\boldsymbol{\mathcal{V}}_x(\mathbf{x},\tau)$ when τ falls into the gap between resonance and cutoff frequencies, and their resurgence in the form of *cones* below resonance frequencies. With this in mind, we can highlight the following distinctions.

Definition 3.9. *[related to Figure 10] For* $(\mathbf{x},\tau) \in \Omega \times \big[0, \min\big(\mathbf{b}_e(\mathbf{x}), \kappa(\mathbf{x})\big)\big]$*, the set* $\boldsymbol{\mathcal{V}}_o(\mathbf{x},\tau)$ *is referred as an ordinary resonance cone.*

Proposition 3.1. *[* $\tau \in \big[0, \min\big(\mathbf{b}_e(\mathbf{x}), \kappa(\mathbf{x})\big)\big]$ *] The ordinary resonance cones* $\boldsymbol{\mathcal{V}}_o(\mathbf{x},\tau)$ *are comprised of exactly two unbounded connected components, say* $\boldsymbol{\mathcal{V}}_o^a(\mathbf{x},\tau)$ *and* $\boldsymbol{\mathcal{V}}_o^b(\mathbf{x},\tau)$*, which are respectively above and below the plane* $\{\xi; \xi^3 = 0\}$ *and given by:*

$$\boldsymbol{\mathcal{V}}_o^a(\mathbf{x},\tau) := \big\{\, \xi = S_{ph}(r,\omega_\xi,\varpi_\xi)\,;\ 0 \le r\,,\ -\pi \le \omega_\xi \le \pi\,, \\ 0 \le \varpi_\xi \le \varpi_\infty^-(\mathbf{x},\tau)\,,\ r^2 = g_+(\mathbf{x},\varpi,\tau)\,\big\}\,, \tag{3.100a}$$

$$\boldsymbol{\mathcal{V}}_o^b(\mathbf{x},\tau) := \big\{\, \xi = S_{ph}(r,\omega_\xi,\varpi_\xi)\,;\ 0 \le r\,,\ -\pi \le \omega_\xi \le \pi\,, \\ \pi - \varpi_\infty^-(\mathbf{x},\tau) \le \varpi_\xi \le \pi\,,\ r^2 = g_+(\mathbf{x},\varpi,\tau)\,\big\}\,. \tag{3.100b}$$

Proof. This statement is a direct consequence of Lemma 3.14, case *i)*. In particular, the asymptotic behaviour (3.94) implies that neither $\boldsymbol{\mathcal{V}}_o^a(\mathbf{x},\tau)$ nor $\boldsymbol{\mathcal{V}}_o^b(\mathbf{x},\tau)$ are bounded. On the contrary, for large values of r, these two sets become close to the two cones:

$$\mathcal{C}_o^a(\mathbf{x},\tau) := \big\{\, \xi\,;\ \varpi_\xi = \varpi_\infty^-(\mathbf{x},\tau)\,\big\}\,, \qquad \mathcal{C}_o^b(\mathbf{x},\tau) := \big\{\, \xi\,;\ \varpi_\xi = \pi - \varpi_\infty^-(\mathbf{x},\tau)\,\big\}\,. \qquad \square$$

The distortion from $\boldsymbol{\mathcal{V}}_l$ is here obvious. As long as τ remains sufficiently small, which means in practice that we deal with Very Low Frequency waves (at approximately 1 kHz), there is no similarity between $\boldsymbol{\mathcal{V}}_o(\mathbf{x},\tau)$ and $\boldsymbol{\mathcal{V}}_l(\tau)$. The same applies to $\boldsymbol{\mathcal{V}}_x(\mathbf{x},\tau)$.

Definition 3.10. *[related to Figure 11] For* $(\mathbf{x},\tau) \in \Omega \times \big[\max(\mathbf{b}_e,\kappa), \sqrt{\mathbf{b}_e^2+\kappa^2}\,\big]$*, the set* $\boldsymbol{\mathcal{V}}_x(\mathbf{x},\tau)$ *is referred as an extraordinary resonance cone.*

Proposition 3.2. *[* $\tau \in \big[\max(\mathbf{b}_e,\kappa), \sqrt{\mathbf{b}_e^2+\kappa^2}\,\big]$ *] The extraordinary resonance cones* $\boldsymbol{\mathcal{V}}_x(\mathbf{x},\tau)$ *are unbounded connected sets given by:*

$$\boldsymbol{\mathcal{V}}_x(\mathbf{x},\tau) := \big\{\ \xi = S_{ph}(r,\omega_\xi,\varpi_\xi)\,;\ 0 \le r\,,\ -\pi \le \omega_\xi \le \pi\,, \\ \varpi_\infty^+(\mathbf{x},\tau) \le \varpi_\xi \le \pi - \varpi_\infty^+(\mathbf{x},\tau)\,,\ r^2 = g_-(\mathbf{x},\varpi_\xi,\tau)\,\big\}\,, \tag{3.101}$$

Proof. This statement is a direct consequence of Lemma 3.15, case *i)*. In particular, the asymptotic behaviour (3.96) implies that the set $\boldsymbol{\mathcal{V}}_x(\mathbf{x},\tau)$ is not bounded. Indeed, for large values of r, it becomes close to the cone:

$$\mathcal{C}_x(\mathbf{x},\tau) := \big\{\, \xi\,;\ \varpi_\xi = \varpi_\infty^+(\mathbf{x},\tau)\,\big\} \cup \big\{\, \xi\,;\ \varpi_\xi = \pi - \varpi_\infty^+(\mathbf{x},\tau)\,\big\}\,. \qquad \square$$

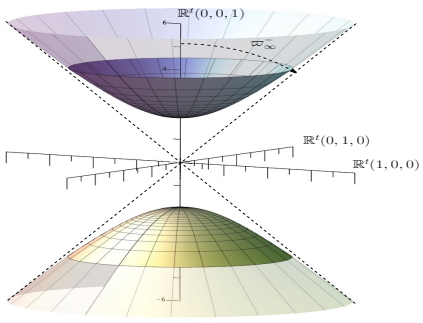

FIGURE 10. Ordinary resonance cone. $\boldsymbol{\mathcal{V}}_o(\mathbf{x},\tau)$ for $\tau \in [0, \min(\mathbf{b}_e(\mathbf{x}), \kappa(\mathbf{x}))]$.

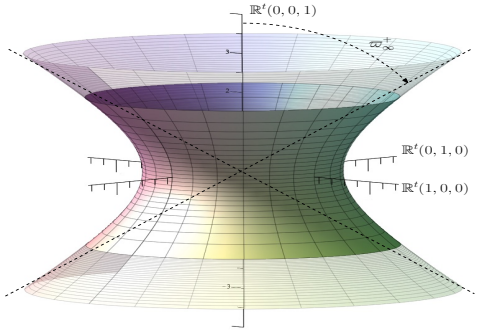

FIGURE 11. Extraordinary resonance cone. $\boldsymbol{\mathcal{V}}_x(\mathbf{x},\tau)$ for $\tau \in [\max(\mathbf{b}_e(\mathbf{x}), \kappa(\mathbf{x})), \sqrt{\mathbf{b}_e(\mathbf{x})^2 + \kappa(\mathbf{x})^2}]$.

Above their corresponding cutoff frequencies, the sets $\mathbf{V}_o(\mathbf{x},\tau)$ and $\mathbf{V}_x(\mathbf{x},\tau)$ are restored in the form of bounded sets which are homeomorphic to spheres.

Definition 3.11. *[related to Figure 12] For $(\mathbf{x},\tau)\in\Omega\times[\kappa(\mathbf{x}),+\infty[$, the set $\mathbf{V}_o(\mathbf{x},\tau)$ is referred as an ordinary sphere.*

Proposition 3.3. *[$\tau\in[\kappa(\mathbf{x}),+\infty[$] The ordinary spheres $\mathbf{V}_o(\mathbf{x},\tau)$ are bounded connected sets given by:*

$$\mathbf{V}_o(\mathbf{x},\tau):=\{\,\xi=S_{ph}(r,\omega_\xi,\varpi_\xi)\,;\;0\le r\,,\;-\pi\le\omega_\xi\le\pi\,,\\ 0\le\varpi_\xi\le\pi\,,\;r^2=g_+(\mathbf{x},\varpi_\xi,\tau)\,\}\,. \tag{3.102}$$

Proof. This statement is a direct consequence of Lemma 3.14, case *ii)*. □

Definition 3.12. *[related to Figure 13] For $(\mathbf{x},\tau)\in\Omega\times[\tau_0^+(\mathbf{x}),+\infty[$, the set $\mathbf{V}_x(\mathbf{x},\tau)$ is referred as an extraordinary sphere.*

Proposition 3.4. *[$\tau\in[\tau_0^+(\mathbf{x}),+\infty[$] The extraordinary spheres $\mathbf{V}_x(\mathbf{x},\tau)$ are bounded connected sets given by:*

$$\mathbf{V}_x(\mathbf{x},\tau):=\{\,\xi=S_{ph}(r,\omega_\xi,\varpi_\xi)\,;\;0\le r\,,\;-\pi\le\omega_\xi\le\pi\,,\\ 0\le\varpi_\xi\le\pi\,,\;r^2=g_-(\mathbf{x},\varpi_\xi,\tau)\,\}\,. \tag{3.103}$$

Proof. This statement is a direct consequence of Lemma 3.15, case *ii)*. □

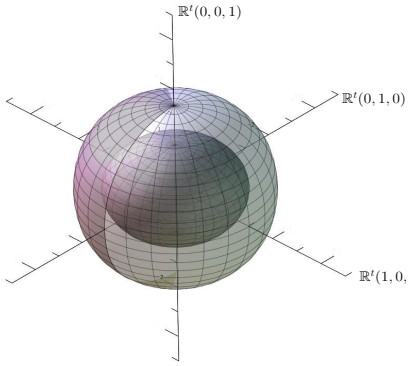

FIGURE 12. The extraordinary sphere nested into the ordinary sphere, for $\tau\gtrsim\tau_0^+(\mathbf{x})$.

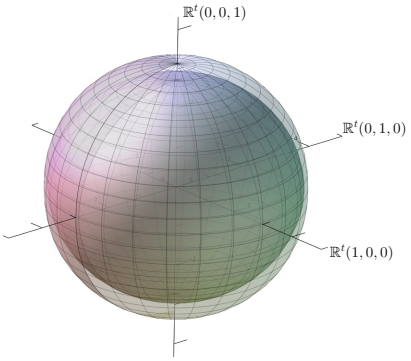

FIGURE 13. Asymptotic merge of the ordinary and extraordinary spheres, for $\tau\gg\tau_0^+(\mathbf{x})$.

The ordinary resonance cone can appear with an ordinary sphere if $\kappa(\mathbf{x})<\sqrt{2}\mathbf{b}_e(\mathbf{x})$ (see Lemma 3.10). An extraordinary resonance cone can occur with an ordinary sphere which, in this case, is located inside. For the sake of clarity such configurations are not made apparent in Figure 10 and 11). For $\tau>\tau_0^+(\mathbf{x})$, the extraordinary sphere and the ordinary sphere coexist (see Figures 12 and 13), the first being included in the second. At higher frequencies, that is concretely above 1 MHz, the distinction between $\mathbf{V}_o(\mathbf{x},\tau)$ and $\mathbf{V}_x(\mathbf{x},\tau)$ becomes almost invisible. For $\tau\gg\tau_0^+(\mathbf{x})$, these both sets just look like $\mathscr{V}_l$. Indeed, from (3.43)-(3.44), we can easily infer that:

$$\lim_{\tau\longrightarrow+\infty}\tau^{-2}\,g_\pm(\mathbf{x},\varpi,\tau)=1\,.$$

3.4.3. *The characteristic variety as a graph of functions depending on τ.* The purpose of this Paragraph 3.4.3 is to convert the condition $(\mathbf{t},\mathbf{x},\tau,\xi)\in\mathscr{V}$ by expressing τ as a function of ξ (in fact of r at fixed angle ϖ). From Definition 3.1, Lemma 3.5 and (3.60), recalling the convention (3.37), we can assert that:

$$(\mathbf{t},\mathbf{x},\tau,\xi)\in\mathscr{V} \iff (|\tau|,r)\in \mathrm{V}(\mathbf{x},\varpi)\cap\mathbb{R}_+^2 \iff \chi_{\mathbf{x},\varpi}(|\tau|,r)=0\,. \tag{3.104}$$

As noted in the article [28], interpreted as a polynomial in the variable τ instead of $|\mathfrak{n}|$, the characteristic equation $\chi_{\mathbf{x},\varpi}(\tau,|\xi|)=0$ turns to be of fourth order in τ^2. More precisely, we have $\chi_{\mathbf{x},\varpi}(\tau,r)=P_{\mathbf{x},\varpi,r}(\tau^2)$ with:

$$\begin{aligned} P_{\mathbf{x},\varpi,r}(X) := {} & X^4-(\mathbf{b}_e^2+3\,\kappa^2+2\,r^2)\;X^3\\ & +\big(r^4+2\,r^2\,(\mathbf{b}_e^2+2\,\kappa^2)+\mathbf{b}_e^2\,\kappa^2+3\,\kappa^4\big)\;X^2\\ & -\big(r^4\,(\mathbf{b}_e^2+\kappa^2)+r^2\,(2\,\kappa^4+\mathbf{b}_e^2\,\kappa^2\,(1+\cos^2\varpi))+\kappa^6\big)\;X\\ & +r^4\,\mathbf{b}_e^2\,\kappa^2\,\cos^2(\varpi)\,. \end{aligned} \tag{3.105}$$

Explicit algebraic expressions $\tau(\mathbf{x},|\xi|,\varpi)$ are of course available, but they are not so easy to implement. We will proceed differently. Another way to extract information is to study the properties of the function $g_\pm(\mathbf{x},\varpi,\cdot)$. We start by looking at the two extreme situations ($\varpi=0$ and $\varpi=\pi/2$). Then, we consider the oblique case $\varpi\in\,]0,\pi/2[$.

∘ 3.4.3.a) Parallel case ($\varpi=0$). To describe the set $\mathrm{V}(\mathbf{x},0)$ as a graph of functions depending on τ, we can come back to Paragraph 3.3.1. With the formulas inside (3.64), (3.66) and (3.67) in mind, we can define:

$$L(\mathbf{x},\tau):=\tau^2-\frac{\kappa(\mathbf{x})^2\,\tau}{\tau+\mathbf{b}_e(\mathbf{x})}\,,\qquad \forall\,(\mathbf{x},\tau)\in\Omega\times\mathbb{R}_+\,, \tag{3.106a}$$

$$R(\mathbf{x},\tau):=\tau^2-\frac{\kappa(\mathbf{x})^2\,\tau}{\tau-\mathbf{b}_e(\mathbf{x})}\,,\qquad \forall\,(\mathbf{x},\tau)\in\Omega\times\big(\mathbb{R}_+\setminus\{\mathbf{b}_e(\mathbf{x})\}\big)\,. \tag{3.106b}$$

Lemma 3.16. *Fix $\mathbf{x}\in\Omega$. The application $L(\mathbf{x},\cdot):[\tau_0^-(\mathbf{x}),+\infty[\longrightarrow\mathbb{R}_+$ as well as the two applications:*

$$R(\mathbf{x},\cdot):[0,\mathbf{b}_e(\mathbf{x})[\longrightarrow\mathbb{R}_+\,,\qquad R(\mathbf{x},\cdot):[\tau_0^+(\mathbf{x}),+\infty[\longrightarrow\mathbb{R}_+\,,$$

are $\mathcal{C}^\infty$-diffeomorphisms.

Proof. For L, remark that:

$$\partial_\tau L(\mathbf{x},\tau)=2\,\tau-\frac{\kappa^2\,\mathbf{b}_e}{(\tau+\mathbf{b}_e)^2}=\frac{2\,\tau\,(\tau^2+\mathbf{b}_e\,\tau)+2\,\mathbf{b}_e\,(\tau^2+\mathbf{b}_e\,\tau)-\kappa^2\,\mathbf{b}_e}{(\tau+\mathbf{b}_e)^2}\,. \tag{3.107}$$

From (3.63), we know that $\tau^2+\mathbf{b}_e\,\tau\geq\kappa^2$ if $\tau\geq\tau_0^-(\mathbf{x})$. Then, looking at the right-hand term of (3.107), we get the first result. Otherwise, just compute $\partial_\tau R(\mathbf{x},\tau)$. □

When $\varpi=0$, there is a mix between ordinary and extraordinary waves. This effect is enhanced under the underdense assumption, see Figure 14. It follows that the independent use of $L(\mathbf{x},\cdot)$ or $R(\mathbf{x},\cdot)$ is not suitable to get inversion formulas that are globally defined in ϖ. The reason is that the expressions $L(\mathbf{x},\cdot)$ or $R(\mathbf{x},\cdot)$ (taken separately) do not allow a continuous connection to $g_\pm(\mathbf{x},\cdot)$ when ϖ goes to 0. To remedy this, we have to blend

the functions $L(\mathbf{x},\cdot)$ and $R(\mathbf{x},\cdot)$ accordingly. This induces the technicalities reproduced below. We start with the overdense case (Definition 3.8) which is simpler. For ordinary waves below the resonance frequency, just take:

$$F^1_{+,ov}(\mathbf{x},r) := \big(\sqrt{R(\mathbf{x},\cdot)}\big|_{[0,\mathbf{b}_e(\mathbf{x})[}\big)^{-1}(r)\,, \tag{3.108}$$

to recover:

$$\mathrm{V}^-_o(\mathbf{x},0) = \{\,(\tau,r)\,;\,0\le r\,,\,\tau = F^1_{+,ov}(\mathbf{x},r)\,\}\,.$$

For extraordinary waves located below the resonance frequency, we have to follow the red curve in Figure 14-(a). This means introducing:

$$F^1_{-,ov}(\mathbf{x},r) := \begin{cases} \big(\sqrt{L(\mathbf{x},\cdot)}\big|_{[\tau_0^-(\mathbf{x}),\kappa(\mathbf{x})[}\big)^{-1}(r) & \text{if} \quad r\le\sqrt{L(\mathbf{x},\kappa(\mathbf{x}))}\,,\\ \kappa(\mathbf{x}) & \text{if} \quad r\ge\sqrt{L(\mathbf{x},\kappa(\mathbf{x}))}\,,\end{cases}$$

in order to obtain:

$$\mathrm{V}^-_x(\mathbf{x},0) = \{\,(\tau,r)\,;\,0\le r\,,\,\tau = F^1_{-,ov}(\mathbf{x},r)\,\}\,.$$

For ordinary waves above the cutoff frequency, we have to reconstruct the blue curve in Figure 14-(a). Just define:

$$F^2_{+,ov}(\mathbf{x},r) := \begin{cases} \kappa(\mathbf{x}) & \text{if} \quad r\le\sqrt{L(\mathbf{x},\kappa(\mathbf{x}))}\,,\\ \big(\sqrt{L(\mathbf{x},\cdot)}\big|_{[\kappa(\mathbf{x}),+\infty[}\big)^{-1}(r) & \text{if} \quad r\ge\sqrt{L(\mathbf{x},\kappa(\mathbf{x}))}\,,\end{cases}$$

that gives access to:

$$\mathrm{V}^+_o(\mathbf{x},0) = \{(\tau,r)\,;\,0\le r\,,\,\tau = F^2_{+,ov}(\mathbf{x},r)\,\}\,.$$

We now move to the underdense case. As already noted in Paragraph 3.3.3, the situation is more intricated when $\mathbf{b}_e(\mathbf{x})>\kappa$. However, the logic is the same. We have to follow the coloured lines (blue and red) at the level of Figure 14-(b). Briefly define:

$$F^1_{+,un}(\mathbf{x},r) := \begin{cases} \big(\sqrt{R(\mathbf{x},\cdot)}\big|_{[0,\kappa(\mathbf{x})[}\big)^{-1}(r) & \text{if} \quad r\le\sqrt{R(\mathbf{x},\kappa(\mathbf{x}))}\,,\\ \kappa(\mathbf{x}) & \text{if} \quad r\ge\sqrt{R(\mathbf{x},\kappa(\mathbf{x}))}\,,\end{cases}$$

$$F^1_{-,un}(\mathbf{x},r) := \begin{cases} \big(\sqrt{L(\mathbf{x},\cdot)}\big|_{[\tau_0^-(\mathbf{x}),\kappa(\mathbf{x})[}\big)^{-1}(r) & \text{if} \quad r\le\sqrt{L(\mathbf{x},\kappa(\mathbf{x}))}\,,\\ \kappa(\mathbf{x}) & \text{if} \quad \sqrt{L(\mathbf{x},\kappa(\mathbf{x}))}\le r\le\sqrt{R(\mathbf{x},\kappa(\mathbf{x}))}\,,\\ \big(\sqrt{R(\mathbf{x},\cdot)}\big|_{[\kappa(\mathbf{x}),+\infty[}\big)^{-1}(r) & \text{if} \quad r\ge\sqrt{R(\mathbf{x},\kappa(\mathbf{x}))}\end{cases}$$

$$F^2_{+,un}(\mathbf{x},r) := \begin{cases} \kappa(\mathbf{x}) & \text{if} \quad r\le\sqrt{L(\mathbf{x},\kappa(\mathbf{x}))}\,,\\ \big(\sqrt{L(\mathbf{x},\cdot)}\big|_{[\kappa(\mathbf{x}),+\infty[}\big)^{-1}(r) & \text{if} \quad r\ge\sqrt{L(\mathbf{x},\kappa(\mathbf{x}))}\,.\end{cases}$$

The sets $\mathrm{V}^\pm_o(\mathbf{x},0)$ and $\mathrm{V}^-_x(\mathbf{x},0)$ are then given by:

$$\mathrm{V}^-_o(\mathbf{x},0) = \{(\tau,r)\,;\,0\le r\,,\,\tau = F^1_{+,un}(\mathbf{x},r)\,\}\,,$$
$$\mathrm{V}^-_x(\mathbf{x},0) = \{(\tau,r)\,;\,0\le r\,,\,\tau = F^1_{-,un}(\mathbf{x},r)\,\}\,,$$
$$\mathrm{V}^+_o(\mathbf{x},0) = \{(\tau,r)\,;\,0\le r\,,\,\tau = F^2_{+,un}(\mathbf{x},r)\,\}\,.$$

The situation of $\mathrm{V}^+_x(\mathbf{x},0)$ is simpler because $\mathrm{V}^+_x(\mathbf{x},0)$ just coincides with $\mathrm{V}^+_r(\mathbf{x},0)$. It suffices to define:

$$F^2_-(\mathbf{x},r) := \big(\sqrt{R(\mathbf{x},\cdot)}\big|_{[\tau_0^+(\mathbf{x}),+\infty[}\big)^{-1}(r)\,,$$

to recover $\mathrm{V}_x^+(\mathbf{x},0)$ through:

$$\mathrm{V}_x^+(\mathbf{x},0) = \big\{(\tau,r)\,;\,0\le r\,,\ \tau = F_-^2(\mathbf{x},r)\,\big\}\,.$$

The sets $\mathrm{V}_o^\pm(\mathbf{x},0)$ and $\mathrm{V}_x^\pm(\mathbf{x},0)$ are represented on Figure 14 below.

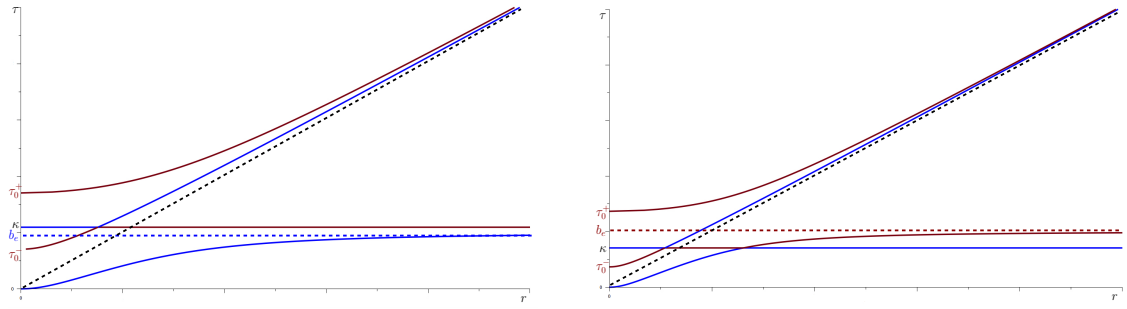

(a) Overdense case. (b) Underdense case.

FIGURE 14. Parallel propagation ($\varpi = 0$) with τ written as a function of r. Mixing of $\mathrm{V}_x(\mathbf{x},0)$ and $\mathrm{V}_o(\mathbf{x},0)$.

∘ 3.4.3.b) Perpendicular case ($\varpi = \pi/2$). We simply find:

$$g_+(\mathbf{x},\pi/2,\tau) = \tau^2 - \kappa(\mathbf{x})^2\,,\qquad g_-(\mathbf{x},\pi/2,\tau) = \frac{(\tau^2-\kappa(\mathbf{x})^2)^2 - \mathbf{b}_e(\mathbf{x})^2\,\tau^2}{\tau^2 - \mathbf{b}_e(\mathbf{x})^2 - \kappa(\mathbf{x})^2}\,.$$

Lemma 3.17. *Fix $\mathbf{x}\in\Omega$. The application $g_+(\mathbf{x},\pi/2,\cdot) : [\kappa(\mathbf{x}),+\infty[\longrightarrow \mathbb{R}_+$ as well as the two applications:*

$$g_-(\mathbf{x},\pi/2,\cdot) : [\tau_0^-(\mathbf{x}),\sqrt{\mathbf{b}_e(\mathbf{x})^2+\kappa(\mathbf{x})^2}[\ \longrightarrow \mathbb{R}_+\,,\quad g_-(\mathbf{x},\pi/2,\cdot) : [\tau_0^+(\mathbf{x}),+\infty[\longrightarrow \mathbb{R}_+\,.$$

are $\mathcal{C}^\infty$-diffeomorphisms.

Proof. This is obvious for $g_+(\mathbf{x},\pi/2,\cdot)$. For $\tau \neq \sqrt{\mathbf{b}_e(\mathbf{x})^2+\kappa^2}$, this follows from:

$$\partial_\tau g_-(\mathbf{x},\pi/2,\tau) \;=\; 2\,\tau\,\frac{(\tau^2-\mathbf{b}_e^2-\kappa^2)^2+\mathbf{b}_e^2\,\kappa^2}{(\tau^2-\mathbf{b}_e^2-\kappa^2)^2} > 0\,. \qquad \square$$

∘ 3.4.3.c) Oblique case ($\varpi\in]0,\pi/2[$). The analog of Lemmas 3.16 and 3.17 would be to show that $\partial_\tau g_\pm(\mathbf{x},\varpi,\cdot)$ has a specific sign. The corresponding calculation seems rather complicated. We use a weaker (more accessible) result, which is sufficient for our purpose.

Lemma 3.18. *Fix $\mathbf{x}\in\Omega$. Select any angle $\varpi\in]0,\pi/2[$. The four applications:*

$$g_+(\mathbf{x},\varpi,\cdot) : [0,\tau_\infty^-(\mathbf{x},\varpi)[\longrightarrow \mathbb{R}_+\,,\qquad g_+(\mathbf{x},\varpi,\cdot) : [\kappa(\mathbf{x}),+\infty[\longrightarrow \mathbb{R}_+\,,$$
$$g_-(\mathbf{x},\varpi,\cdot) : [\tau_0^-(\mathbf{x}),\tau_\infty^+(\mathbf{x},\varpi)[\longrightarrow \mathbb{R}_+\,,\qquad g_-(\mathbf{x},\varpi,\cdot) : [\tau_0^+(\mathbf{x}),+\infty[\longrightarrow \mathbb{R}_+\,,$$

are homeomorphisms.

Proof. Fix $r\in\mathbb{R}_+$. From (3.104) and (3.105), we can easily infer that:

$$\#\,\{\tau\in\mathbb{R}_+\,;\,(\tau,r)\in \mathrm{V}(\mathbf{x},\varpi)\}\le 4\,. \tag{3.109}$$

On the other hand, from Paragraph 3.3.2, we have (3.90). As recorded in Lemmas 3.11 and 3.13, the function $g_+(\mathbf{x},\varpi,\cdot)$ is continuous on $[0,\tau_\infty^-(\mathbf{x},\varpi)[$, and it satisfies:

$$g_+(\mathbf{x},\varpi,0)=0\,,\qquad \lim_{\tau\to(\tau_\infty^-)-} g_+(\mathbf{x},\varpi,\tau)=+\infty\,.$$

In this context, given $r\in\mathbb{R}_+$, the intermediate value theorem states that $r^2=g_+(\mathbf{x},\varpi,\tau)$ for some $\tau\in[0,\tau_\infty^-(\mathbf{x},\varpi)[$. In other words, we have $(\tau,r)\in \mathrm{V}_o^-(\mathbf{x},\varpi)$. Similarly, applying again Lemmas 3.11 and 3.13 but arguing this time with $g_-(\mathbf{x},\varpi,\cdot)$ and $g_+(\mathbf{x},\varpi,\cdot)$ on well-chosen intervals, we get:

$$\#\left\{\tau\in\mathbb{R}_+\,;\,(\tau,r)\in\mathrm{V}_*^\sigma(\mathbf{x},\varpi)\right\}\geq 1\,,\qquad \forall\,(*,\sigma)\in\{o,x\}\times\{\pm\}\,. \tag{3.110}$$

Combining (3.109) and (3.110), we can assert that:

$$\#\left\{\tau\in\mathbb{R}_+\,;\,(\tau,r)\in\mathrm{V}(\mathbf{x},\varpi)\right\}=4\,,\qquad \#\left\{\tau\in\mathbb{R}_+\,;\,(\tau,r)\in\mathrm{V}_*^\sigma(\mathbf{x},\varpi)\right\}=1\,. \tag{3.111}$$

This means that the function $g_+(\mathbf{x},\varpi,\cdot)$ is a bijection from $[0,\tau_\infty^-(\mathbf{x},\varpi)[$ to $[0,+\infty[$, and from $[\kappa,+\infty[$ to $[0,+\infty[$. This implies also that the function $g_-(\mathbf{x},\varpi,\cdot)$ is a bijection from the interval $[\tau_0^-(\mathbf{x}),\tau_\infty^+(\mathbf{x},\varpi)[$ to $[0,+\infty[$, and from $[\tau_0^+(\mathbf{x}),+\infty[$ to $[0,+\infty[$. Since both $g_+(\mathbf{x},\varpi,\cdot)$ and $g_-(\mathbf{x},\varpi,\cdot)$ are continuous and injective on their respective intervals of definition, the corresponding inverse functions are continuous. □

∘ 3.4.3.d) Synthesis of the results ($\varpi\in[0,\pi/2]$). By combining the results of the preceding paragraphs, a *global* description of the parts $\mathrm{V}_*^\sigma(\mathbf{x},\varpi)$ inside $\mathrm{V}(\mathbf{x},\varpi)$ becomes available. To this end, for all position $\mathbf{x}\in\Omega$, for all angle $\varpi\in[0,\pi]$, for all symbol $*\in\{ov,un\}$, and for all $r\in\mathbb{R}_+$, define:

$$f^1_{+,\star}(\mathbf{x},\varpi,r):=\begin{cases}\left(\sqrt{g_+(\mathbf{x},\varpi,\cdot)}\big|_{[0,\tau_\infty^-(\mathbf{x},\varpi)[}\right)^{-1}(r) & \text{if}\quad \varpi\in\,]0,\pi[\,,\\ F^1_{+,\star}(\mathbf{x},r) & \text{if}\quad \varpi=0(\pi)\,,\end{cases} \tag{3.112a}$$

$$f^2_{+,\star}(\mathbf{x},\varpi,r):=\begin{cases}\left(\sqrt{g_+(\mathbf{x},\varpi,\cdot)}\big|_{[\kappa(\mathbf{x}),+\infty[}\right)^{-1}(r) & \text{if}\quad \varpi\in\,]0,\pi[\,,\\ F^2_{+,\star}(\mathbf{x},r) & \text{if}\quad \varpi=0(\pi)\,,\end{cases} \tag{3.112b}$$

$$f^1_{-,\star}(\mathbf{x},\varpi,r):=\begin{cases}\left(\sqrt{g_-(\mathbf{x},\varpi,\cdot)}\big|_{[\tau_0^-(\mathbf{x}),\tau_\infty^+(\mathbf{x},\varpi)[}\right)^{-1}(r) & \text{if}\quad \varpi\in\,]0,\pi[\,,\\ F^1_{-,\star}(\mathbf{x},r) & \text{if}\quad \varpi=0(\pi)\,,\end{cases} \tag{3.112c}$$

$$f^2_{-}(\mathbf{x},\varpi,r)\quad:=\begin{cases}\left(\sqrt{g_-(\mathbf{x},\varpi,\cdot)}\big|_{[\tau_0^+(\mathbf{x}),+\infty[}\right)^{-1}(r) & \text{if}\quad \varpi\in\,]0,\pi[\,,\\ F^2_{-}(\mathbf{x},r) & \text{if}\quad \varpi=0(\pi)\,.\end{cases} \tag{3.112d}$$

Then, the components of the characteristic variety $\mathscr{V}$ can be viewed as the graphs of continuous functions on $\Omega\times[0,\pi]\times\mathbb{R}_+$. As a matter of fact, for all $(\mathbf{x},\varpi)\in\Omega\times[0,\pi]$, the sets $\mathrm{V}_o^\pm(\mathbf{x},\varpi)$ and $\mathrm{V}_x^\pm(\mathbf{x},\varpi)$ are given by:

$$\mathrm{V}_o^-(\mathbf{x},\varpi):=\left\{\,(\tau,r)\,;\,0\leq r\,,\,\tau=f^1_{+,\star}(\mathbf{x},\varpi,r)\,\right\}, \tag{3.113a}$$

$$\mathrm{V}_o^+(\mathbf{x},\varpi):=\left\{\,(\tau,r)\,;\,0\leq r\,,\,\tau=f^2_{+,\star}(\mathbf{x},\varpi,r)\,\right\}. \tag{3.113b}$$

$$\mathrm{V}_x^-(\mathbf{x},\varpi):=\left\{\,(\tau,r)\,;\,0\leq r\,,\,\tau=f^1_{-,\star}(\mathbf{x},\varpi,r)\,\right\}, \tag{3.113c}$$

$$\mathrm{V}_x^+(\mathbf{x},\varpi):=\left\{\,(\tau,r)\,;\,0\leq r\,,\,\tau=f^2_{-}(\mathbf{x},\varpi,r)\,\right\}. \tag{3.113d}$$

3.4.4. *The eikonal equation.* In Paragraph 3.1, we have approximated the RVM equations by using the WKB theory. The first outcome of this procedure is an eikonal equation which provides a simplified but pertinent representation of electromagnetic wave propagation in terms of geometric optics.

∘ 3.4.4.a) The concrete form of the eikonal equation. Paragraph 3.4.3 allows to formulate *globally in space* the Cauchy problem *in time* satisfied by ϕ. To produce the eikonal equation, introduce the angle $\varpi(\mathbf{x},\xi) \in [0,\pi]$ between the directions ξ and $\mathbf{B}_e(\mathbf{x})$. When ξ and $\mathbf{B}_e(\mathbf{x})$ are not parallel vectors, this angle is accessible through:

$$\varpi(\mathbf{x},\xi) := arccotan\left(\frac{\xi\cdot\mathbf{B}_e(\mathbf{x})/|\xi|\,\mathbf{b}_e(\mathbf{x})}{\sqrt{1-\left(\xi\cdot\mathbf{B}_e(\mathbf{x})/|\xi|\,\mathbf{b}_e(\mathbf{x})\right)^2}}\right), \qquad (\mathbf{x},\xi)\in\Omega\times\mathbb{R}^3\,. \tag{3.114}$$

When ξ and $\mathbf{B}_e(\mathbf{x})$ are parallel vectors, just adopt the conventions:

$$\varpi(\mathbf{x},\xi) := \left\{\begin{array}{lllll} \pi & \text{if} & \xi = s\,\mathbf{B}_e(\mathbf{x}) & \text{with} & s<0\,, \\ 0 & \text{if} & \xi = s\,\mathbf{B}_e(\mathbf{x}) & \text{with} & s>0 \end{array}\right., \qquad (\mathbf{x},\xi)\in\Omega\times\mathbb{R}^3\,. \tag{3.115}$$

For all $(\mathbf{x},\xi)\in\Omega\times\mathbb{R}^3$, we can also define:

$$\lambda^i_{+,*}(\mathbf{x},\xi) := -f^i_{+,*}\left(\mathbf{x},\varpi(\mathbf{x},\xi),|\xi|\right), \qquad (i,*)\in\{1,2\}\times\{ov,un\}\,, \tag{3.116a}$$

$$\lambda^1_{-,*}(\mathbf{x},\xi) := -f^1_{-,*}\left(\mathbf{x},\varpi(\mathbf{x},\xi),|\xi|\right), \qquad *\in\{ov,un\}\,, \tag{3.116b}$$

$$\lambda^2_{-}(\mathbf{x},\xi) := -f^2_{-}\left(\mathbf{x},\varpi(\mathbf{x},\xi),|\xi|\right). \tag{3.116c}$$

Lemma 3.19. *Let $\phi\in\mathcal{C}^\infty(M;\mathbb{R})$ be a function subjected to (3.57) with $l=1$. The choice of the value $l=1$ is to simplify the presentation. Then, the condition:*

$$\left(\varpi(\mathbf{x},\nabla_{\mathbf{x}}\phi(\mathbf{t},\mathbf{x})),\,\partial_{\mathbf{t}}\phi(\mathbf{t},\mathbf{x}),\,|\nabla_{\mathbf{x}}\phi(\mathbf{t},\mathbf{x})|\right)\in\mathcal{V}^\dagger_\ell(\mathbf{x}), \qquad (\dagger,\ell)\in\{+,-\}\times\{o,x\}$$

amounts to the same thing as:

$$\partial_{\mathbf{t}}\phi(\mathbf{t},\mathbf{x}) + \lambda^i_{\pm,*}(\mathbf{x},\nabla_{\mathbf{x}}\phi(\mathbf{t},\mathbf{x})) = 0\,, \qquad (i,*)\in\{1,2\}\times\{ov,un\} \tag{3.117}$$

with the following correspondences:

$$(\dagger,\ell)=(-,o)\implies(i,\pm)=(1,+)\,, \qquad (\dagger,\ell)=(+,o)\implies(i,\pm)=(2,+)\,,$$
$$(\dagger,\ell)=(-,x)\implies(i,\pm)=(1,-)\,, \qquad (\dagger,\ell)=(+,x)\implies(i,\pm)=(2,-)\,,$$

and $*$ is given by ov (resp. un) if $\mathbf{b}_e(\mathbf{x})<\kappa(\mathbf{x})$ (resp. $\mathbf{b}_e(\mathbf{x})>\kappa(\mathbf{x})$).

Proof. This follows directly from (3.113). □

Lemma 3.18, together with the definitions (3.113) and (3.116), only yields the continuity of the functions $\lambda^i_{\pm,*}(\cdot)$. This is not enough to ensure the existence and the uniqueness of solutions to the Hamilton-Jacobi equation (3.117). However, when dealing in the overdense case with the so-called whistler dispersion relation $\lambda^1_{+,ov}(\cdot)$, this can be avoided by selecting large values of $|\nabla_{\mathbf{x}}\phi(\mathbf{t},\mathbf{x})|$.

Lemma 3.20. *For all relatively compact open set $O\subset\Omega$, there exists a constant C such that $\lambda^1_{+,ov}(\cdot)$ is of class $\mathcal{C}^1$ on $O\times B(0,C)^c$.*

Proof. The expression $\lambda^1_{+,ov}(\cdot)$ can be accessed via (3.116a) and (3.112a). Thus, the aim is to study the regularity of the functions $g_+(\cdot)$ and $F^1_{+,ov}(\cdot)$. The first difficulty is to examine what happens when $\varpi = 0$ and $\varpi = \pi$.

On the one hand, the function $\varpi(\cdot)$ of (3.114) is not differentiable when ξ and $\mathbf{B}_e(\mathbf{x})$ have parallel directions. Note however that this singularity is artificial. Indeed, the definition of $g_+(\cdot)$ only involves terms in $\sin^2\varpi(\cdot)$ and $\cos^2\varpi(\cdot)$ which both are of class $\mathcal{C}^1$. On the other hand, the two extreme situations $\varpi = 0$ (i.e. study of $F^1_{+,ov}$) and $\varpi = \pi/2$ have already been treated in Lemmas 3.16 and 3.17. It follows that the discussion may be limited to the case $\varpi \in]\delta, \pi - \delta[$ with $\delta \in \mathbb{R}^*_+$ small enough. From now on, the matter is to show that, for some well chosen $\delta > 0$, we have:

$$\forall\, (\varpi, \tau) \in]\delta, \pi - \delta[\times]\tau^-_\infty(\mathbf{x}, \varpi) - \delta, \tau^-_\infty(\mathbf{x}, \varpi)[\,, \qquad \partial_\tau g_+(\mathbf{x}, \varpi, \tau) > 0\,. \tag{3.118}$$

For $\varpi \in]0, \pi/2[$ and $\tau < \tau^-_\infty(\mathbf{x}, \varpi)$, we can compute:

$$\partial_\tau g_+(\mathbf{x}, \varpi, \tau) \,=\, \frac{1}{(\tau^2 - (\tau^+_\infty)^2)(\tau^2 - (\tau^-_\infty)^2)} \left(P(\varpi, \tau) - \frac{Q(\varpi, \tau)}{(\tau^2 - (\tau^+_\infty)^2)} - \frac{Q(\varpi, \tau)}{(\tau^2 - (\tau^-_\infty)^2)} \right),$$

where:

$$P(\mathbf{x}, \varpi, \tau) := 2\ \tau\ \mathcal{P}(\mathbf{x}, \varpi, \tau) + \tau^2\, \partial_\tau \mathcal{P}(\mathbf{x}, \varpi, \tau) + \frac{\mathbf{b}_e\, \kappa^2\, \partial_\tau \mathcal{Q}(\mathbf{x}, \varpi, \tau)}{2\ \sqrt{\mathcal{Q}(\mathbf{x}, \varpi, \tau)}}\,, \tag{3.119a}$$

$$Q(\mathbf{x}, \varpi, \tau) := 2\ \tau^3 \left[\mathcal{P}(\mathbf{x}, \varpi, \tau) + \mathbf{b}_e\ \kappa^2 \sqrt{\tau^{-4}\, \mathcal{Q}(\mathbf{x}, \varpi, \tau)} \right]. \tag{3.119b}$$

Combining (3.77) and (3.78), we easily get that:

$$Q\big(\mathbf{x}, \varpi, \tau^-_\infty(\mathbf{x}, \varpi)\big) := 4\ \tau^-_\infty(\mathbf{x}, \varpi)^3\ \mathcal{P}\big(\mathbf{x}, \varpi, \tau^-_\infty(\mathbf{x}, \varpi)\big) > 0\,. \tag{3.120}$$

It follows that:

$$\lim_{\tau\, \to\, \tau^-_\infty(\mathbf{x}, \varpi)^-} \partial_\tau g_+(\mathbf{x}, \varpi, \tau) = +\infty\,.$$

This is sufficient to deduce (3.118). □

∘ 3.4.4.b) Deviation from parallel propagation. In the constant coefficient case, if $\xi \wedge \mathbf{B}_e = 0$ at time $t = 0$, this remains true along the characteristics at all times $t \in \mathbb{R}^*_+$. Now, in the presence of spatial inhomogeneities, parallel propagation would mean that the well prepared rays of geometrical optics, i.e. the rays associated to (3.117) and started from positions $(\mathbf{x}, \xi) \in T^*M$ such that $\xi \wedge \mathbf{B}_e(\mathbf{x}) = 0$, would follow the field lines. The aim of this Paragraph is precisely to dismiss this possibility.

To simplify, we focus on the whistler dispersion relation $\lambda^1_{+,ov}(\cdot)$. Moreover, to detect only the effects of the variations of $\mathbf{B}_e(\cdot)$, we assume that κ does not depend on $\mathbf{x}$. This amounts to suppose that there are no variations in density. Let $O \Subset \Omega$. With C as in Lemma 3.20, consider a function $\phi_0 \in \mathcal{C}^\infty(O; \mathbb{R})$ satisfying:

$$\forall\, \mathbf{x} \in O\,, \qquad \varpi\big(\mathbf{x}, \nabla_{\mathbf{x}}\phi_0(\mathbf{x})\big) = 0\,, \qquad C < |\nabla_{\mathbf{x}}\phi_0(\mathbf{x})|\,.$$

Complete the Hamilton-Jacobi equation (3.117) with the initial data:

$$\forall\, \mathbf{x} \in O\,, \qquad \phi(0, \mathbf{x}) = \phi_0(\mathbf{x})\,. \tag{3.121}$$

The smoothness of $\lambda^1_{+,ov}(\cdot)$ guarantees the local in time well-posedness of the Cauchy problem (3.117)-(3.121). More precisely, restricting a little the size of O if necessary, we can find $T \in]0,1]$ small enough and a unique function ϕ of class $\mathcal{C}^1$ satisfying:

$$\forall\, (\mathbf{t},\mathbf{x}) \in [0,T]\times O\,, \quad \partial_{\mathbf{t}}\phi(\mathbf{t},\mathbf{x}) + \lambda^1_{+,ov}\big(\mathbf{x}, \nabla_{\mathbf{x}}\phi(\mathbf{t},\mathbf{x})\big) = 0\,, \quad \phi(0,\mathbf{x}) = \phi_0(\mathbf{x})\,. \tag{3.122}$$

To show that purely parallel propagation does not occur for whistler waves, it suffices to exhibit some $(\mathbf{t},\mathbf{x}) \in [0,T]\times O$ such that $\varpi\big(\mathbf{x}, \nabla_{\mathbf{x}}\phi(\mathbf{t},\mathbf{x})\big) > 0$. To this end, it is more convenient to work in the straightened coordinates of [7]. With the notations from Discussion 2.1 in mind, introduce the diffeomorphism $\mathrm{Y}_e : \Omega \longrightarrow \mathrm{Y}_e(\Omega)$ which is defined through the curvilinear coordinates:

$$\mathrm{Y}^1_e := z\,(\rho^2+z^2)^{-3/2} \in \mathbb{R}\,, \qquad \mathrm{Y}^2_e := -\,\rho^4\,(\rho^2+z^2)^{-3} \in \mathbb{R}^*_-\,, \qquad \mathrm{Y}^3_e := \phi \in \mathbb{R}\,.$$

This gives rise to a triply orthogonal system $(\nabla_{\mathbf{x}}\mathrm{Y}^j_e)_{1\leq j\leq 3}$ satisfying $\nabla_{\mathbf{x}}\mathrm{Y}^1_e = \mathbf{B}_e$. Adopt the conventions:

$$d^j_e := |\nabla_{\mathbf{x}}\mathrm{Y}^j_e \circ \mathrm{Y}_e^{-1}|\,, \qquad \forall\, j \in \{1,2,3\}\,. \tag{3.123}$$

In particular, we have $d^1_e \equiv \mathbf{b}_e \circ \mathrm{Y}_e^{-1}$. From now on, we will note $\mathbf{y}$ the current variable in the domain $\mathrm{Y}_e(\Omega)$. With these conventions, the coordinates $\mathbf{y}^1$, $\mathbf{y}^2$ and $\mathbf{y}^3$ can be interpreted respectively as a sort of latitude, (negative) altitude and longitude. Define:

$$\phi(\mathbf{t},\mathbf{y}) := \phi(\mathbf{t}, \mathrm{Y}_e^{-1}(\mathbf{y}))\,, \qquad \phi_0(\mathbf{y}) := \phi_0(\mathrm{Y}_e^{-1}(\mathbf{y}))\,.$$

The new expression ϕ is subjected to:

$$\partial_{\mathbf{t}}\phi(\mathbf{t},\mathbf{y}) + \Lambda^1_{+,ov}\big(\mathbf{y}, \nabla_{\mathbf{y}}\phi(\mathbf{t},\mathbf{y})\big) = 0\,, \qquad \phi(0,\mathbf{y}) = \phi_0(\mathbf{y})\,, \tag{3.124}$$

where, for $\xi = {}^t(\xi^1,\xi^2,\xi^3) \in \mathbb{R}^3$, we have introduced:

$$\Lambda^1_{+,ov}(\mathbf{y},\xi) := -f^1_{+,ov}\big(\mathrm{Y}_e^{-1}(\mathbf{y}), \varpi(\mathbf{y},\xi), N(\mathbf{y},\xi)\big)\,, \tag{3.125}$$

with:

$$N(\mathbf{y},\xi) := \sqrt{\sum_{1\leq j\leq 3} (\xi^j)^2\; d^j_e(\mathbf{y})^2}\,, \tag{3.126a}$$

$$\varpi(\mathbf{y},\xi) := \mathrm{arccotan}\left(\frac{d^1_e\;\xi^1}{\sqrt{(d^2_e)^2\,(\xi^2)^2 + (d^3_e)^2\,(\xi^3)^2}}\right)\,. \tag{3.126b}$$

Lemma 3.21. *[characterization of purely parallel propagation] The following assertions are equivalent:*

(i) For all $(\mathbf{t},\mathbf{x}) \in [0,T]\times O$, we have $\varpi\big(\mathbf{x}, \nabla_{\mathbf{x}}\phi(\mathbf{t},\mathbf{x})\big) = 0$.

(ii) For all $(\mathbf{t},\mathbf{y}) \in [0,T]\times \mathrm{Y}_e(O)$, we have $\partial_{\mathbf{y}^2}\phi(\mathbf{t},\mathbf{y}) = \partial_{\mathbf{y}^3}\phi(\mathbf{t},\mathbf{y}) = 0$.

Proof. With $\mathbf{x} = \mathrm{Y}_e^{-1}(\mathbf{y})$, the condition $\varpi\big(\mathbf{x}, \nabla_{\mathbf{x}}\phi(\mathbf{t},\mathbf{x})\big) = 0$ is equivalent to:

$$0 = \mathbf{B}_e(\mathbf{x}) \wedge \nabla_{\mathbf{x}}\phi(\mathbf{t},\mathbf{x}) = \partial_{\mathbf{y}^2}\phi(\mathbf{t},\mathbf{y})\; \mathbf{B}_e(\mathbf{x}) \wedge \nabla_{\mathbf{x}}\mathrm{Y}^2_e(\mathbf{x}) + \partial_{\mathbf{y}^3}\phi(\mathbf{t},\mathbf{y})\; \mathbf{B}_e(\mathbf{x}) \wedge \nabla_{\mathbf{x}}\mathrm{Y}^3_e(\mathbf{x})\,.$$

Since the three vectors $\mathbf{B}_e(\mathbf{x})$, $\nabla_{\mathbf{x}}\mathrm{Y}^2_e(\mathbf{x})$ and $\nabla_{\mathbf{x}}\mathrm{Y}^3_e(\mathbf{x})$ are orthogonal two by two, this can be achieved if and only if $\partial_{\mathbf{y}^2}\phi(\mathbf{t},\mathbf{y}) = \partial_{\mathbf{y}^3}\phi(\mathbf{t},\mathbf{y}) = 0$. □

We are now able to prove that purely paralel propagation does not exist:

Theorem 2. *Assume that κ is constant on Ω. Then, there exists some $(\mathbf{t},\mathbf{x}) \in [0,T]\times O$ such that $\varpi(\mathbf{x}, \nabla_{\mathbf{x}}\phi(\mathbf{t},\mathbf{x})) > 0$.*

Proof. The function $\Lambda^1_{+,ov}(\cdot)$ introduced at the level of (3.124) cannot depend on $\mathbf{y}^3$ since we have $\partial_{\mathbf{y}^3} d^j \equiv 0$ for all $j \in \{1,2,3\}$ (see [7], Lemma 2.1). As a consequence, we have:

$$\forall\,(\mathbf{t},\mathbf{y}) \in [0,T]\times \mathrm{Y}_e(O)\,, \qquad \partial_{\mathbf{y}^3}\phi(\mathbf{t},\mathbf{y}) = 0\,.$$

Taking into account Lemma 3.21, the matter is to obtain $\partial_{\mathbf{y}^2}\phi(\mathbf{t},\mathbf{y}) \neq 0$ for some $(\mathbf{t},\mathbf{y})$. By contradiction, let us assume that we have $\partial_{\mathbf{y}^2}\phi(\cdot) \equiv 0$. Then, the equation (3.124) reduces to:

$$\partial_{\mathbf{t}}\phi(\mathbf{t},\mathbf{y}) + f^1_{+,ov}(\mathrm{Y}_e^{-1}(\mathbf{y}), 0, d^1_e(\mathbf{y})\,|\partial_{\mathbf{y}^1}\phi(\mathbf{t},\mathbf{y})|) = 0\,. \tag{3.127}$$

Moreover, looking at the derivative of (3.124) with respect to $\mathbf{y}^2$, we get:

$$\forall\,(\mathbf{t},\mathbf{y}) \in [0,T]\times \mathrm{Y}_e(O)\,, \qquad \partial_{\mathbf{y}^2}\Lambda^1_{+,ov}(\mathbf{y}, {}^t(\partial_{\mathbf{y}^1}\phi(\mathbf{t},\mathbf{y}), 0, 0)) = 0\,. \tag{3.128}$$

From (3.125), we can deduce:

$$\partial_{\mathbf{y}^2}\Lambda^1_{+,ov} = \nabla_{\mathbf{x}} f^1_{+,ov}\cdot \partial_{\mathbf{y}^2}\mathrm{Y}_e^{-1} + \partial_{\varpi} f^1_{+,ov}\times \partial_{\mathbf{y}^2}\varpi + \partial_r f^1_{+,ov}\times \partial_{\mathbf{y}^2} N\,.$$

On the one hand, we have the relations:

$$\nabla_{\mathbf{x}} f^1_{+,ov} = -\frac{\nabla_{\mathbf{x}}\sqrt{g_+}}{\partial_\tau\sqrt{g_+}}\,, \qquad \partial_\varpi f^1_{+,ov} = -\frac{\partial_\varpi\sqrt{g_+}}{\partial_\tau\sqrt{g_+}}\,, \qquad \partial_r f^1_{+,ov} = \frac{1}{\partial_\tau\sqrt{g_+}}\,.$$

On the other hand, the dependence of $g_+(\cdot)$ on $\mathbf{x}$ and ϖ is achieved through $b_e(\mathbf{x})$ and $\cos^2\varpi$. It follows that:

$$\nabla_{\mathbf{x}}\sqrt{g_+}\cdot\partial_{\mathbf{y}^2}\mathrm{Y}_e^{-1}(\mathbf{y}) = \partial_{b_e}\sqrt{g_+}\times\partial_{\mathbf{y}^2} d^1_e\,, \qquad \partial_\varpi\sqrt{g_+}\times\partial_{\mathbf{y}^2}\varpi = \partial_{\cos^2\varpi}\sqrt{g_+}\times\partial_{\mathbf{y}^2}\cos^2\varpi\,.$$

Remark also that $\varpi(\mathbf{y},\xi^1,0,0) = 0(\pi)$ so that $\sin\varpi(\mathbf{y},\xi^1,0,0) = 0$. By combining the preceding information, we can assert that:

$$(\partial_{\mathbf{y}^2}\Lambda^1_{+,ov})(\mathbf{y}, {}^t(\xi^1,0,0)) = \frac{\partial_{\mathbf{y}^2} d^1_e(\mathbf{y})}{\partial_\tau\sqrt{g_+}}\left(|\xi^1| - \partial_{\mathbf{b}_e}\sqrt{g_+}\right)\,, \tag{3.129}$$

where $\partial_{\mathbf{b}_e}\sqrt{g_+}$ and $\partial_\tau\sqrt{g_+}$ are evaluated at the position:

$$(\mathbf{x},\varpi,\tau) = (\,\mathrm{Y}_e^{-1}(\mathbf{y})\,,\,0\,,\,f^1_{+,ov}(\mathrm{Y}_e^{-1}(\mathbf{y}),0,|\xi^1 d^1_e|)\,)\,.$$

Knowing that $\partial_{\mathbf{y}^2} d^1_e < 0$ - see [7], Lemma 2.1 - and that $\sqrt{g_+} \equiv F^1_{+,ov} \equiv \sqrt{R}$ when $\varpi = 0$ - see (3.108) and (3.112a)-, the condition (3.128) amounts to the same thing as:

$$\forall\,(\mathbf{t},\mathbf{y})\,, \qquad |\partial_{\mathbf{y}^1}\phi(\mathbf{t},\mathbf{y})| - \partial_{\mathbf{b}_e}\sqrt{R}(\mathrm{Y}_e^{-1}(\mathbf{y}), \partial_{\mathbf{t}}\phi(\mathbf{t},\mathbf{y})) = 0\,. \tag{3.130}$$

Another way to express (3.127) is to write:

$$|\partial_{\mathbf{y}^1}\phi(\mathbf{t},\mathbf{y})| = d^1_e(\mathbf{y})^{-1}\ \sqrt{R}(\mathrm{Y}_e^{-1}(\mathbf{y}), \partial_{\mathbf{t}}\phi(\mathbf{t},\mathbf{y}))\,.$$

With (3.106b), the left hand side of (3.130) is therefore:

$$\frac{1}{d^1_e}\ \sqrt{R}(\mathrm{Y}_e^{-1}(\mathbf{y}),\tau) + \frac{\kappa^2\,\tau}{2\,(\tau-b_e)^2\,\sqrt{R}(\mathrm{Y}_e^{-1}(\mathbf{y}),\tau)}\,, \qquad \tau := \partial_{\mathbf{t}}\phi(\mathbf{t},\mathbf{y})\,. \tag{3.131}$$

Since $\tau > 0$, this expression cannot be zero as required at the level of (3.130). This is the expected contradiction. □

3.4.5. *Physical interpretations.* Chorus emissions are the most common and most intense electromagnetic plasma waves that are observed in the radiation belts of the Earth. They must be related to radio science phenomena. They have long stimulated both experimental and theoretical research [17, 18, 35], see especially the fairly old review [31]. During the last years [3, 29, 37], with the advent of satellite-based investigation systems, they have received renewed interest. Today, they are studied even more intensively, especially because of their role as a viable mechanism for accelerating electrons [24, 34].

There is a general agreement that the mechanisms underlying the generation of very low frequency waves does rely on the cyclotron resonance interactions between the waves and the particles. The current discussions rather relate to the modalities of these interactions. In the recent contribution [7], the origin of the monochromatic elements forming the fine structure of chorus (see Figure 15) is mathematically interpreted as a mesoscopic caustic effect.

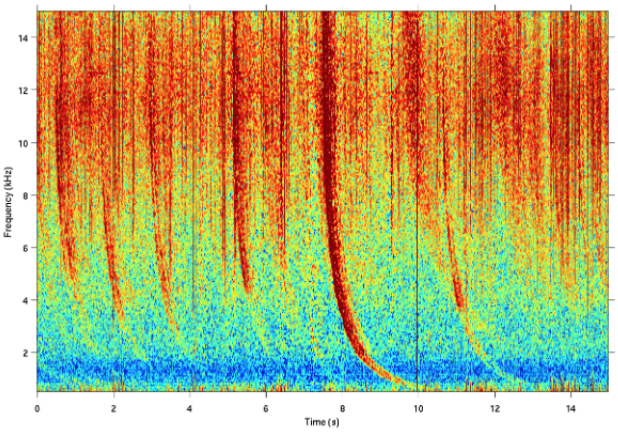

FIGURE 15. Spectrogram of chorus emission.

As a matter of fact, the deviation from parallel propagation which has been fully justified in Paragraph 3.4.4 comes to reinforce this principle. Indeed, this confirms that the waves (unlike the particles) do not travel along the field lines. Thus, instead of coming from the propagation along the field lines of some original wave packet, most electromagnetic signals would be the result of the procedure of creation of light detailed in [7]. The analysis of [7] was based on the classical whistler dispersion relation, as found in [11, 27, 33]. Below, by combining the refined model exhibited in Theorem 1 with the information from [7], we can get a better understanding of what happens.

According to [7], the wave packets are emitted inside the characteristic variety $\mathscr{V}$, all along the resonance cones (drawn at the level of Figures 10 and 11). Moreover, a signal which is generated at the time $\mathbf{t}$ from the position $(\mathbf{t}, \mathbf{x}, \tau, \xi) \in \mathscr{V}$ starts to travel at the velocity $|\nabla_\xi \lambda^i_{-,\star}(\mathbf{x}, \xi)|$. In view of the dispersion relations, the size of $|\nabla_\xi \lambda^i_{-,\star}(\mathbf{x}, \xi)|$ may be significant when ξ is located away from the resonance frequencies $\tau^\pm_\infty(\mathbf{x}, \varpi)$ with ϖ given by (3.38). Then, as described in Theorem 2 of [7], the electromagnetic signals should appear again and again over consecutive periods of almost equal length. They are marked by light-coloured vertical lines in the spectrograms, see Figure 17. On the contrary, the size of $|\nabla_\xi \lambda^i_{-,\star}(\mathbf{x}, \xi)|$ becomes small when ξ approaches $\tau^\pm_\infty(\mathbf{x}, \varpi)$. Then, there is almost no propagation. This could account for the creation of quasi-electrostatic waves. This difference in behaviour could explain why chorus emissions are usually composed of discrete narrowband wave elements accompanied by banded incoherent waves [24].

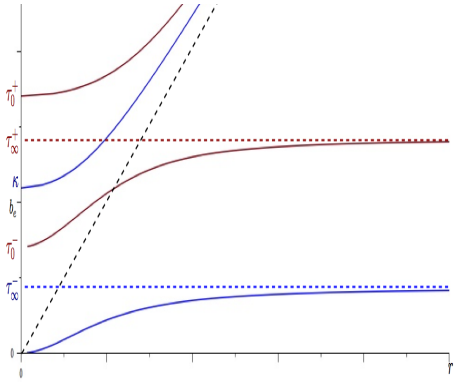

FIGURE 16. The characteristic variety as a graph of functions depending on τ.

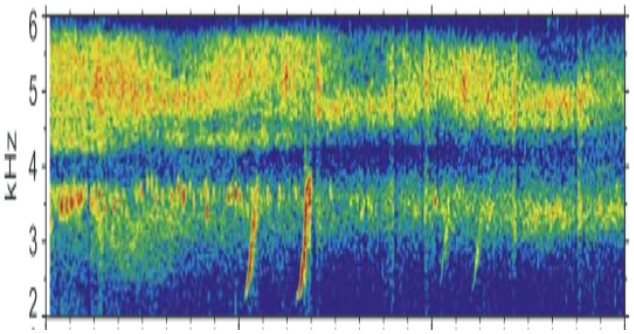

FIGURE 17. Whistler-mode chorus: Spectrogram of the electromagnetic field.

Moreover, chorus emissions usually occur in two frequency ranges, a *lower* band and some *upper* band, which are separated by a gap [24, 29, 31]. The high part of the lower band might correspond to the resonance frequency τ_∞^-. On the other hand, the upper band could be demimited from below by the cutoff frequency τ_0^- and at the top by the resonance frequency τ_∞^+. To well illustrate these correspondences, the comparison between Figures 16 and 17 is facilitated above. Note also that the lower and upper bands would be associated with respectively the ordinary and extraordinary modes of propagation,

The fact [29] that lower-band waves tend to be field-aligned ($\varpi \simeq 0$) whereas upper-band waves seem to be highly oblique ($\varpi \simeq \pi/2$) is another aspect that can be interpreted as a consequence of our analysis. Indeed, away from the emission points, the (non propagating) electrostatic waves should not be detected. Such waves are generated from the vertical lines in Figures 6 and 7. This yields the line $\tau \equiv \tau_\infty^+ = \kappa$ in the perpendicular case $\varpi = 0$, and $\tau \equiv \tau_\infty^- = 0$ in the parallel case $\varpi = \pi/2$. As a result, away from the emitting regions, one would expect to observe principally a lower-band (related to τ_∞^-) when $\varpi \simeq 0$, and a upper band (related to τ_∞^+) when $\varpi \simeq \pi/2$.

In conclusion, the refined structures of the characteristic variety $\mathscr{V}$ help to improve our understanding of the morphological properties of chorus emissions.

Acknowledgments. This work received the support of the *Agence Nationale de la Recherche*: projet NOSEVOL (ANR 2011 BS01019 01) and ANR blanc DYFICOLTI.

REFERENCES

[1] E. V. Appleton. Wireless studies of the ionosphere. *J. Inst. Electr. Eng*, 71:642–650, 1932.
[2] A. Back, T. Hattori, S. Labrunie, J.-R. Roche, and P. Bertrand. Electromagnetic wave propagation and absorption in magnetised plasmas: variational formulations and domain decomposition, 2014.
[3] J. Bortnik, R. M. Thorne, and N. P. Meredith. The unexpected origin of plasmaspheric hiss from discrete chorus emissions. *Nature*, 452:62–66, 2008.

[4] M. Bostan and C. Negulescu. Mathematical models for strongly magnetized plasmas with mass disparate particles. *Discrete Contin. Dyn. Syst. Ser. B*, 15(3):513–544, 2011.
[5] M. Braun. Mathematical remarks on the Van Allen radiation belt: a survey of old and new results. *SIAM Rev.*, 23(1):61–93, 1981.
[6] J.-Y. Chemin, B. Desjardins, I. Gallagher, and E. Grenier. *Mathematical geophysics*, volume 32 of *Oxford Lecture Series in Mathematics and its Applications*. The Clarendon Press Oxford University Press, Oxford, 2006. An introduction to rotating fluids and the Navier-Stokes equations.
[7] C. Cheverry. Can One Hear Whistler Waves? *Comm. Math. Phys.*, 338(2):641–703, 2015.
[8] R. Ciurea-Borcia, G. Matthieussent, E. Le Bel, F. Simonet, and J. Solomon. Oblique whistler waves generated in cold plasma by relativistic electron beams. *Physics of plasmas*, 7(1):359–370, 2000.
[9] M.H. Denton, J.E. Borovsky, and T.E. Cayton. A density temperature description of the outer electron radiation belt during geomagnetic storms. *Journal of Geophysical Research: Space Physics*, 115, 2010.
[10] Bruno Després, Lise-Marie Imbert-Gérard, and Ricardo Weder. Hybrid resonance of Maxwell's equations in slab geometry. *J. Math. Pures Appl. (9)*, 101(5):623–659, 2014.
[11] R. Fitzpatrick. *Plasma Physics: An Introduction*. Hardcover, 2014.
[12] E. Frénod and E. Sonnendrücker. Long time behavior of the two-dimensional Vlasov equation with a strong external magnetic field. *Math. Models Methods Appl. Sci.*, 10(4):539–553, 2000.
[13] C. Gillmor. Wilhelm Altar, Edward Appleton, and the magneto-ionic theory. *Proceedings of the American Philosophical Society*, 126(5):395–440, 1982.
[14] R. T. Glassey and J. W. Schaeffer. Global existence for the relativistic Vlasov-Maxwell system with nearly neutral initial data. *Comm. Math. Phys.*, 119(3):353–384, 1988.
[15] F. Golse and L. Saint-Raymond. The Vlasov-Poisson system with strong magnetic field. *J. Math. Pures Appl. (9)*, 78(8):791–817, 1999.
[16] F. Golse and L. Saint-Raymond. The Vlasov-Poisson system with strong magnetic field in quasineutral regime. *Math. Models Methods Appl. Sci.*, 13(5):661–714, 2003.
[17] D. R. Hartree. The propagation of electromagnetic waves in a stratified medium. *Mathematical Proceedings of the Cambridge Philosophical Society*, 25:97–120, 1929.
[18] R. A. Helliwell. *Whistlers and Related Ionospheric Phenomena*. Stanford University Press. 1965.
[19] C.F. Kennel. Low frequency whistler mode. *Journal of Plasma Physics*, 71:1– 28, 1966.
[20] C.F. Kennel and H.E. Petschek. Limit on stably trapped particles. *Journal of Geophysical Research*, 9:2190–2202, 1966.
[21] E. Le Bel. *Etude physique et numérique de la saturation des ceintures de Van Allen*. PhD thesis, Paris 11, Orsay, 2001.
[22] W. Li, J. Bortnik, R. M. Thorne, Y. Nishimura, V. Angelopoulos, and L. Chen. Modulation of whistler mode chorus waves: 2. role of density variations. *Journal of Geophysical Research*, 116, Issue A6, 2011.
[23] Z. Lin and W. A. Strauss. Linear stability and instability of relativistic Vlasov-Maxwell systems. *Comm. Pure Appl. Math.*, 60(5):724–787, 2007.
[24] K. Liu, S.P. Gary, and D. Winske. Excitation of banded whistler waves in the magnetosphere. *Geophysical Research Letters*, 38, 2011.
[25] J. D. Menietti, J. S. Pickett, D. A. Gurnett, and J. D. Scudder. Electrostatic electron cyclotron waves observed by the plasma wave instrument on board polar. *Journal of Geophysical Research*, 106, 2001.
[26] G. Métivier. *The Mathematics of Nonlinear Optics*. 2009.
[27] D. C. Montgomery and D. A. Tidman. *Plasma kinetic theory*. McGraw-Hill Book Company, 1964.
[28] M. E. Oakes, R. B. Michie, K. H. Tsui, and J. E. Copeland. Cold plasma dispersion surfaces. *Journal of Plasma Physics*, 21:205–224, 1979.
[29] Y. Omura, M. Hikishima, Y. Katoh, D. Summers, and S. Yagitani. Nonlinear mechanisms of lower-band and upper-band vlf chorus emissions in the magnetosphere. *Journal of Geophysical Research*, 114, 2009.
[30] J. Rauch. *Hyperbolic Partial Differential Equations and Geometric Optics*. Graduate Studies in Mathematics. American Mathematical Society, 2012.

[31] S.S. Sazhin and M. Hayakawa. Magnetospheric chorus emissions: A review. *Planetary and Space Science*, 40:681–697, 1992.
[32] D. Sidhu and H. Unz. The magneto-ionic theory for drifting plasma: The whistler mode. *Transactions of the Kansas Academy of Science*, 70(4):432–450, 1967.
[33] T. H. Stix. *Waves in plasma*. American Institute of Physics, 1992.
[34] Harid V. *Coherent interactions between whistler mode waves and energetic electrons in the earth's radiation belts*. PhD thesis, Stanford, 2015.
[35] R. Woollett. *Electromagnetic wave propagation in a cold, collisionless atomic hydrogen plasma*. Nasa technical note, Nasa TN D-2071, 1964.
[36] F. Xiao, Thorne R. M., and D. Summers. Intsability of electromagnetic r-mode waves in a relativistic plasma. *Physics of plasmas*, 5:2489–2497, 1998.
[37] K. Yamaguchi, T. Matsumuro, Y. Omura, and D. Nunn. Ray tracing of whistler-mode chorus elements. *Ann. Geophys.*, 31:665–673, 2013.

(C. Cheverry) Institut Mathématique de Rennes, Campus de Beaulieu, 263 avenue du Général Leclerc CS 74205 35042 Rennes Cedex, FRANCE
E-mail address: christophe.cheverry@univ-rennes1.fr

(Adrien Fontaine) Institut Mathématique de Rennes, Campus de Beaulieu, 263 avenue du Général Leclerc CS 74205 35042 Rennes Cedex, FRANCE
E-mail address: adrien.fontaine@ens-rennes.fr